Polyurethane Materials: Insights on Dynamic Properties and Self-Healing Applications

A manuscript submitted to the

Universidad del País Vasco (UPV/EHU)
Donostia-San Sebastián – España

PhD THESIS

Presented by

Fermin Elizalde Iraizoz

Under the supervision of

Dr. Haritz Sardon (UPV/EHU)

Dr. Robert Aguirresarobe (UPV/EHU)

Donostia, October 2022

eman ta zabal zazu

Universidad del País Vasco
Euskal Herriko Unibertsitatea

(cc)2022 FERMIN ANDONI ELIZALDE IRAIZOZ (cc by-nc-nd 4.0)

Summary

Thermoset materials are the main choice when high dimensional stability, great chemical resistance and good mechanical properties are a need. Nevertheless, their fixed crosslinked structure is the biggest obstacle to overcome once their lifetime reaches to the end. For this reason, novel molecular architectures tagged as covalent adaptable networks (CANs) have been proposed recently, and ideally combine the reprocessability of thermoplastics at high temperatures and the application requirements of thermosets. These new class of polymers contain dynamic bonds that can undergo exchange reactions to enable their correct recycling, reshaping or reprocessing. And not less interestingly, this dynamic chemistry adds self-healing properties to them.

Among all the different kind of polymers formulated as crosslinked materials, polyurethane (PU) is the bestseller of the market, as very versatile and different kind of products can be synthesized changing the initial reagents. For this reason, is essential to understand the potential dynamic character contribution of network dynamics, implemented exchangeable bonds, and the role of catalysts in this polymer family.

To provide context to this, **Chapter 1** offers an introduction to the main characteristics of CANs, from synthesis and exchange mechanisms, to rheological characterization and lifetime enlarging opportunities, highlighting the most important aspects and recent discoveries found in literature. Mainly, most of the reviewing work performed in this chapter has been focused in PUs. Finally, the potential application of this kind of networks in a smart application (self-healing electrolyte in Li-ion batteries) has been also disclosed.

Chapter 2 approached the synthesis and characterization of different aliphatic and aromatic PU networks, from non-catalyzed formulations to catalyzed ones. Their dynamic behavior was characterized by small molecular weight model reactions and rheology, attending to transcarbamoylation exchange reactions that may occur at mild-high temperatures. It has been proven that the introduction of different catalysts such as *p*-Toluenesulfonic acid (PTSA) and Dibutyltin dilaurate (DBTDL) has a tremendous importance to trigger urethane exchangeability in aromatic compositions, even promoting different exchange mechanisms.

To add dynamic character to aliphatic PU networks, in **Chapter 3** two alkoxyamine-based diols have been synthesized and introduced replacing different amounts of the non-dynamic chain extender employed in the Chapter 2. It has been proved that small modifications in the alkoxyamine structure can lead to bond dissociation energy variation and thus, the whole dynamic character of the network changes. Moreover, secondary reactions that may be present at certain conditions have been also analyzed.

In **Chapter 4**, another strategy has been used to trigger dynamicity in aliphatic polyurethane networks, in this case, to finally apply this formulation as self-healing electrolyte in Li-ion batteries. Hindered urea bonds (HUBs) have been introduced as crosslinking points by reacting a trifunctional bulky secondary amine with hexamethylene diisocyanate (HDI), to subsequently add polyethylene glycol (PEG) as conductive soft segment. The electrochemical performance of this membrane has been compared to commercially available Celgard® 2500 and afterwards, both electrolytes have been physically damaged and cycled. HUB-PU membrane shows

specific capacity values close to the ones obtained before the scratch, meanwhile the commercial separator has shown poor electrochemical performance at this stage.

To finish, **Chapter 5** holds the conclusions of the contributions achieved in this work, from understanding the importance of the employed synthetic strategy to the potential application of self-healing membranes in energy storage. In addition, a perspective on the implementation of the different compositions performed is given, revealing the advantages and drawbacks of each system. Although there is still way ahead, there is no doubt that further progresses must continue in this field in order to enable the design of more industrially scalable dynamic materials.

Laburpena

Material termoegonkorrak erabilienak dira dimentsio-egonkortasun altuko, erresistentzia kimiko handiko eta propietate mekaniko onak eskatzen dituzten aplikazioetarako. Hala ere, behin euren aplikazio bizitza amaierara iritsitakoan, euren elkargurutzatutako egitura finkoa gainditzeko beharra oztopo handia da. Honengatik, sare moldakor dinamiko (CAN, ingelesez) bezala izendatutako arkitektura molekular berriak proposatu dira azkenaldian, hauek tenperatura altuetako termoplastikoen birprozesaketa eta termoegonkorren aplikazio eskakizunak betetzeko gaitasuna idealki konbinatzen dituzte. Polimero klase berri hauek barne lotura dinamikoak dauzkate, trukaketa erreakzioak eman ditzaketenak, birziklapen, birmoldaketa eta birprozesaketa egokiak lortzeko asmoz. Azkenik, kimika dinamiko honek auto-konpontze propietateak gehitzen dizkiete.

Material elkargurutzatu bezala formulatzen diren polimero guztien artean, poliuretanoak (PU) merkatuan gehien saltzen direnak dira, izan ere, oso moldaerrazak dira eta mota desberdineko produktuak sintetizatu daitezke hasierako erreaktiboak aldatuz. Horregatik, potentzialki eduki dezaketen izaera dinamikoa ulertzeko berebizikoa da aditzea bai sare dinamikak, bai ezarritako trukaketa loturak, baita katalitzaileek eduki dezaketen papera polimero familia honetan.

Testuinguruan kokatzeko asmoz, **lehenengo kapitulua**k sare moldagarri kobalenteen propietate orokorren inguruko sarrera bat eskeintzen du, sintesi eta trukaketa mekanismoetatik abiatuz, karakterizazio erreologikora eta materialen bizitza luzatzeko aukeretara iritsi arte, azkenaldian literaturan publikatu diren aspektu garrantzitsuenak eta aurkikuntzak nabarmenduz. Bereziki, atal honetan egindako berrikuspen lan gehiena poliuretanoetan (PU) zentratua izan da. Azkenik, sare mota hauen erabilera

potentziala aplikazio adimentsu batean (elektrolito auto-konpongarria Li-ioizko baterietan) ezagutarazi da.

2. Kapituluak poliuretano (PU) saretu aromatiko eta alifatiko desberdinen sintesia eta karakterizazioa gerturatu ditu, katalizatzaile gabeko formulazioetatik hasita, katalizatuetaraino iritsiz. Euren izaera dinamikoa karakterizatua izan da bai pisu molekular txikiko erreakzio ereduekin eta baita erreologiarekin ere, tenperatura epel eta altuetan eman daitezkeen transkarbamoilazio trukaketa erreakzioetan zentratuz. Egiaztatua izan da, katalizatzaile desberdinen sarrerak, hala nola, azido *para*-toluen sulfonikoarenak (PTSA ingelesez) eta dibutiltin dilauratoarenak (DBTDL), berebiziko garrantzia dutela uretano loturaren dinamismoa bultzatzeko konposizio aromatikoetan, baita trukaketa mekanismo desberdinak sustatzeko gai direla ere.

Poliuretano alifatiko saretuetan dinamismoa garatzeko asmoz, **3. Kapitulua**n, alkoxiaminetan oinarritutako bi diol sintetizatu dira, eta aurreko kapituluan erabilitako kate-luzapen molekula ez dinamikoaren proportzio desberdinak molekula hauekin ordezkatu dira. Egiaztatu da, alkoxiamina hauen egitura molekularrean aldaketa txikiak egonik, loturaren disoziazio energia aldatzen dela eta ondorioz, sare osoaren dinamismoa aldatu daitekeela. Bestalde, baldintza zehatzetan agertu daitezkeen erreakzio sekundarioak ere karakterizatu dira.

4. Kapituluan, poliuretano alifatikozko sareetan dinamismoa sustatzeko bestelako estrategia bat erabili da, izan ere, bukaeran formulazio hau Li-ioizko baterietan auto-konpontze mintz elektrolitiko bezala erabili nahi izan da. Eragotzitako urea loturak (HUB, ingelesez), elkargurutzapen puntu bezala sartu dira, amina sekundario trifuntzional bat hexametilen diisozianatoarekin (HDI) erreakzionaraziz eta ondoren polietilen glikola (PEG) gehituz, azken honek segmentu bigun eroale bezala jarduten duelarik. Mintz honen propietate elektrokimikoak Celgard® 2500 mintz komertzialarekiko alderatu dira eta ondoren, bi mintzak moztu eta zikloak egiten jarri dira berriz. HUB-PU mintzak erakutsi dituen balioak, moztu aurretik erakutsitakoen gertukoak dira. Aldiz, puntu honetan, mintz komertzialak erakutsitako prestazio elektrokimikoak oso pobreak izan dira.

Amaitzeko, **5. Kapitulua**k lan honetan lortutako ondorio eta kontribuzioak nabarmentzen ditu, erabilitako estrategia sintetikoak daukan garrantzitik hasita, energia-biltegi aplikazioan erabili daitekeen auto-konpontze mintzeraino iritsiz. Gainera, garatutako konposizio desberdinek etorkizunean inplementatzeko daukaten aukeren ikuspuntua ere ematen da, sistema bakoitzaren alde onak eta txarrak azpimarratuz. Nahiz eta oraindik bidea dagoen egiteko, zalantzarik gabe garatzen jarraitu behar du arlo honek, industrialki eskalatu daitezkeen material dinamikoen diseinuan bideratzeko.

Table of content

Summary.. I

Laburpena... IV

List of Acronyms and Symbols XI

CHAPTER 1

Chapter 1: Polyurethane Covalent Adaptable Networks: State of the art 1

1.1 Polyurethanes (PUs): current market and applications **......... 1**

1.2 Polyurethane thermosets: molecular architecture, performance and end-of-life **5**

1.3 Covalent Adaptable Networks (CANs): Growing alternative to classic thermosets **... 10**

1.4 Covalent Adaptable Networks (CANs): Exchange mechanisms**11**

1.5 Rehological differences of classic thermosets, thermoplastics and CANs **13**

1.6 Essential elements to create effective Covalent Adaptable Networks (CANs) **15**

  1.6.1 Introduction of dynamic bonds into polyurethane networks 16

  1.6.2 Characteristics of the polymer network.. 23

  1.6.3 Common catalysts and their application in dynamic networks 28

1.7 Enlarging lifetime of CANs: from self-healing to reprocessing**30**

1.8 Application of self-healing materials as polymer electrolytes**32**

1.9 Objectives of this thesis**.. 33**

1.10 References **... 35**

CHAPTER 2

Chapter 2. Influence of catalysts in the dynamicity of polyurethane networks 47

2.1. Introduction 47

2.2. Results and discussion 50

- 2.2.1. Dynamic behavior of polyurethane thermosets 50
- 2.2.2. Exchange in catalyst free polyurethanes 52
- 2.2.3. Effect of the catalyst in the exchange reaction of aromatic and aliphatic polyurethanes 54
- 2.2.4. Model study of associative and dissociative exchange mechanisms in presence of PTSA and DBTDL catalysts 58

2.3. Conclusion 63

CHAPTER 3

Chapter 3. Introduction of alkoxyamine based diols to tune the dynamic behavior of aliphatic polyurethanes 71

3.1. Introduction 71

3.2. Results and discussion 74

- 3.2.1. Synthesis and characterization of different alkoxyamine based diols 74
- 3.2.2. Synthesis of aliphatic polyurethane network containing PV2 alkoxyamine 79
- 3.2.3. Effect of chemical structure and concentration of alkoxyamines in the dynamic behavior of aliphatic polyurethane thermosets 81
- 3.2.4. Reprocessing capabilities of alkoxyamine based polyurethanes 83
- 3.2.5. Limitations of synthesized alkoxyamine based polyurethane thermosets 85

3.3. Conclusion 87

3.4. References 88

CHAPTER 4

Chapter 4. Applying hindered urea bonds as self-healing poly(urea-urethane) electrolytes for Lithium Batteries 95

4.1. Introduction 95

4.2. Results and discussion.. 99

4.2.1. Synthesis of self-healable crosslinked poly(urea-urethane) network: HUB-PU network.................................99

4.2.2. Self-healing ability of HUB-PU network..100

4.2.3. Electrochemical characterization of gel-polymer electrolyte based on swollen HUB-PU network 102

4.2.4. Li-metal cells performance after mechanical damage and healing of the HUB-PU gel polymer electrolyte ...107

4.3. Conclusion.. 109

4.4 References 110

CHAPTER 5

Chapter 5: Conclusions and perspective........................ 118

Methods 120

Appendix... 131

Experimental section 159

Materials... 169

List of Publications 173

List of Acronyms and Symbols

®	Registered mark
°C	Celsius degree
^{1}H-NMR	Proton Nuclear Magnetic Resonance
ATR	Attenuated Total Reflectance
ATRA	Atom transfer radical addition
BDE	Bond Dissociation Energy
C	Coulomb
C-65	Carbon black powder
CAN	Covalent Adaptable Network
$CDCl_3$	Deuterated Chloroform
COSY	Homonuclear Correlation Spectroscopy
Cu	Copper
DA	Diels-Alder
DBTDL	Dibutyltin dilaurate
DBU	1,8-Diazabicyclo[5.4.0]undec-7-ene
DEC	Diethyl carbonate
DFT	Density Functional Theory
DMSO-d_6	Deuterated Dymethyl sulfoxide
DMTA	Dynamic Mechanical Thermal Analysis
$E_{(t)}$	Relaxation Modulus
$E_{(0)}$	Initial Modulus
E_a	Activation Energy
EC	Ethylene carbonate
ECC-std	Electrochemical test cell for two-electrode battery testing
EPR	Electron Paramagnetic Resonance
eq.	Equation
equiv.	Equivalent
ESW	Electrochemical Stability Window
FTIR	Fourier-Transform Infrared Spectroscopy
g	Gram
G´	Storage Modulus
h	Hour
H_{12}-MDI	Dicyclohexylmethane-4,4'-diisocyanate
HCl	Hydrochloric acid
HDI	Hexamethylene diisocyanate
HDO	1,6-Hexanediol
HUB	Hindered Urea Bond
Hz	Hertz
IPDI	Isophorone diisocyanate

K	Kelvin degree
KCal	Kilocalories
kDa	Kilodalton
kJ	Kilojoule
LFP	Lithiium-iron-phosphate
Li	Lithium
LIB	Lithium Ion Battery
$LiPF_6$	Lithium hexamfluorophospate
N_2	Nitrogen
NMP	N-methyl-2-pyrrolidinone
mA	Milliamp
MALDI	Matrix-Assisted Laser Desorption/Ionization
m-CPBA	meta-Chloroperoxybenzoic acid
MDI	4,4′-Methylene diphenyl isocyanate
mg	Miligram
min	Minute
mm	Milimeter
M_n	Number-average molar mass
MS	Mass spectometry
MSA	Methanesulfonic Acid
M_w	Weight-average molar mass
NaOH	Sodium Hydroxyde
NCO	Isocyanate
Pa	Pascal
PEG	Polyehylene glycol
PET	Polyethylene terephtalate
PHU	Poly(Hydroxy Urethane)
PTSA	p-Toluenesulfonic acid
PPG	Polypropylene glycol
ppm	Parts per million
PU	Polyurethane
PVDF	Poly(vynilidenedifluoride)
RT	Room Temperature
s	Second
S	Siemens
SEC	Size Exclusion Chromatography
SPE	Solid Polymer Electrolyte
τ	Relaxation time
TBD	1,5,7-triazabicyclo[4.4.0]dec-5-ene

TDI	Toluene diisocyanate
TEA	Triethylamine
T_g	Glass Transition Temperature
THF	Tetrahydrofuran
T_m	Melting Temperature
TOF	Time of flight
TPU	Thermoplastic Polyurethane
T_v	Freezing Transition Temperature
UPV/EHU	University of the Basque Country
V	Volt
ZPVE	Zero-point vibrational energy

Chapter 1

Chapter 1: Polyurethane Covalent Adaptable Networks: State of the art

1.1 Polyurethanes (PUs): current market and applications

Discovered 85 years ago by Otto Bayer, polyurethanes have become a class of materials that has versatility as their main property[1]. Due to their chemical and morphological structure, polyurethanes are one of the few classes of polymers that can act as thermoplastic, elastomeric, and thermoset materials[2].

Industrially available polyurethane based materials are synthesized by reacting polyisocyanates and polyols, giving as a result carbamate groups within the polymer chain, but can be also included in this polymer family other related materials synthesized using other nucleophiles (such as polyureas by reaction of amines with isocyanates)[3]. Additionally, several reactions may occur with high reactive isocyanate groups at different conditions (high temperatures, moisture…)[4]. Moreover, Polyurethanes (PUs) have a segmented structure that cannot be found in other polymer families. The hard segments are composed of rigid molecular groups such as urethane, urea and trimers. Less frequently, biuret and allophanate groups also can be part of the hard part of PUs. On contrary, soft segments are constituted by flexible (and entangled) polyether or polyester polymers. The combination of this segmented structure and the highly tunable chemisty make polyurethanes to fit a wide variety of applications. Different pathways can be followed to obtain the final polyurethane material, and normally the direction taken is driven by the target application. For this reason, the correct choice of the following components becomes crucial.

First of all, PUs properties and nature depend on the building blocks, thus, the initial reactants. Herein, we find isocyanates, which react with polyols and small molecular weight nucleophiles. These isocyanates can be cycled aliphatic, such as H_{12}-MDI or IPDI, or linear, being HDI the most well known compound. Nevertheless, aromatic isocyanates are more reactive than the aliphatic analogs, being MDI and TDI industrially the most employed ones[5].

Isocyanates react easily with most of the nucleophiles. In order to adquire a flexible and resistant material, these compounds react with polyols. Also, diols, diamines and similar small molecular weight nucleophiles are add it to polyurethane formulations as chain extenders.

The reaction of isocyanate and nucleophiles is speed up industrially. Normally organotin catalysts are added to industrial formulation in part per million (ppm) scales, increasing the reactivity and lowering the temperatures required for the carbamate formation. Organocatalysts have been also employed as a greener alternative for polyurethane synthesis[6]. The discussion about the types of catalysts will be more deeply discussed in the section *1.6.3 Common catalysts and their application in dynamic networks*.

Finally, PUs can be synthesized as crosslinked or not crosslinked materials. If the target application demands the high dimensional stability of covalently crosslinked networks, trifunctional or even more functional isocyanates and nucleophiles are introduced.

As can be seen in Scheme 1, for most of the applications where polyurethane materials are applied, high solvent resistance, great mechanical properties and good resistance are required. These properties can be only achieved when materials are covalently crosslinked, forming fixed polymer networks. For this reason, this family of polymers is predominantly thermoset materials. Thermoplastic polyurethanes (TPUs) are just formulated in few applications, such as adhesives (hot-melt adhesives) and TPU elastomers (trainers).

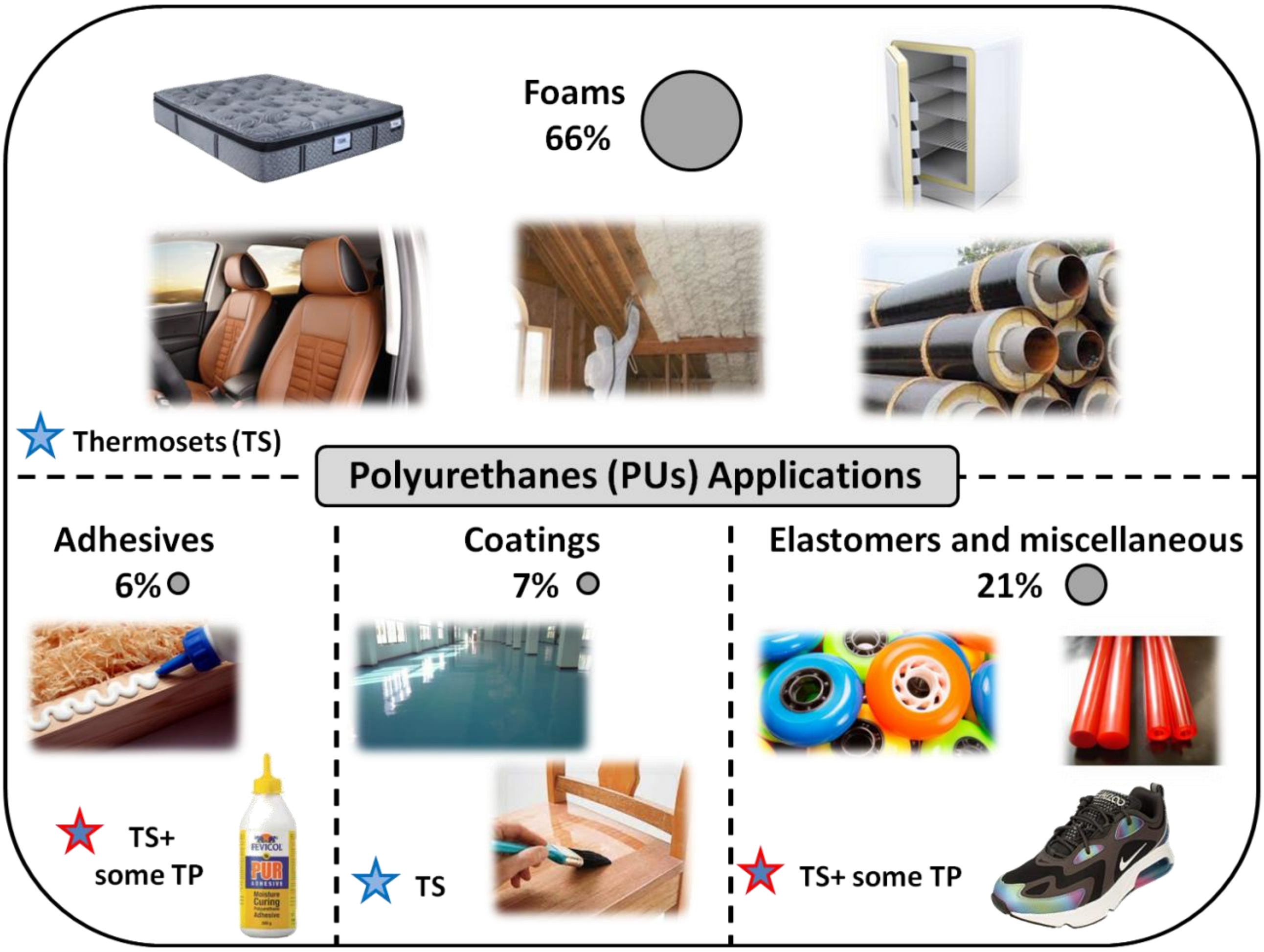
Foams
66%
Thermosets (TS)
Polyurethanes (PUs) Applications
Adhesives
6%
Coatings
7%
Elastomers and miscellaneous
21%
TS+
some TP
TS
TS+ some TP

Scheme 1. Main polyurethane (PU) applications where foams (rigid and flexible) represent the largest group among adhesives (6%), coatings (7%) and elastomers (around 20%).

This synthetic flexibility gives us multiple possible applications, such as high abrasion resistant coatings, skate wheels, adhesives, pipe and building insulating foams to mattresses and trainers. Main polyurethane applications can be found in Scheme 1, with industrial examples shown in pictures. Clearly, PU thermosets are preferred in all kind of applications. Their importance is hughe, as foams and coatings are totally formulated as cured materials. In the case of elastomers, just around 25% are thermoplastic elastomers, and in the case of adhesives, only hot-melt adhesives are produced from TPUs[7].

As abovementioned, foams are the first kind of polyurethane thermosets. Can be formulated as rigid or flexible, and they represent the largest group (around 66% of total PU production) among adhesives, coatings, elastomers and others (Scheme 1). To produce the foaming, water reacts with isocyanates giving carbamic acid[5]. This unstable compound rapidly decomposes in amine and CO_2. Amines finally react giving ureas and the carbon dioxide works as blowing agent. Flexible foams have been used for example in mattresses, cushions and seats in automotive industry. But lightweight structures are highly demanded nowadays, moreover taking into account actual requirements of energy and resource efficiency. As an example, rigid foams are particularly interesting for constructing industry, refrigerators and piping/tubing industry. These close cell materials are particularly interesting as insulator materials and as consequence, big amounts of energy are saved every year. To obtain these rigid foams, MDI is the most employed isocyanate in industry, combined with polyether/polyester polyols[8].

Next application where PU crosslinked materials represent the majority is in adhesive application. Polyurethane based adhesives are well known due to their good bonding strength. Industrially, can be formulated as single component (moisture curing), or dual component adhesives. Taking into account the versatility of PU chemistry, the landscape of PU adhesives includes different materials such as construction sealants with high elongation at break, two component (2C) and windshield-type adhesives with medium elongation at break values and also high strength 2C PU adhesives and crash performing Epoxy/PU hybrids (low elongation)[7,9].

Cured polyurethanes are able to achieve great chemical resistivity, good adhesion, low temperature flexibility and high abrasion resistance that make this family of polymers suitable for coating applications[10]. PU coatings are more elastic and softer than epoxy coatings, keeping their mechanical properties and flexibility at low temperatures, and hence, making them more durable. Polyurethane coatings have been also tailor made adding anticorrosive properties[11].

Last but not least, we find the last application where polyurethanes are preferentially synthesized as networks. Elastomers (about 20% of global PU consumption) have accompanied polyurethanes ever since their discovery in 1937 by Otto Bayer, and they achieve an optimum set of physical properties required for any kind of application. Around 40% of PU elastomers are cellular elastomers, being footwear elastomers the most produced group of this kind. The remaining 60% are solid elastomers were cast elastomers, thermoplastic (TPU) elastomers, elastomeric fibers and synthetic leader are quite equally produced and are followed by spray elastomers (highly reactive blends) and RIM (reaction injection molding) elastomers[12].

It is worthy to mention that casting have been the basic technology underlying both solid and cellular elastomers. This manufacturing method can be divided in hot casting (over 60°C), cold casting (ambient temperature) and rotational casting systems.Cast elastomers include in their formulation isocyanates, polyols, chain extenders and additives[10].

Ascan be noticed from Scheme 1, most of the applications shown in this section require very versatile crosslinked materials. Thermoplastic polyurethanes (TPUs) are also employed, but they only represent a small percentage inside of total polyurethane production.

1.2 Polyurethane thermosets: molecular architecture, performance and end-of-life

As previously mentioned, thermosets offer significant benefits regarding mechanical properties and solvent resistance compared to thermoplastic materials, as a consequence of their crosslinked structure. Thus, their industrial relevance is more than understandable.

As can be seen in Scheme 2, in the case of polyurethane networks different components are highlighted in three main groups.

Generally speaking, to obtain this fixed molecular architecture, different reactants, catalysts and processing methods should be correctly followed to obtain the final crosslinked material. Commonly, in PU preparation reactants are mixed in liquid state. When the system is cooled, hard segments aggregate and link due to the weak hydrogen bonds, forming two separate phase system. The quantity and nature of the segmentation becomes crucial for the final properties of the PU material.[10]

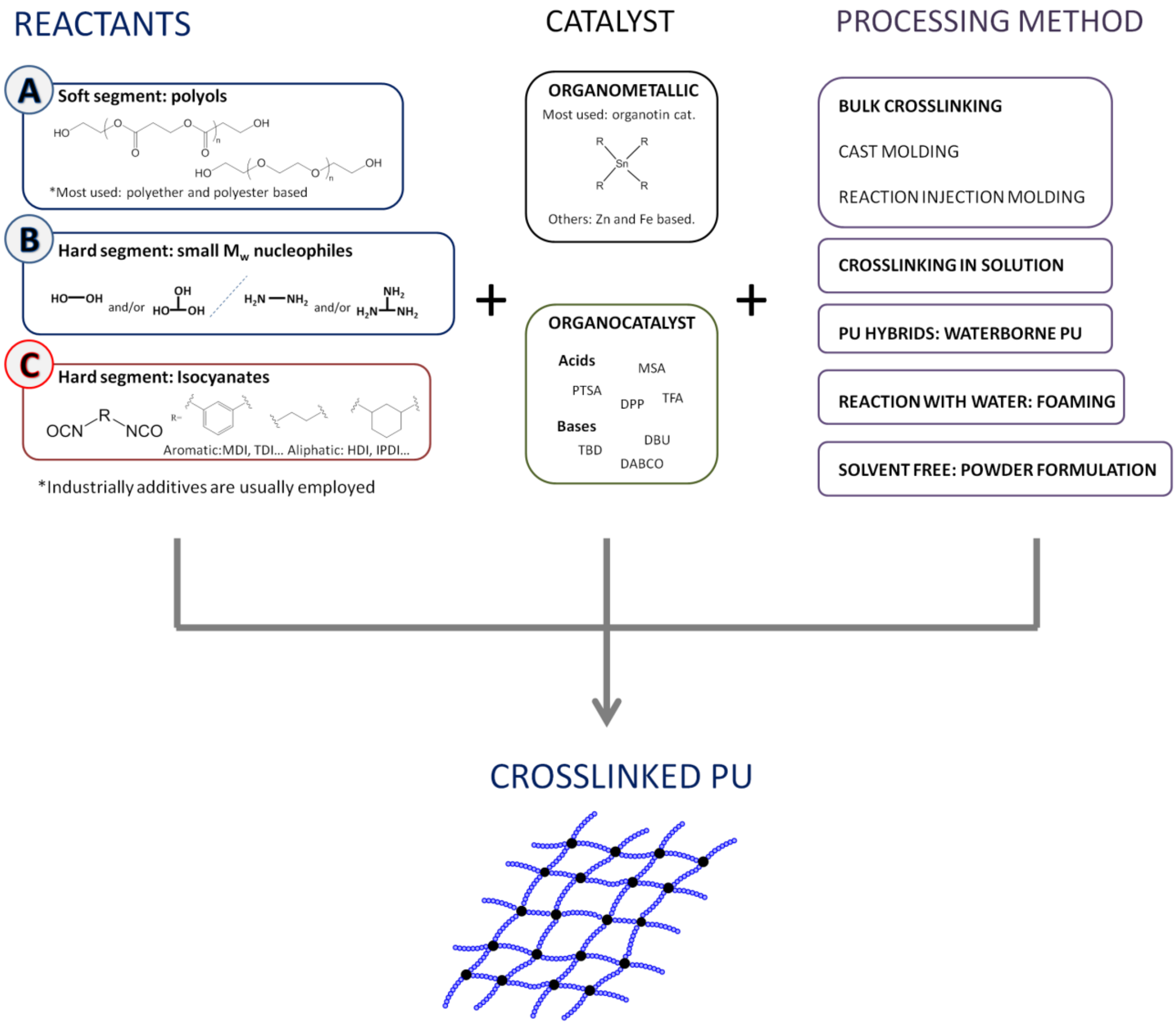
REACTANTS
CATALYST
PROCESSING METHOD
A
Soft segment: polyols
HO
OH
O
n
*Most used: polyether and polyester based
B
Hard segment: small M_w nucleophiles
HO—OH
and/or
HO
OH
OH
H_2N—NH_2
and/or
H_2N
NH_2
NH_2
C
Hard segment: Isocyanates
OCN
R
NCO
Aromatic:MDI, TDI... Aliphatic: HDI, IPDI...
*Industrially additives are usually employed
+
ORGANOMETALLIC
Most used: organotin cat.
R
Sn
Others: Zn and Fe based.
ORGANOCATALYST
Acids
MSA
PTSA
DPP
TFA
Bases
TBD
DBU
DABCO
+
BULK CROSSLINKING
CAST MOLDING
REACTION INJECTION MOLDING
CROSSLINKING IN SOLUTION
PU HYBRIDS: WATERBORNE PU
REACTION WITH WATER: FOAMING
SOLVENT FREE: POWDER FORMULATION
CROSSLINKED PU

Scheme 2. Common reactants, catalysts and processing methods employed in polyurethane thermoset synthesis. Depending on reactant, catalyst and additives different kind of networks can be obtained.

First, reactants are classified according to their reactivity and position in the polyurethane backbone. As abovementioned, PUs contain hard and soft segments. Polyols, commonly based on polyether or polyester chains, represent the more flexible part of the polyurethane. These compounds react with the boundary reactant of the hard segment; diisocyanates. Industrially, aromatic isocyanates are preferred to aliphatic due to their higher reactivity[13]. The other essential group of reactants of the hard segment is the chain extender, small molecular weight nucleophiles such as diols, diamines or similar reactants with even higher functionalities that act as crosslinking points[14].

Second, catalytic compounds are industrially employed to accelerate network formation, assure complete isocyanate/nucleophiles reaction and as a consequence, increase network stability[2]. Mainly, catalysts can be divided into two different groups. On the one hand, organometallic catalysts are employed industrially due to their high reactivity and required small quantities (generally, parts per million). However, the toxicity and inability to be separated from the final polyurethane material is understood as an environmental risk that should be deleted. For this purpose, organocatalysts have been studied more recently and different acids and bases have shown their catalytic effectiveness for the urethane formation[15]. In this case, higher catalytic quantities are required.

Finally, the processing method to acquire the ultimate cured material is also relevant. Mostly, bulk crosslinking is employed industrially, where cast molding is the preferred option. Nonetheless, reaction injection molding (RIM) is another processing method to obtain polyurethane materials with well defined shapes[16]. Other processing methods are crosslinking in solution, where high volatile solvents are used and solid content is around 25%[12].

However, their permanent molecular structure is also their main drawback, as classic thermosets are static materials that cannot undergo any processing once are totally cured[17].

Thus, reprocessing of thermosets has become the main issue of this class of materials. In the case of these classic permanent networks, once they are polymerized they become unable to flow upon heating as thermoplastics do when they melt. Their remolding, reshaping and reprocessing is impossible and principally are discarded once the materials life is over[18]. Thus, classic thermosets offer high performance but cannot undergo thermal treatments such as those required for mechanical recycling. As a result, it is uniqueness to develop methods to obtain their chemical reversion[19,20].

In the case of classic polyurethane thermosets, glycolysis is the only recycling method applied industrially among hydrolysis and aminolysis. Nevertheless, this process requires temperatures up to 200°C, and high molecular-weight polymers are broken to small molecules with free OH groups. Finally, these compounds can be mix with other polyols and polyisocyanates[8]. The last alternative to avoid the arrival of polyurethane waste to landfill is the energy recovery. The heat content of PUs varies between 24 and 30 MJ kg^{-1}, and is comparable to coal. This is actually the last opportunity to somehow obtain some benefits at the end-of-life of polyurethane thermosets[10].

For this purpose, two different alternatives appear as future solutions with a common quality. On the one hand, chemical recycling represents one of the upcoming alternatives. This process can be given in order to permanently break crosslinked molecular structures, recovering initial monomers to recreate equal original materials. More interestingly, different, new building units can be obtained in some cases, novel monomers with higher added value that could lead to innovative polymers[21]. This last alternative is widely known as upcycling[22]. Nevertheless, for several reasons, the implementation of chemical recycling of thermosets represents a major challenge in comparison with its application in thermoplastic polymers. Commonly, chemical recycling requires solvents, catalysts, reactants and in most of the cases high temperatures to depolymerize polymer chains. These temperatures are often compulsory for the activation of catalysts, nucleophiles and not less important, to melt targeted polymers creating a homogeneous media. In thermosets, this process is hindered due to the higher solvent resistance and lack of melting of crosslinked materials in comparison with thermoplastics.

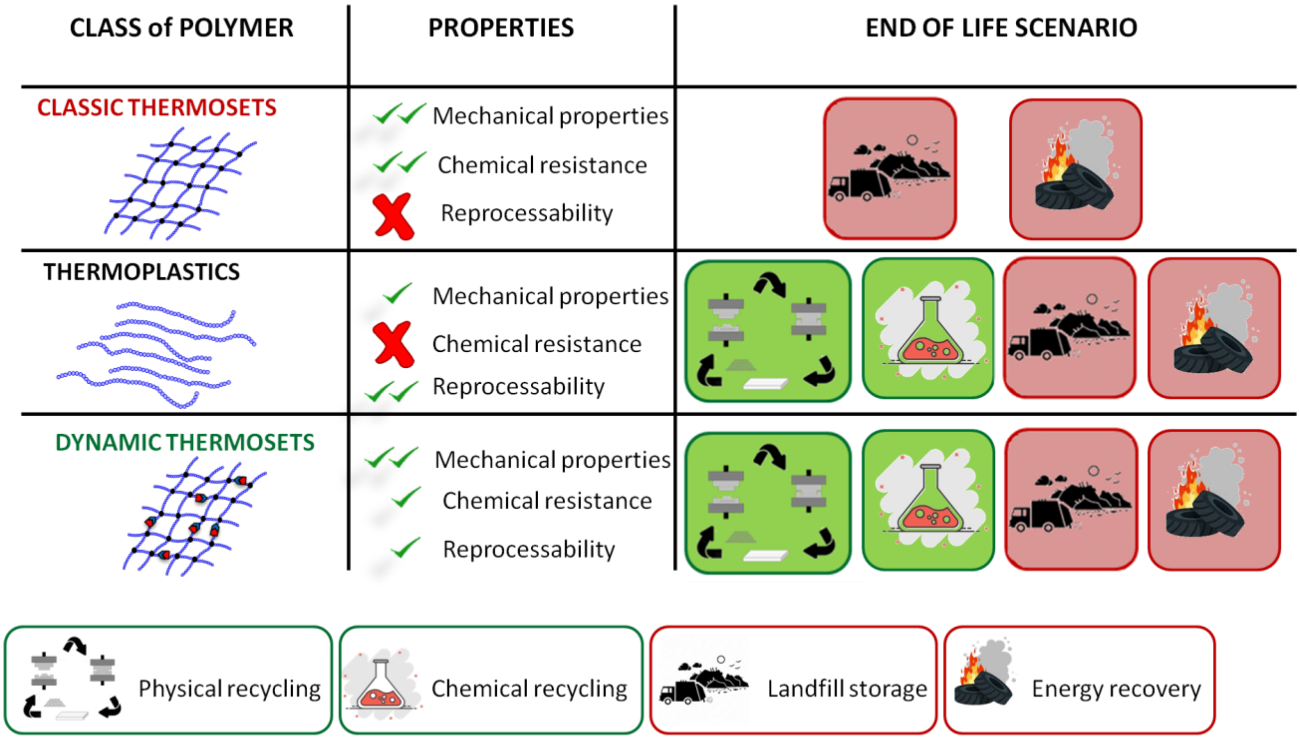
CLASS of POLYMER
PROPERTIES
END OF LIFE SCENARIO
CLASSIC THERMOSETS
✓✓ Mechanical properties
✓✓ Chemical resistance
✗ Reprocessability
THERMOPLASTICS
✓ Mechanical properties
✗ Chemical resistance
✓✓ Reprocessability
DYNAMIC THERMOSETS
✓✓ Mechanical properties
✓ Chemical resistance
✓ Reprocessability
Physical recycling
Chemical recycling
Landfill storage
Energy recovery

Scheme 3. Properties and end of life scenario recycling alternatives for each class of polymers: classic thermosets, thermoplastics and dynamic thermosets or CANs.

As shown in Scheme 3, abovementioned recycling alternatives are available for thermoplastic polymers but also for an emerging new class of polymers that combines the mechanical properties and chemical resistance of classic thermosets but keeping the open door for reprocessability. These novel materials are known as covalent adaptable networks (CANs) and have been defined by Bowman and Kloxin[23], as crosslinked materials with sufficient reversible covalent bonds into polymer networks to respond chemically to an applied stimulus. Thus, these new class of materials are able to change their physical structure, state and/or shape of the network.

This new concept brings new possibilities to PU thermosets such as the capacity of being reprocessed and to recover from damage. In most cases, mild-high temperatures and pressure are employed to rapidly reprocess[24]. In some cases, catalysts also improve the recyclability of the networks, as explained in the section below. Not less important, CANs will present self-healing characteristics that can provide the opportunity to enlarge the lifetime of the material without removing it from the application site[25]. To be able to carry out physical recycling with CANs is the main advantage in comparison with classic thermosets, which cannot be recycled and are usually discarded in the landfill or used for energy recovery. Overall, physical recycling of CANs provides a faster and less expensive recycling alternative.

1.3 Covalent Adaptable Networks (CANs): Growing alternative to classic thermosets

As shown in Scheme 4, substantial differences can be found between classic thermosets and covalent adaptable networks (CANs). Non dynamic crosslinked materials (Scheme 4 A), due to their static architecture, even when a stretch is applied there is not a topology change. Alternatively dynamic networks contain, apart from fixed crosslinking points, exchangeable bonds across the polymer backbone. For the correct activation of the dynamic network several requirements should be fulfilled. As shown in Scheme 4 B, mechanical activation of the material is needed to reshape the network. But, in order to allow the correct chain mobility and bond activation, at least higher temperatures than the T_g of the materials are required. As a result of the stretching of the material, CANs rearrange in the direction of the major stretching forces, and therefore plastic deformation[26] is achieved.

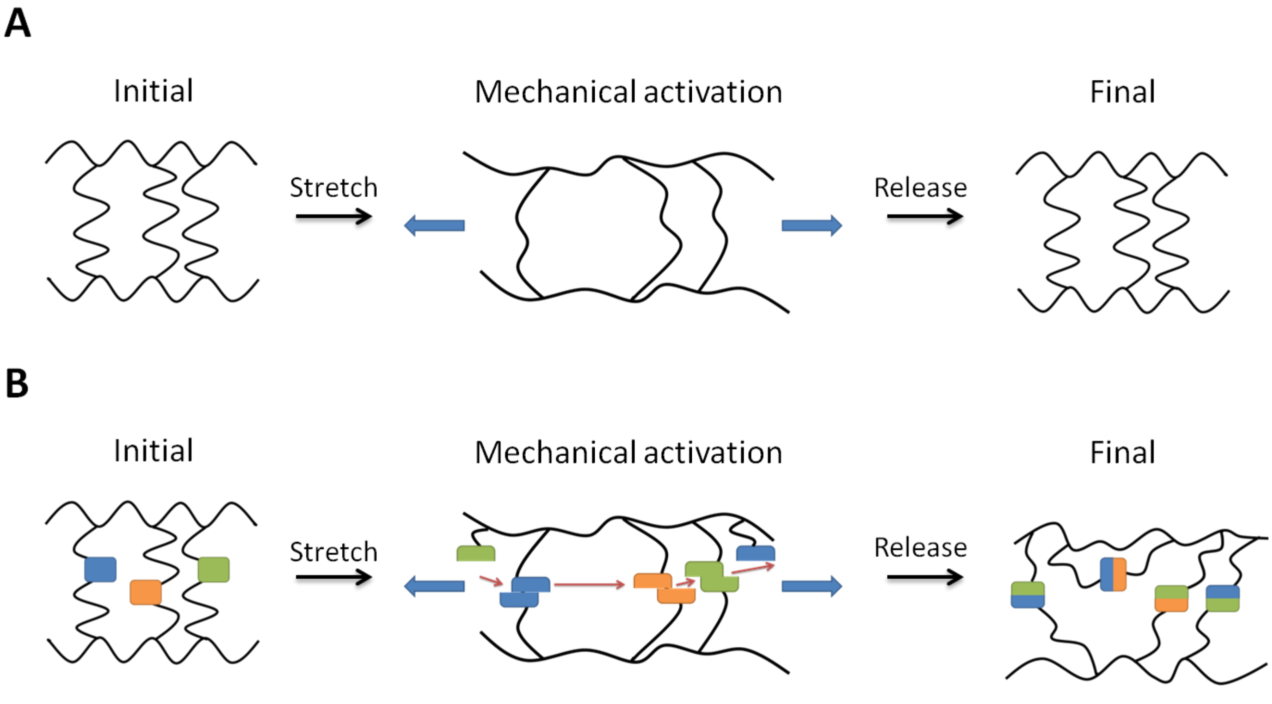

Scheme 4. Representation of network rearrangement process when strained in non dynamic or classic thermosets A) and covalent adaptable networks (CANs) B).

1.4 Covalent Adaptable Networks (CANs): Exchange mechanisms

The main difference between a dynamic thermoset in comparison with a classic thermoset is that exchangeable bonds are able to trigger plastic deformation of the network. Normally this reshaping occurs at mild-high temperatures, and usually these dynamic bonds are included into the formulation[27].

One of the most employed orderliness to classify dynamically crosslinked materials is according to the exchange reaction mechanism that undergoes the reactive group for the reprocessing/self-healing process. In fact, distinctive differences are supposed between each class of exchangeable groups, in terms of controlling the reprocessability conditions upon heating[28]. Mostly, the state of the art is focused on highlighting associative and dissociative materials, but some recent reviews[29] and experimental works has also detailed the dissociative/associative exchange mechanism given in radical mediated reactions.

In the associative case, as can be seen in Figure 1 A, free groups present in the network are able to react with the functional groups of the polymer backbone before the old linkage is broken. Once this step is given and new bone is formed, the old bond breaks forming a new free group, which can subsequently continue with exchange reactions. In these associative rearrangements, the crosslinking density of the network remains permanently fixed. For this reason, the decrease of viscosity is gradual and these kinds of materials are also known as *vitrimers*[17,18].

In the case of dissociative exchange reactions (Figure 1 B), the rearrangement process takes place by first breaking/opening the old bond, and later these newly formed stable free groups are able to react with other free groups to effectively finish the recombination step. In the majority of the cases, to trigger this exchange, heating up to mild-high temperatures is necessary to enable sufficient dissociation and chain mobility to effectively reprocess or self-heal materials. In some cases, also light has been needed. If we compare this exchange mechanism with the associative one, the main disadvantage that we face is when high temperatures are used for shifting dissociative equilibrium to the open state site, because at this point, dynamic materials can suffer the lost of network integrity and thus, giving a radical drop of the viscosity and affect the reprocessing[28]. On the contrary, the creep resistance of dissociative materials is intended to be better than in associative ones, taking into account that at low temperatures the dissociative bond equilibrium is shifted to the dormant state.

The last mechanism that can be found in CANs is the dissociative/associative one (Figure 1 C), which involves both steps described in just mentioned pure dissociative and pure associative exchanges. Mostly, this kind of exchange is given in radical mediated reactions. In the first step, bond dissociation is given and active species are formed. Following, these groups are able to exchange with the neighbor groups *via* the associative step. Overall, the network dynamics in this type of rearrangement depends on the contribution of the first step[29].

Therefore, each type of chemistry should be selected depending on the reprocessing conditions and application of the material. It is not a secondary matter to regard carefully about this, taking into account that avoiding unwanted secondary reactions is also one of the actual challenges remaining in network recycling.

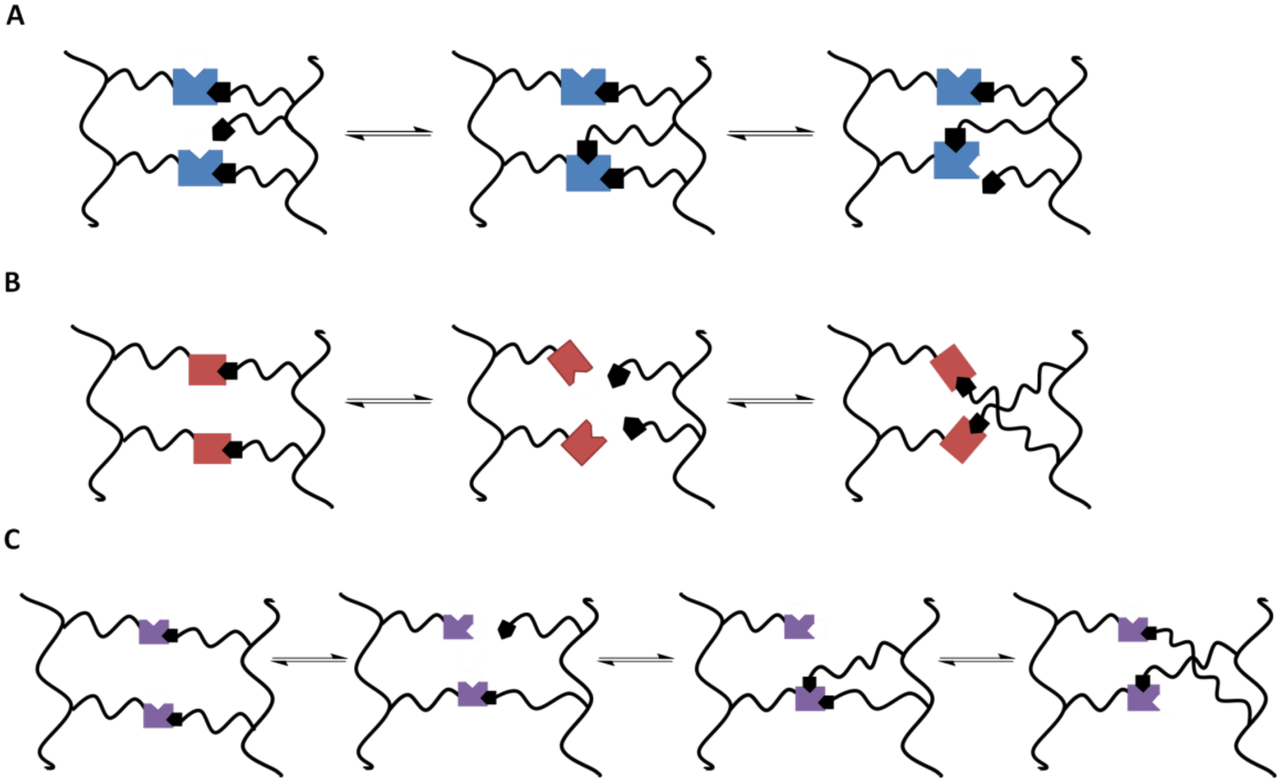

Figure 1. Representation of different dynamic exchange mechanisms that can follow covalent adaptable networks (CANs). A) Associative exchange. B) Dissociative exchange. C) Dissociative-associative exchange, mostly given in radical mediated reactions.[29]

1.5 Rehological differences of classic thermosets, thermoplastics and CANs

Most research works focused on this topic include stress-relaxation measurements to understand the dynamicity of CANs. In these transient measurements, samples are in a constant strain, and the decrease of stress is measured during time. Thus, this kind of measurement explains how polymers relieve stress under continous strain[30]. The relaxation of a material depends on the temperature applied and how is applied (isothermal or non-isothermal). Commonly, in stress-relaxation measuremnts of CANs, different isothermal are performed with the material, and upon increased temperature, relaxation is shifted to shorter times[24]. This is a consecuence of higher chain mobility and the enhancement of rearrangement kinetics.

Up to now, the reprocessability of dynamic networks has been linked entirely to the temperature dependence of relaxation times. To obtaine relaxation times (τ), normalized stress-relaxation data is taken ($E(t)/E_0 = f(t/\tau)$) and values are estimated based on the Maxwell model for viscoelastic fluids at $E(t)/E_0 = 1/e$. Adquired values follow an Arrhenius dependence, $\tau\,(T) \approx e^{\frac{E_{a\tau}}{RT}}$, and activation energy ($E_{a\tau}$) is measured[28].

These stress-relaxation values can be tuned or modified by changing different variables such as dynamic bond concentration, network architecture or added catalyst load and nature. These alternatives to shift relaxation times to shorter (or even longer) times will be discussed in the next section, as they represent important factors in order to obtain effective dynamic networks.

As can be seen in Scheme 5, stress-relaxation times really differ between each class of polymeric materials. In the case of thermoplastic materials, above T_g, a fast decay in the relaxation moduli is expected as chain movement is totally facilitated. In the case of classic thermosets, the fixed crosslinked structure makes impossible the chain reorganization in the force direction; thus, a constant value of the relaxation moduli is measured along measurement time. CANs, otherwise, as the molecular structure is not totally fixed due to the dynamic linkages, chain mobility is not totally restricted and are able to reorganize when the constant strain is applied. As a consequence, a relaxation moduli decay is obtained.

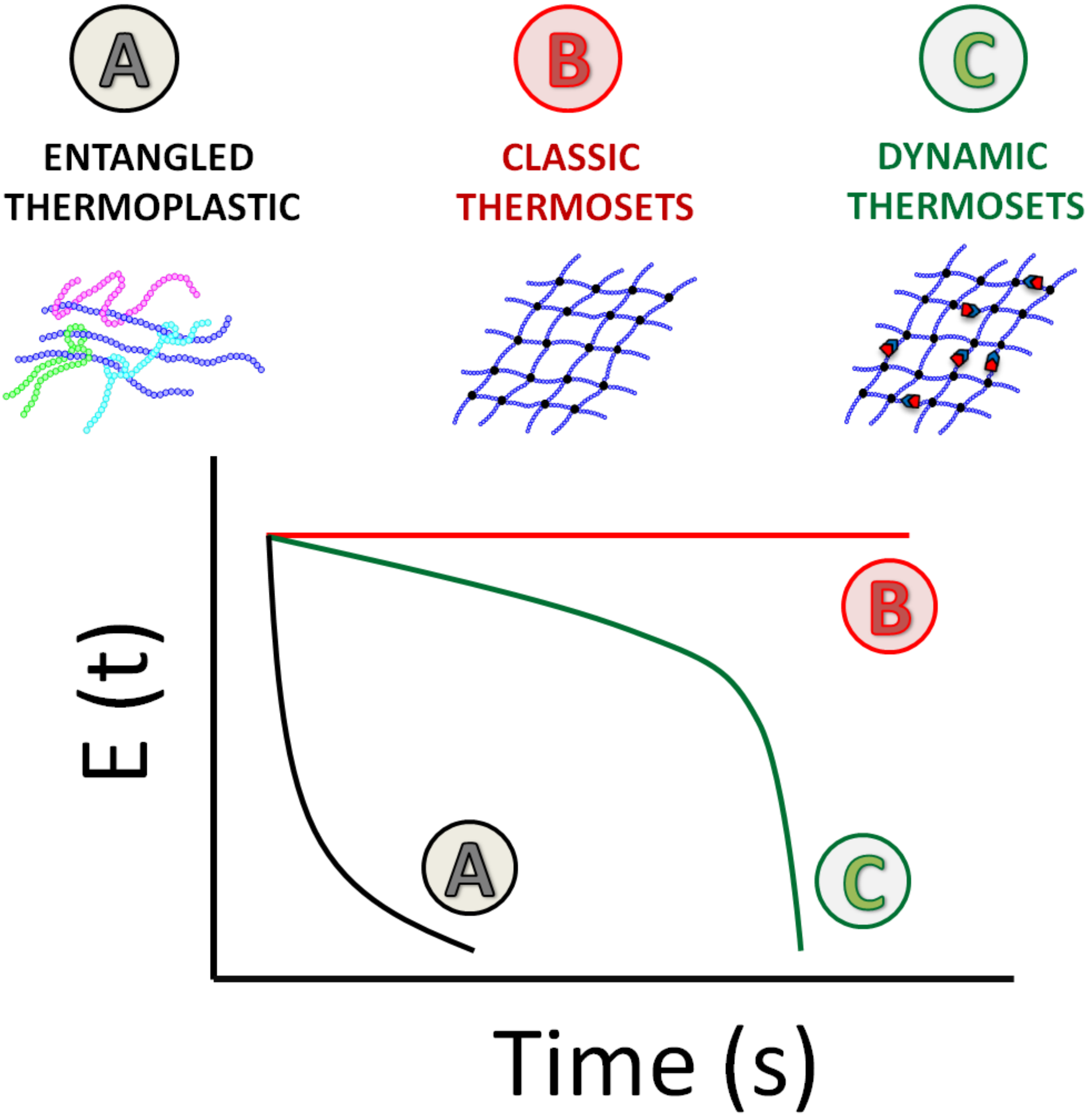
A
ENTANGLED THERMOPLASTIC
B
CLASSIC THERMOSETS
C
DYNAMIC THERMOSETS
E (t)
Time (s)
B
A
C

Scheme 5. Representation of stress-relaxation measurements for A) thermoplastics B) Classic thermosets and covalent adaptable networks (CANs) C).

1.6 Essential elements to create effective Covalent Adaptable Networks (CANs)

In order to produce CANS different elements have to be considered:

- Introduction of dynamic bonds
- Characteristics of the polymer network
- Effect of present catalyst

The proper combination of these elements leads to obtain dynamic networks with optimum relaxation times. In this section, first, the introduction of dynamic bonds into polymer networks will be discussed according to their exchange mechanisms. Note that the different exchangeable chemistries shown herein are the ones applied in polyurethane networks. Other dynamic bonds can be found in literature, but will not be added to this discussion. With the same purpose, when characteristics of polymer networks are explained, polyurethane networks will get most of our attention. Finally, the introduction of different catalysts and their importance will be analyzed predominantly for the most relevant and industrially produced thermosets.

1.6.1 Introduction of dynamic bonds into polyurethane networks

The main characteristic of CANs is the presence of certain groups that are susceptible to suffer exchange reactions. Therefore, one of the most straightforward strategies to provide dynamism is the incorporation of dynamic groups in the polymer network.

Bowman and coworkers have highlighted that reversible bonds and their incorporation to networks should be taken into account simultaneously[24]. This incorporation can be given in two different manners. Using reversible chemistry as crosslinking chemistry is the first option to create dynamic linkages in the polymer backbone. This alternative is particularly interesting due to the different set of network architectures that can be achieved[24]. This strategy takes advantage of preexisting bonds (*i.e.* urea and urethane groups) to achieve the desire dynamism (Scheme 6, strategy A and A´).

On the other hand, the incorporation of polymerizable monomers that contain the dynamic linkage in the monomer backbone represents a more versatile alternative. This allows new recombination mechanisms not commonly present in day-to-day polymers (Scheme 6, strategy B).

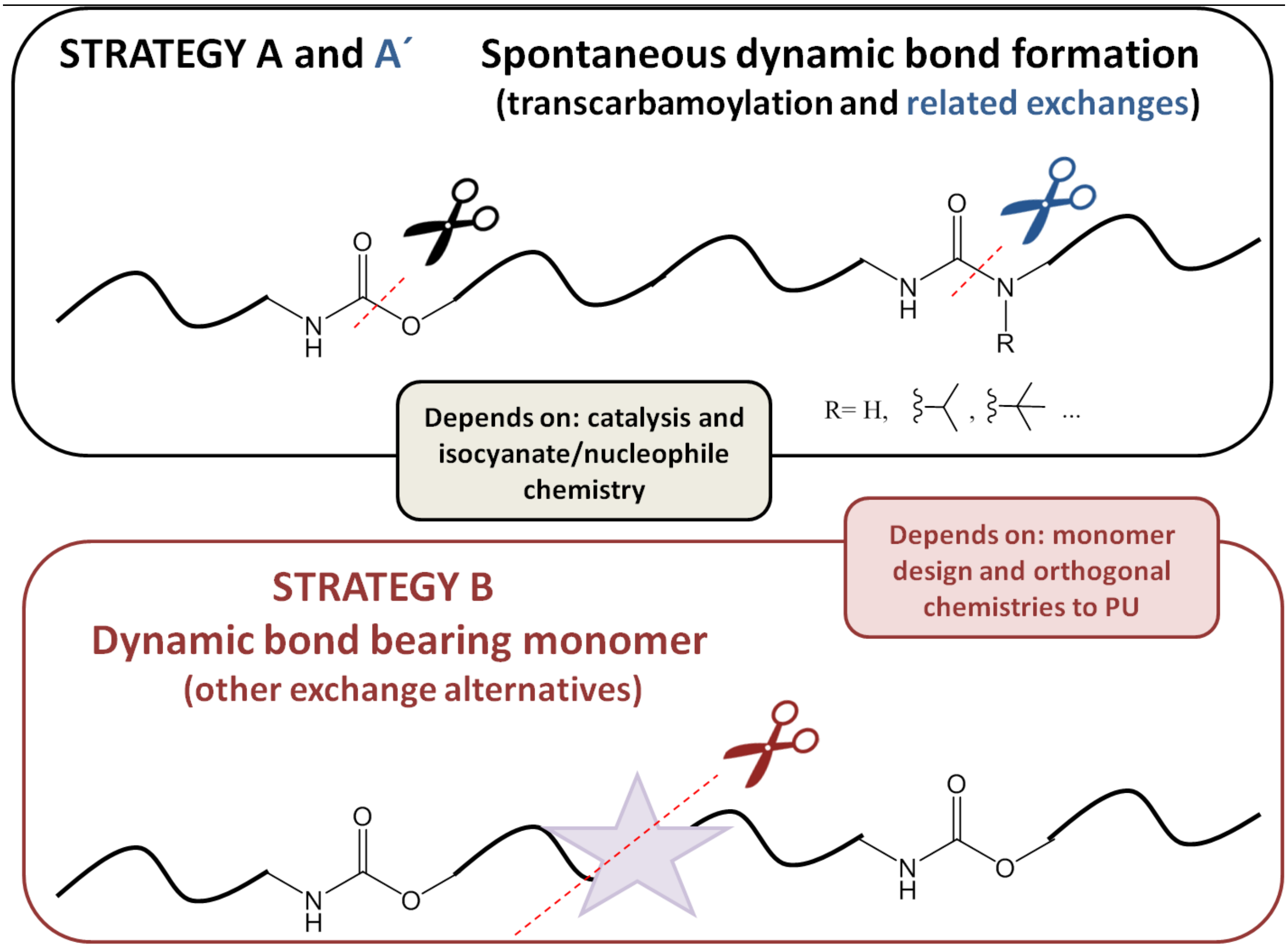
STRATEGY A and A´
Spontaneous dynamic bond formation
(transcarbamoylation and related exchanges)
O
N
H
O
O
N
H
N
R
Depends on: catalysis and isocyanate/nucleophile chemistry
R= H, ...
Depends on: monomer design and orthogonal chemistries to PU
STRATEGY B
Dynamic bond bearing monomer
(other exchange alternatives)
O
N
H
O
O
N
H
O

Scheme 6. Synthetic strategies in polyurethane covalent adaptable networks. In the strategy A (top side), urethane bonds creating reactive groups are shown as potential dynamic groups for transcarbamoylation and related exchange reactions. In the bottom side, strategy B, where most common orthogonal chemistries to urethane exchanges are shown.

Regarding strategy A and A´, researchers from all over the world focus their efforts in the understanding of the dynamicity of poly (urea-urethane) materials[31]. Last works suggest that some excess of aromatic amines can increase amine/urea exchange in poly(urea-urethane) materials when are hot-pressed at 160°C for 1 hour, under pressure[32,33]. Although amine/urea exchange has worked effectively, next steps related to this chemistry were given looking for lower exchange temperatures.

Recently, Cheng and coworkers found the dynamic nature of hindered urea bonds (HUB), and their work was focus analyzing how the use of different bulky alkyl parts affect the bond dissociation equilibrium in molecular model reactions. They select t-butylamino groups as the most promising bulky substituent for the development of poly(hindered urea/urethane) networks. Clearly, bulky substituents can weaken amide bonds breaking the conjugation effect between the lone electron pair on the nitrogen atom and the π-electrons on the carbonyl p-orbital. The next step in this work was to introduce N,N'-di-tert-butylethylenediamine in polyurethane network, demonstrating remarkable self-healing properties after 12 hours at 37°C[34].

This effect does not occur in classic urea bonds, where the general amide bond has remarkable stability due to the aforementioned conjugation effect[35,36].

In order to corroborate this hypothesis, experimental results have been compared to density functional theory (DFT) calculations carried out in one of the latest reviews published about these exchangeable bonds. Zhang and coworkers have shown that the free energy of the formation of classic urea bond from -NH_2 is exergonic with ΔG = -7.64 kcal/mol, while the formation of HUB from hindered amine bond is endergonic with ΔG =10.43 kcal/mol. Thus, these free energy values indicate that the HUB prefers to undergo the reverse reaction, and dissociates into isocyanate and hindered amine moieties[37].

With the aim of increasing the dynamic behavior in polyurethane networks several external and more complex exchangeable bonds have been introduced following the strategy B. These dynamic linkages can follow either dissociative or associative mechanisms (a third option is also available, the dissociative/associative combined mechanism) and are expected to activate faster and at lower temperatures than urethane bonds. In this section most employed orthogonal chemistries are explained preferentially focusing in polyurethane networks. These groups have been classified according to the review recently published by our group[29].

1.6.1.1 Dissociative dynamic exchanges

Diels-Alder cycloadducts

Diels-Alder/retro Diels-Alder chemistry involves de formation of cycloadducts commonly formed from the cycloaddition of maleimide and furan groups. When high temperatures are reached, these original cycloadducts are able to open following a dissociative step forming the starting maleimide and furan groups[38]. This process is broadly known as retro Diels-Alder reaction. Usually, the reformation of the bond (cycloadduct) is given at lower temperatures, thus, recovering network integrity[39]. In order to introduce this chemistry into PU networks, the most employed strategy has been to first, synthesize functional polyols[40] or smaller molecular weight diols[41,42] to finally react with polyisocyanates. Nevertheless, due to the temperatures required for these exchangeable bonds, in most of the examples found in literature crosslinked polyurethane networks are reprocessed above 120°C[43,44].

Alkoxyamine exchangeable bonds

Alkoxyamines are compounds that can thermally cleave in nitroxides and carbon centered radicals (commonly referred as the alkyl fragment). Even though this dynamic chemistry was found in the beginning of the 20th century, they were applied around 1990s, for nitroxide mediated polymerization (NMP), inspired by control radical polymerization (CRP)[45,46].

Nevertheless, their introduction to smart materials has been given in the last decade. Otsuka and coworkers made one of the first approaches proving the crossover in dynamic covalent polymers based on the reversible alkoxyamine homolysis[47].

Based on this previous research, self-healable polymer networks containing dynamic alkoxyamine moieties have been synthesized in the last decade. Yuan and coworkers polymerized dimethacrylic ester alkoxyamine and polystyrene to successfully create reversible polystyrene networks with healing temperatures of 130°C[48].

More interestingly, Zhang and coworkers synthesized alkoxyamine diols from TEMPOL (nitroxide part) and ACPO (a general free radical initiator) to reduce homolysis temperature[49]. Crosslinked polyurethane networks where acquired after reacting with IPDI isocyanate and polyethylene glycol (PEG2000). Self-healing testing was performed after healing for 48h. This group reported around 90% of healing efficiency between 15°C and 25°C under argon, and same result at 15°C under air. Nevertheless, this interesting approach could be suffering of creep taking into account the T_g and scission temperatures of the alkoxyamine diols.

As the main drawback expected from this fast exchangeable bond, we found that healing efficiency is expected to decrease with time. As a rule, to induce dissociation, mild-high temperatures (90-130°C) are usually employed. This fact, combined with radical sensitivity to oxygen and irreversible combination of carbon radical centers, could lead to the lost of efficiency and degradation[50].

Overall, alkoxyamines can be incorporated into different polymer networks and above mentioned approaches contribute convenient methods to introduced self-healing properties into common polymer materials[44].

Boronic esters

The dynamic activity of boronic esters has been also analyzed for different polymer systems and in small molecular weight compounds. One of the first attempts to understand the dynamic nature of boronic esters was made by Cromwell *et al*, using two telechelic di-boronic ester small molecules to dynamically crosslink with 1-2 diol-containing polymer backbones, proving boronic transesterification reactions and significant healing at slightly elevated temperatures (50°C)[51]. Summerlin and coworkers also proved boronic ester metathesis of 5-membered rings at room temperature[50].

This exchangeable linkage was later introduced in polyurethane elastomers. For example, Li *et al*. introduced catechol derived boronic esters in the absence of moisture, obtaining healable networks at mild conditions[52]. In a recent work, catechol-boronic ester crosslinked PU networks were synthesized adding hydrophilic quaternary ammonium salts. Networks were reprocessed in a pH range of 7 to 9 at room temperature[53]. Lastly, the synergetic effect between covalent adaptable boronic ester bonds and nitrogen coordination has been also reported[54,55].

1.6.1.2 Associative dynamic exchanges

Vinylogous urethanes and Vinylogous Ureas

The amine exchange in vinylogous urethanes was reported firstly by Du Prez and coworkers[56]. This linkage was proven to work effectively above 100°C, with fast stress-relaxation times as short as 85 seconds at 170°C, and in absence of catalyst, without exchange properties at room temperature that could lead to creep. This kind of vitrimer materials were reprocessed up to four times without significant degradation. In a more recent work carried out by the same research group, in order to control exchange kinetics from service temperature to higher temperatures, simple additives were added to modify exchange kinetics depending on the purpose. If the target was to achieve more dimensional stability, exchange reactions were decelerated. On the contrary, if the aim was to increase processing ability, the dynamicity was increased for example in high T_g thermosets by introducing acid-catalysts[17].

The same group implemented vynilogous ureas in composite materials. After analyzing different vynilogous acyl compounds, secondary vynilogous urea showed the fastest intrinsic exchange kinetic. They obtained fast stress-relaxation at 110°C and composites were termoconformed multiple times at 150°C[57].

Lastly, Abetz and coworkers designed a synthetic route to acetoacetilate aromatic alcohols employed commonly (such as Bisphenol A), obtaining acetoacetate monomers that easily react with primary amines to obtain mixtures of vynilogous ureas and vynilogous urethane bonds. The ratio can be modulated by solvent and catalyst changes. Finally, different elastomeric materials were synthesized showing very different activation energies (44-150 kJ/mol). These materials were reprocessed for two consecutive cycles[58].

Other functional groups such as ester and urethanes are able to undergo this mechanism, but as they are commonly present in commodity polymers, their exchangeability will be discussed later in another section.

1.6.1.3 Dissociative/associative dynamic exchanges

Dichalcogenides: Disulfide and Diseleinide bonds

Disulfide chain extenders are one of the most studied dynamic exchangeable linkages in polyurethane networks. One of the first attempts was made by Rekondo and co workers using aromatic disulfide moieties into poly (urea-urethane) elastomers to enable the self-healing at room temperature[59]. Following works also attended the effect of isocyanate structure in presence of different aromatic disulfide chain extenders[60]. More recently aliphatic disulfides have been also analyzed as they are a cheaper alternative in comparison with the aromatic compounds. Nevertheless to trigger their dynamism UV light or an increased temperature is necessary[61,62].

Several works have shown that the disulfide exchange can happen following an dissociative/associative mechanism[63,64]. Also it has been concluded that the use of catalysts can speed up the exchange by the formation of S-based anions in addition to radical mechanism[29,64]. Finally, the associative exchange given between thiols and disulfides has been also shown as another alternative present with these dynamic groups[65].

In comparison with disulfides, diseleinides have been proved to have lower bond energies (172 kJ/mol) than its counterpart of disulfide (240 kJ/mol)[66]. As occurs with previously explained aliphatic disulfur bonds, aliphatic diseleinides also can be triggered with light, and in the case of aromatic compounds, also their exchange can be given at room temperature. In terms of self-healable efficiency, in this last example, aromatic diseleinides have shown to be more efficient than their disulfur analogs[67]. However, and even though diseleinides are a great alternative to improve dynamicity into polyurethane networks, their toxicity and price result as big drawbacks for their future implementation.

1.6.2 Characteristics of the polymer network

One of the key factors that should be deeply analyzed to understand the overall dynamicity of the material is the polymer network itself.

Mostly, new and more complex reversible dynamic bonds and their incorporation to polymer networks have centered the majority of the research works published recently, not excessively focusing in the variables that are highlighted in this section.

Crosslinking density, dynamic bond location and distribution, and reactant stoichiometry play pivotal role in the overall dynamicity of the material. These parameters are intrinsic characteristics of the network itself. Through the complete control of these variables and the correct choice of the synthetic pathway, the behavior of the network can be tuned to achieve expected performance as a thermoset combined with recyclable properties.

Looking into the molecular architecture, the crosslinking density of the network is one of the key factors that should be taken into account. In the one hand, networks with high crosslinking density could present mobility issues for the exchange of dynamic linkages. In this case, one of the solutions that could be applied to enhance dynamicity is to locate dissociative covalent adaptable bonds along the network, decreasing this crosslinking density at reprocessing temperature. In this scenario, the control of the expected sudden drop of material´s viscosity has to be controlled.

On the other hand, low crosslinking density can enable more chain mobility for the reprocessing but can affect material´s properties, as in thermosets high solvent resistance and good mechanical properties are a must. In some cases, when dynamic bonds are formed during curing step, another drawback is that the cuantity of exchangeable functional groups is usually low. Thus, a correct balance should be achieved to combine material´s properties and mobility that could affect to solid state exchangeable kineticks[19]. In polyurethanes, the functionality of isocyanates and low molecular weight nucleophiles can change the crosslinking degree and are easily modified to our choice.

Chain characteristics are the next key factor for overall network dynamicity. As it is well known, polymer network mobility depends on T_g (in case of totally amorphous polymers) and also T_m in the case of semicrystalline polymers. For CANs a new transition temperature is defined: topoly freezing transition temperature (T_v).This intrinsic T_v is defined as the temperature at which the melt viscosity is equal to 10^{12}Pa·s[68,69]. Thus, the T_v drops the line between the freezing of the topology network due to the absence of exchange reactions and bond exchange activation to flow following an Arrhenius dependence. The location of this temperature compared to T_g (in only amorphous) and T_m (for semicrystalline materials) defines the thermomechanical profile of the material[70].

In amorphous polymer networks, we find two different scenarios. If the topology freezing transition temperature (T_v) is above the T_g, as shown in Scheme 7A), the network will be in a rubbery state below T_v and above T_g. If we continue increasing the temperature above T_v, dynamic bonds are activated and viscosity decays following an Arrhenius dependence. On the contrary, in the case of Scheme 7B), long range segmental motions of polymers limit macroscopic flow when T_g is above T_v.

In the case of semicrystalline materials, the same explanation can be adapted but taking into account T_m and T_v locations. These behaviours are summarized inScheme 7 C) and Scheme 7D) respectively.

Elastomers are particularly interesting as their T_g is lower than room temperature. Thus, mobility is highly activated and bond activation energy of the dynamic linkage totally determines the reprocessability.

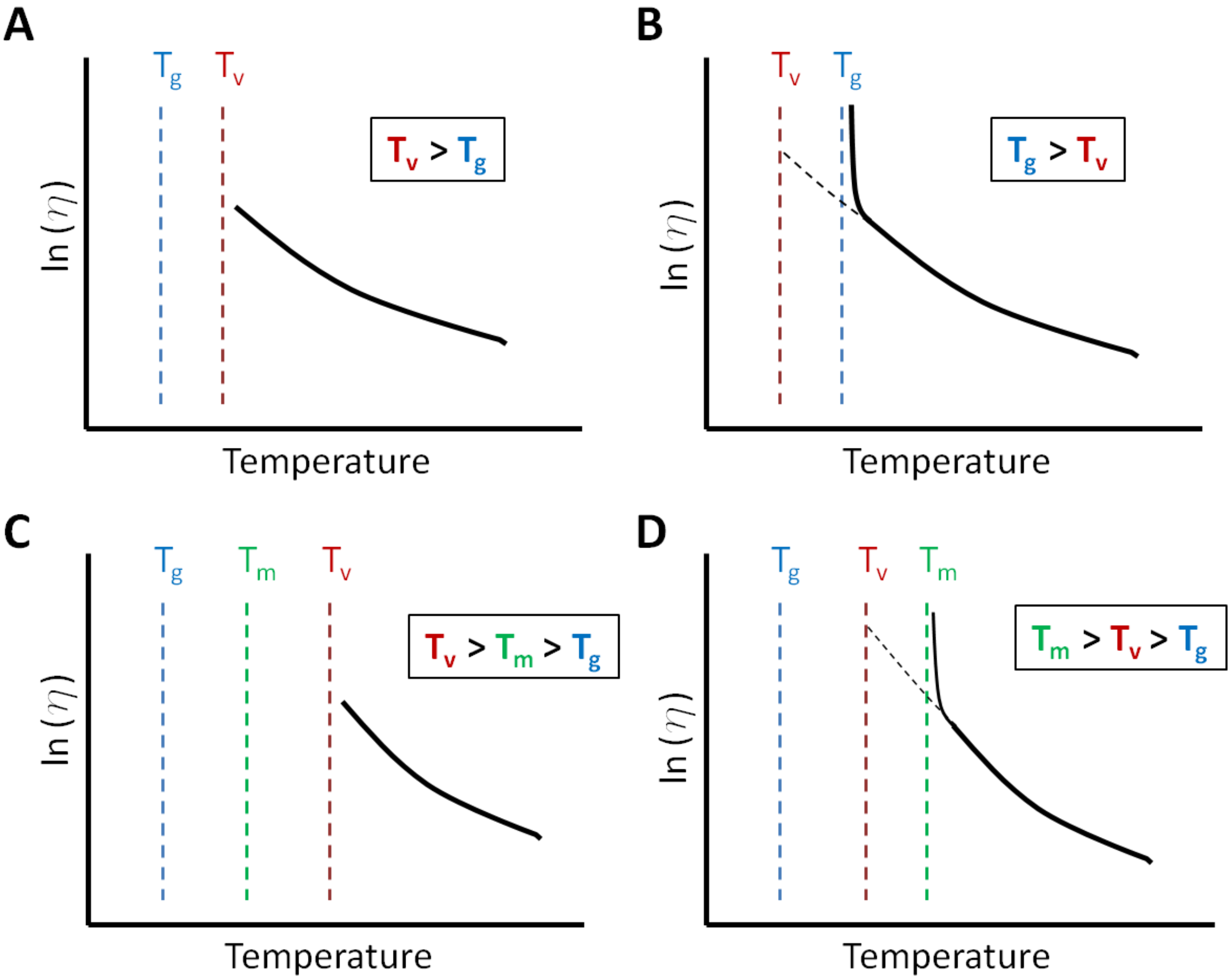

Scheme 7. Plot of Ln (η) versus Temperature when, A) the topology freezing temperature (T_v) is higher than glass transition temperature (T_g); B) glass transition temperature (T_g) is higher than the topology freezing temperature (T_v); C) the topology freezing temperature (T_v) is higher than glass transition temperature (T_g) and melting temperature (T_m); and D) the topology freezing temperature (T_v) is lower than melting temperature (T_m).

PU networks and more precisely PU elastomers offer significant advantages to tune abovementioned thermomechanical behaviors. The polyol (thus, soft segment) affects the overall mobility of the chain, and determines the T_g (and T_m) of the network. Changing the type of polyol, for example from amorphous polypropylene glycol (PPG) to semicrystalline polyethylene glycol (PEG), changes the overall network behavior.

Low molecular weight oligomers (M_n < 5000 g/mol) are preferred to avoid physical entanglement while facilitating chain mobility[71].

Last but not least, functional groups present along the polymer backbone can be susceptible of reversible reactions. Attending to polyurethane materials, the networks that will be deeply analyzed in this thesis, urethane groups are present in different concentrations depending on the employed reactant nature (for example, longer the polyol, less urethane bonds along the network) and stoichiometry (free alcohol or amines can be present on purpose). These pendant nucleophiles can be present in the material to increase exchange reaction rates. As a consequence of these stoichiometry variations to include free functional groups, also crosslinking density decreases, which can enable higher mobility. The location of urea-urethane bonds (or other bonds susceptible to exchanghe reactions) in the network (hard/soft segments) has to be also kept it in mind. In PUs, apart from transcarbamoylation reactions given in the hard segments, transesterification reactions can be also performed in the soft segment, as shown by Ditchel and coworkers in polyester based polyurethane networks[72].

Focusing in these last exchangeable linkages, their importance is as well proved in epoxy based thermosets. In this thermosets, transesterification reactions require free alcohol groups present in the network (as this exchange reaction follows associative exchange reaction) and the presence of suitable catalysts to enable the exchange. Several works have studied these parameters since the discovery of Leibler and coworkers[69].

In any case, the importance of common catalysts employed in industrially relevant thermosets (such as polyurethanes and epoxys) and their use in other exchangeable chemistries have started very recently to be attended. These findings are explained in the section below.

1.6.3 Common catalysts and their application in dynamic networks

Catalysts are widely present in most of the formulations of synthetic polymers[15]. These catalytic compounds are able to decrease synthesis time and energy and with very little loadings.

Focusing on dynamic networks, few research works have found that catalysts can play an important role to trigger the exchangeability of dynamic linkages. And even more remotely, few works have explored deeply and in a more complete manner the existence of catalytic alternative tools for the dynamic activation and the kinetic control of CANs.

The first approaches that have been made in order to improve the dynamic behavior of common polymer networks is to analyze already employed industrially available catalysts and their ability to speed up exchange reactions. Usually, looking for faster stress-relaxation, the correct choice in terms of catalyst load and nature could lead to the achievement of this target[70]. Hence, reprocessing alternatives and broadening of the reprocessing temperature window of catalyzed crosslinked materials are given[73].

In this section, principal metal-based catalysts and organocatalysts employed in dynamic networks are discussed according to each dynamic bond.

Organometallic complexes have been firstly and widely used in polymer synthesis. More specifically, organotin catalysts are the most employed catalytic compounds of the world[74], and their use is widely known in polyurethane synthesis[75], transesterification reactions[76], as stabilizers (and catalysts) in PVC production[77], foam synthesis[78], and in other condensation reactions that require Lewis acid catalysts[79].

Attending to tin based (Sn) catalysts, among a wide variety of catalysts stannous octoate ($SnOct_2$) and Dibutyltin Dilaurate (DBTDL) are the most employed in literature to trigger dynamicity of carbamate exchanges. The first catalyst has been analyzed in vitrimers by Hillmyer and coworkers[80], but actually, DBTDL is the most employed for transcarbamoylation reactions, being much more studied. Several examples can be found in literature to catalyze urethane exchange[72,81,82]. Xie and coworkers triggered the dynamic behavior at 130°C analyzing how different loads of abovementioned catalyst affect the exchangeability[82]. Ditchel and coworkers also employed DBTDL, and compared the stress-relaxation results obtained with other Lewis acid catalysts, Bi(neo)$_3$ and Fe(acac)$_3$ at high temperatures[72]. To enable plasticity, Yan and coworkers[81] also introduced DBTDL (1 wt%, 2 wt% and 3 wt%) and reshape aliphatic polyurethanes at 140°C.

Organotin catalysts also have been employed to trigger transesterification reactions as shown by Retout *et al*[83] and Da Silva and coworkers[84]. In vitrimer materials, DBTDL was used to trigger dynamicity in epoxy/anhydride networks[25].

For this dynamic linkage, other alternatives have been also analyzed in the last decade. Several works can be found of the pioneer(s) of this chemistry. Leibler and coworkers analyzed how the load and nature of three different catalysts (1,5,7-triazabicyclo[4.4.0]dec-5-ene (TBD), triphenylphosphine (PPH$_3$) organocatalysts and Zn(OAc)$_2$) affect to the transesterification reaction rate in epoxy-based vitrimers[85]. Tournilhac *et al.* continued studying metal-catalyzed transesterifications and proved that coordinated Zn^{2+} is structurally bonded to the network. Thus, diffusivity of the catalysts plays a prominent role in the overall efficiency of the catalyst as the metal-based compound is not present everywhere[86].

Later, also to increase exchangeability of ester bonds in epoxy materials, Williams and coworkers took advantage of in-situ generated tertiary amines in the network to increase the exchange rate[87]. This strategy is particularly interesting because the catalytic groups are not externally introduce, on contrary, are induced by the chosen synthetic pathway. And moreover, it has been also applied for transcarbamoylation reactions, mostly in polyhydroxyurethane networks[88].

The addition of organotin and organocatalyst has been also studied for vinylogous urethanes, one of the most studied dynamic groups of recent literature. The transamination reaction was firstly found by Du Prez and coworkers[56] as mentioned in previous section, but more interestingly, this group also developed a complete study on the activation/ inhibition effect of several catalysts and additives. This work was carried out in hard and soft polymer networks, and completed with molecular model kinetic studies. This deep study showed how in presence of Lewis and Brønsted acids the reaction rate of amine exchange is tremendously increased. 1 mol % of *para*-Toluenesulfonic acid (PTSA) showed the best performance, surprisingly being better than Dibutyltin Dilaurate (DBTDL) and sulphuric acid (H_2SO_4). On the contrary, TBD showed very slow exchange rate, even at high concentrations (5%). Thus, the inhibition effect of bases was notorious, and they conclude that vitrimer elastomers materials based on this linkage can be designed to display different viscoelastic properties[17].

1.7 Enlarging lifetime of CANs: from self-healing to reprocessing

The final purpose in covalent adaptable networks is to enlarge the lifetime of the beginning thermoset, keeping original mechanical properties (at least as close as it is possible). To do so, different lifetime enlarging alternatives have been studied recently. These options can be mainly classified into complete reprocessing (where different processing techniques such as hot-press compression and extrusion have been applied to granulated or powdered CANs) and self-healing (where a broken part of the material is healed). Actually, the beginning of this topic has been centered in this second lifetime enlarging method[89]. Self-healing materials can recover their initial functionality after healing the damage. In each case, the usefulness of the polymer can be very different, and thus, the properties to recover are not only mechanical ones, also others such as electric and ionic conductivity, anticorrosive and isolating properties, among others.

Self-healing processes can follow two main routes to recover initial functionality[90]. Extrinsic self-healing is a non autonomic process and requires the exhaustion of healing agents that are pre-embedded in the polymer matrix during the fabrication step. For this mechanism, microcapsules or microvessels designed to be broken by mechanical ruptures are required.

The other route is the intrinsic self-healing with reversible bonds. In this group, we can also differenciate between reversible covalent bond based and non-covalent bond based self-healing. Up to now, supramolecular dynamic bonds have gained most of the attention, but recently numerous advantages have been made in covalent adaptable networks to achieve good mechanical properties and effective healing properties[91].

Previously, self-healing has been studied with supramolecular chemistries such as hydrogen bonding. Nevertheless, covalent adaptable linkages have given a new re-awakening to this field. The presence of dynamic covalent linkages allows the intrinsic self-healing of the materials.

The most employed dynamic thermo reversible reactions in polyurethane networks have been furan-maleimide DA adducts[40,42], disulfide and diseleinide bonds[63,67], and alkoxyamines[48,49].

According to reprocessing of dynamic materials, the most employed technique has been compression moulding. Dynamic networks have been powdered or grounded and reprocess at mild-high temperatures in most of the works published in this field. Attending to reprocessing techniques for dynamic networks, is particularly interesting the work of Zhu and coworkers[92], that compared the mechanical properties of PET vitrimers after using different reprocessing techniques (extrusion, injection and compression) molding. Polyethylene vitrimers bearing sylil ether exchange reactions were also reprocess by compression and injection molding in other recent work[93]. Reprocessing of PU dynamic materials has been studied predominantely by Dichtel and coworkers[72].

Finally, to end with this section, it is northworthy to mention the possible application of CANs in additive manufacturing techniques. For example, PU based dynamic network has been reprocessed by powder bed fusion (PBF) technique[94]. For sure, more research will be performed in this topic in the close future.

1.8 Application of self-healing materials as polymer electrolytes

Taking into account the increasing needs for renewable energy and sustainable development, the area of energy harvesting and storage has been playing an important role in the global low/zero-carbon energy strategy[95]. Researchers have explored new materials and designed new rational structures to ensure highly performant and effective electrochemical energy storage and conversion devices, such as, batteries, fuel cells, supercapacitors, etc. The practicality and cycling-life of these devices is limited by the internal and external damages that can undergo over time[96]. Thus, one of the remaining particular challenges is to develop suitable self-healing electrical and ionic materials to enlarge the device lifetime.

Lithium ion batteries (LIBs) have been employed in several kind of portable electronic devices, electric vehicles and implantable medical devices. Using Li metal as anode material has been considered as a promising approach to increase the specific capacity of this technology. However, the main drawback of Li-metal batteries is the undesired lithium dendrite growth given during electrochemical deposition and stripping. More specifically, active Li-metal and most of the liquid organic electrolytes and lithium salts reacts causing spontaneus solid electrolyte interphase (SEI) on the Li anode surface. Throughout Li deposition/striping, volume changes are given and this unstable and heterogeneus SEI layer cannot resist, leading to the formation of cracks and defects that concentrate Li^+ flux and promotes Li dendrite growth[97].

To overcome this issue, self-healing electrodes and electrolytes have been developed recently for supercapacitators and lithium batteries. Nevetheless, the attention has been centered in self-healing electrodes more than in electrolytes, and novel preparation processes should emerge for the preparation of highly ionic conductive, flexible and thermally stable self-healing electrolytes[95].

1.9 Objectives of this thesis

In the recent chapter the main characteristics of covalent adaptable networks (CANs) and more precisely the ones based on polyurethane networks have been highlighted. With that background in mind the main objective of this work **is to explore and expand the potential of polyurethanes (PUs) as covalent adaptable networks (CANs) understanding the potential advantages and limitations and looking forward to their implementation in advanced applications.**

In order to fulfill this general objective, the work has been divided in two major parts, as presented in the manuscript. First chapters (**Chapters 2 and 3**), contain both the characterization and optimization of dynamic polyurethane thermosets. This characterization is also carried out in the last part of this work (**Chapter 4**), but this final chapter is more focused in the application: the use of PUs as self-healing polymer electrolytes in lithium-ion batteries.

In order to understand the dynamicity of polyurethane networks, **Chapter 2** will depict the synthesis and rheological characterization of non catalyzed and catalyzed aliphatic and aromatic polyurethane networks. The best catalysts (DBTDL and PTSA) to trigger carbamate exchange reactions in aromatic polyurethane compositions will be analyzed in different polyurethane formulations and also in small molecular weight model reactions to understand the exchange mechanisms of the urethane bond in presence of abovementioned catalytic compounds.

In **Chapter 3** novel alkoxyamine based diols will be introduced by replacing at different proportions the chain extender employed in the previous chapter (1,6-Hexanediol). The objective of this section is to trigger dynamicity in aliphatic polyurethane networks owing to the fast radical exchange reactions of alkoxyamines. These dynamicity changes depend on the molecular structure of these novel alkyl nitroxides, and their advantanges and drawbacks will be also explained.

Going upon the second part of the thesis, in **Chapter 4**, with the aim of synthesizing self-healable polyurea-urethane separators for Lithium ion batteries, hindered urea bonds (HUBs) have been tested as dynamic groups located in the crosslinking points. The electrochemical performance of this novel material and its self-healibility have been characterized and compared with the performances of one of the most employed separators in the energy storage industry, Celgard 2500®.

Finally, the results and the most relevant conclusions in regard to the gains and the challenges considered in this work and in the respective field will be commented.

1.10 References

(1) Das, A.; Mahanwar, P. A Brief Discussion on Advances in Polyurethane Applications. *Adv. Ind. Eng. Polym. Res.* **2020**, *3* (3), 93–101. https://doi.org/10.1016/j.aiepr.2020.07.002.

(2) Delebecq, E.; Pascault, J.; Boutevin, B.; Ganachaud, F. On the Versatility of Urethane / Urea Bonds : Reversibility, Blocked Isocyanate, and Non-Isocyanate Polyurethane. *Chem. Rev.* **2013**, *113* (1), 80–118.

(3) Wang, H. H.; Lin, M. S. Poly(Urea-Urethane) Polymers with Multi-Functional Properties. *J. Polym. Res.* **2000**, *7* (2), 81–90. https://doi.org/10.1007/s10965-006-0107-y.

(4) Cherng, J. Y.; Hou, T. Y.; Shih, M. F.; Talsma, H.; Hennink, W. E. Polyurethane-Based Drug Delivery Systems. *Int. J. Pharm.* **2013**, *450* (1–2), 145–162. https://doi.org/10.1016/j.ijpharm.2013.04.063.

(5) Sharmin, E.; Zafar, F. Polyurethane: An Introduction. In *Polyurethane*; 2012; pp 3–16. https://doi.org/10.5772/51663.

(6) Kreye, O.; Mutlu, H.; Meier, M. A. R. Sustainable Routes to Polyurethane Precursors. *Green Chem.* **2013**, *15* (6), 1431–1455. https://doi.org/10.1039/c3gc40440d.

(7) Burchardt, B. Advances in Polyurethane Structural Adhesives. In *Advances in Structural Adhesive Bonding*; Woodhead Publishing Limited, 2010; pp 35–65. https://doi.org/10.1533/9781845698058.1.35.

(8) Avar, G.; Meier-Westhues, U.; Casselmann, H.; Achten, D. *Polyurethanes*; Elsevier, 2012; Vol. 10. https://doi.org/10.1016/B978-0-444-53349-4.00275-2.

(9) Comyn, J. *What Are Adhesives and Sealants and How Do They Work?*, 2nd ed.; Elsevier Ltd., 2021. https://doi.org/10.1016/b978-0-12-819954-1.00003-4.

(10) Avar, G.; Meier-Westhues, U.; Casselmann, H.; Achten, D. *Polyurethanes*; 2012; Vol. 10. https://doi.org/10.1016/B978-0-444-53349-4.00275-2.

(11) Diniz, F. B.; Andrade, G. F. De; Martins, C. R.; Azevedo, W. M. De. A Comparative Study of Epoxy and Polyurethane Based Coatings Containing Polyaniline-DBSA Pigments for Corrosion Protection on Mild Steel. *Prog. Org. Coatings* **2013**, *76* (5), 912–916. https://doi.org/10.1016/j.porgcoat.2013.02.010.

(12) Engels, H. W.; Pirkl, H. G.; Albers, R.; Albach, R. W.; Krause, J.; Hoffmann, A.; Casselmann, H.; Dormish, J. Polyurethanes: Versatile Materials and Sustainable Problem Solvers for Today's Challenges. *Angew. Chemie - Int. Ed.* **2013**, *52* (36), 9422–9441. https://doi.org/10.1002/anie.201302766.

(13) Mudri, N. H.; Abdullah, L. C.; Aung, M. M.; Salleh, M. Z.; Biak, D. R. A.; Rayung, M. Comparative Study of Aromatic and Cycloaliphatic Isocyanate Effects on Physico-Chemical Properties of Bio-Based Polyurethane Acrylate Coatings. *Polymers (Basel).* **2020**, *12* (7), 1–17. https://doi.org/10.3390/polym12071494.

(14) Cherng, J. Y.; Hou, T. Y.; Shih, M. F.; Talsma, H.; Hennink, W. E. Polyurethane-Based Drug Delivery Systems. *Int. J. Pharm.* **2013**, *450* (1–2), 145–162. https://doi.org/10.1016/j.ijpharm.2013.04.063.

(15) Sardon, H.; Pascual, A.; Mecerreyes, D.; Taton, D.; Cramail, H.; Hedrick, J. L. Synthesis of Polyurethanes Using Organocatalysis: A Perspective. *Macromolecules* **2015**, *48* (10), 3153–3165. https://doi.org/10.1021/acs.macromol.5b00384.

(16) Yacoub, F.; MacGregor, J. F. Analysis and Optimization of a Polyurethane Reaction Injection Molding (RIM) Process Using Multivariate Projection Methods. *Chemom. Intell. Lab. Syst.* **2003**, *65* (1), 17–33. https://doi.org/10.1016/S0169-7439(02)00088-6.

(17) Denissen, W.; Droesbeke, M.; Nicola, R.; Leibler, L.; Winne, J. M.; Du Prez, F. E. Chemical Control of the Viscoelastic Properties of Vinylogous Urethane Vitrimers. *Nat. Commun.* **2017**, *8*. https://doi.org/10.1038/ncomms14857.

(18) McBride, M. K.; Worrell, B. T.; Brown, T.; Cox, L. M.; Sowan, N.; Wang, C.; Podgorski, M.; Martinez, A. M.; Bowman, C. N. Enabling Applications of Covalent Adaptable Networks. *Annu. Rev. Chem. Biomol. Eng.* **2019**, *10* (1), 175–198. https://doi.org/10.1146/annurev-chembioeng-060718-030217.

(19) Kloxin, C. J.; Scott, T. F.; Adzima, B. J.; Bowman, C. N. Covalent Adaptable Networks (CANs): A Unique Paradigm in Cross-Linked Polymers. *Macromolecules* **2010**, *43* (6), 2643–2653. https://doi.org/10.1021/ma902596s.

(20) Rahimi, A. R.; Garciá, J. M. Chemical Recycling of Waste Plastics for New Materials Production. *Nat. Rev. Chem.* **2017**, *1*, 1–11. https://doi.org/10.1038/s41570-017-0046.

(21) Jehanno, C.; Pérez-Madrigal, M. M.; Demarteau, J.; Sardon, H.; Dove, A. P. Organocatalysis for Depolymerisation. *Polym. Chem.* **2019**, *10* (2), 172–186. https://doi.org/10.1039/c8py01284a.

(22) Jehanno, C.; Demarteau, J.; Mantione, D.; Arno, M. C.; Ruipérez, F.; Hedrick, J. L.; Dove, A. P.; Sardon, H. Selective Chemical Upcycling of Mixed Plastics Guided by a Thermally Stable Organocatalyst. *Angew. Chemie - Int. Ed.* **2021**, *60* (12), 6710–6717. https://doi.org/10.1002/anie.202014860.

(23) Bowman, C. N.; Kloxin, C. J. Covalent Adaptable Networks: Reversible Bond Structures Incorporated in Polymer Networks. *Angew. Chemie - Int. Ed.* **2012**, *51* (18), 4272–4274. https://doi.org/10.1002/anie.201200708.

(24) Kloxin, C. J.; Bowman, C. N. Covalent Adaptable Networks: Smart, Reconfigurable and Responsive Network Systems. *Chem. Soc. Rev.* **2013**, *42* (17), 7161–7173. https://doi.org/10.1039/c3cs60046g.

(25) Liu, W.; Schmidt, D. F.; Reynaud, E. Catalyst Selection, Creep, and Stress Relaxation in High-Performance Epoxy Vitrimers. *Ind. Eng. Chem. Res.* **2017**, *56* (10), 2667–2672. https://doi.org/10.1021/acs.iecr.6b03829.

(26) Guerre, M.; Taplan, C.; Winne, J. M.; Du Prez, F. E. Vitrimers: Directing Chemical Reactivity to Control Material Properties. *Chem. Sci.* **2020**, *11* (19), 4855–4870.

https://doi.org/10.1039/d0sc01069c.

(27) Wemyss, A. M.; Ellingford, C.; Morishita, Y.; Bowen, C.; Wan, C. Dynamic Polymer Networks: A New Avenue towards Sustainable and Advanced Soft Machines. *Angew. Chemie - Int. Ed.* **2021**, *60* (25), 13725–13736. https://doi.org/10.1002/anie.202013254.

(28) Jourdain, A.; Asbai, R.; Anaya, O.; Chehimi, M. M.; Drockenmuller, E.; Montarnal, D. Rheological Properties of Covalent Adaptable Networks with 1,2,3-Triazolium Cross-Links: The Missing Link between Vitrimers and Dissociative Networks. *ACS Appl. Mater. Interfaces* **2020**. https://doi.org/10.1021/acs.macromol.9b02204.

(29) Aguirresarobe, R. H.; Nevejans, S.; Reck, B.; Irusta, L.; Sardon, H.; Asua, J. M.; Ballard, N. Healable and Self-Healing Polyurethanes Using Dynamic Chemistry. *Prog. Polym. Sci.* **2021**, *114*. https://doi.org/10.1016/j.progpolymsci.2021.101362.

(30) Xu, X.; Hou, J. A Stress Relaxation Model for the Viscoelastic Solids Based on the Steady-State Creep Equation. *Mech. Time-Dependent Mater.* **2011**, *15* (1), 29–39. https://doi.org/10.1007/s11043-010-9122-9.

(31) Chen, T.; Fang, L.; Li, X.; Gao, D.; Lu, C.; Xu, Z. Self-Healing Polymer Coatings of Polyurea-Urethane/Epoxy Blends with Reversible and Dynamic Bonds. *Prog. Org. Coatings* **2020**, *147* (July), 105876. https://doi.org/10.1016/j.porgcoat.2020.105876.

(32) Erice, A.; Ruiz de Luzuriaga, A.; Matxain, J. M.; Ruipérez, F.; Asua, J. M.; Grande, H. J.; Rekondo, A. Reprocessable and Recyclable Crosslinked Poly(Urea-Urethane)s Based on Dynamic Amine/Urea Exchange. *Polymer (Guildf).* **2018**, *145*, 127–136. https://doi.org/10.1016/j.polymer.2018.04.076.

(33) Erice, A.; Azcune, I.; Ruiz De Luzuriaga, A.; Ruipérez, F.; Irigoyen, M.; Matxain, J. M.; Asua, J. M.; Grande, H. J.; Rekondo, A. Effect of Regioisomerism on Processability and Mechanical Properties of Amine/Urea Exchange Based Poly(Urea-Urethane) Vitrimers. *ACS Appl. Polym. Mater.* **2019**, *1* (9), 2472–2481. https://doi.org/10.1021/acsapm.9b00589.

(34) Ying, H.; Zhang, Y.; Cheng, J. Dynamic Urea Bond for the Design of Reversible and Self-Healing Polymers. *Nat. Commun.* **2014**, *5*. https://doi.org/10.1038/ncomms4218.

(35) Ramey, K. X 10-5. **1974**, *2448* (15), 2448–2449.

(36) Hutchby, M.; Houlden, C. E.; Gair Ford, J.; Tyler, S. N. G.; Gagné, M. R.; Lloyd-Jones, G. C.; Booker-Milburn, K. I. Hindered Ureas as Masked Isocyanates: Facile Carbamoylation of Nucleophiles under Neutral Conditions. *Angew. Chemie - Int. Ed.* **2009**, *48* (46), 8721–8724. https://doi.org/10.1002/anie.200904435.

(37) Zhang, Q.; Wang, S.; Rao, B.; Chen, X.; Ma, L.; Cui, C.; Zhong, Q.; Li, Z.; Cheng, Y.; Zhang, Y. Hindered Urea Bonds for Dynamic Polymers: An Overview. *React. Funct. Polym.* **2021**, *159* (November 2020). https://doi.org/10.1016/j.reactfunctpolym.2020.104807.

(38) Chen, X.; Dam, M. A.; Ono, K.; Mal, A.; Shen, H.; Nutt, S. R.; Sheran, K.; Wudl, F. A Thermally Re-Mendable Cross-Linked Polymeric Material. *Science (80-.).* **2002**, *295* (5560), 1698–1702.

https://doi.org/10.1126/science.1065879.

(39) Tasdelen, M. A. Diels-Alder "Click" Reactions: Recent Applications in Polymer and Material Science. *Polym. Chem.* **2011**, *2* (10), 2133–2145. https://doi.org/10.1039/c1py00041a.

(40) Li, M.; Ding, H.; Yang, X.; Xu, L.; Xia, J.; Li, S. Preparation and Properties of Self-Healing Polyurethane Elastomer Derived from Tung-Oil-Based Polyphenol. *ACS Omega* **2020**, *5* (1), 529–536. https://doi.org/10.1021/acsomega.9b03082.

(41) Rivero, G.; Nguyen, L. T. T.; Hillewaere, X. K. D.; Du Prez, F. E. One-Pot Thermo-Remendable Shape Memory Polyurethanes. *Macromolecules* **2014**, *47* (6), 2010–2018. https://doi.org/10.1021/ma402471c.

(42) Heo, Y.; Sodano, H. A. Self-Healing Polyurethanes with Shape Recovery. *Adv. Funct. Mater.* **2014**, *24* (33), 5261–5268. https://doi.org/10.1002/adfm.201400299.

(43) Irusta, L.; Fernández-Berridi, M. J.; Aizpurua, J. Polyurethanes Based on Isophorone Diisocyanate Trimer and Polypropylene Glycol Crosslinked by Thermal Reversible Diels Alder Reactions. *J. Appl. Polym. Sci.* **2017**, *134* (9), 1–9. https://doi.org/10.1002/app.44543.

(44) Liu, Y. L.; Chuo, T. W. Self-Healing Polymers Based on Thermally Reversible Diels-Alder Chemistry. *Polym. Chem.* **2013**, *4* (7), 2194–2205. https://doi.org/10.1039/c2py20957h.

(45) Zou, W.; Dong, J.; Luo, Y.; Zhao, Q.; Xie, T. Dynamic Covalent Polymer Networks: From Old Chemistry to Modern Day Innovations. *Adv. Mater.* **2017**, *29* (14). https://doi.org/10.1002/adma.201606100.

(46) Audran, G.; Brémond, P.; Marque, S. R. A. Labile Alkoxyamines: Past, Present, and Future. *Chem. Commun.* **2014**, *50* (59), 7921–7928. https://doi.org/10.1039/c4cc01364f.

(47) Otsuka, H.; Aotani, K.; Higaki, Y.; Takahara, A. A Dynamic (Reversible) Covalent Polymer: Radical Crossover Behaviour of TEMPO–Containing Poly(Alkoxyamine Ester)S. *Chem. Commun.* **2002**, *2* (23), 2838–2839. https://doi.org/10.1039/b209193c.

(48) Yuan, C.; Rong, M. Z.; Zhang, M. Q.; Zhang, Z. P.; Yuan, Y. C. Self-Healing of Polymers via Synchronous Covalent Bond Fission/Radical Recombination. *Chem. Mater.* **2011**, *23* (22), 5076–5081. https://doi.org/10.1021/cm202635w.

(49) Zhang, Z. P.; Rong, M. Z.; Zhang, M. Q.; Yuan, C. Alkoxyamine with Reduced Homolysis Temperature and Its Application in Repeated Autonomous Self-Healing of Stiff Polymers. *Polym. Chem.* **2013**, *4* (17), 4648–4654. https://doi.org/10.1039/c3py00679d.

(50) Cash, J. J.; Kubo, T.; Bapat, A. P.; Sumerlin, B. S. Room-Temperature Self-Healing Polymers Based on Dynamic-Covalent Boronic Esters. *Macromolecules* **2015**, *48* (7), 2098–2106. https://doi.org/10.1021/acs.macromol.5b00210.

(51) Cromwell, O. R.; Chung, J.; Guan, Z. Malleable and Self-Healing Covalent Polymer Networks through Tunable Dynamic Boronic Ester Bonds. *J. Am. Chem. Soc.* **2015**, *137* (20), 6492–6495. https://doi.org/10.1021/jacs.5b03551.

(52) Yang, Y.; Du, F. S.; Li, Z. C. Highly Stretchable, Self-Healable, and Adhesive Polyurethane Elastomers Based on Boronic Ester Bonds. *ACS Appl. Polym. Mater.* **2020**, *2* (12), 5630–5640. https://doi.org/10.1021/acsapm.0c00941.

(53) Xia, N. N.; Rong, M. Z.; Zhang, M. Q. Stabilization of Catechol-Boronic Ester Bonds for Underwater Self-Healing and Recycling of Lipophilic Bulk Polymer in Wider PH Range. *J. Mater. Chem. A* **2016**, *4* (37), 14122–14131. https://doi.org/10.1039/c6ta05121a.

(54) Song, K.; Ye, W.; Gao, X.; Fang, H.; Zhang, Y.; Zhang, Q.; Li, X.; Yang, S.; Wei, H.; Ding, Y. Synergy between Dynamic Covalent Boronic Ester and Boron-Nitrogen Coordination: Strategy for Self-Healing Polyurethane Elastomers at Room Temperature with Unprecedented Mechanical Properties. *Mater. Horizons* **2021**, *8* (1), 216–223. https://doi.org/10.1039/d0mh01142h.

(55) Zhang, X.; Wang, S.; Jiang, Z.; Li, Y.; Jing, X. Boronic Ester Based Vitrimers with Enhanced Stability via Internal Boron-Nitrogen Coordination. *J. Am. Chem. Soc.* **2020**, *142* (52), 21852–21860. https://doi.org/10.1021/jacs.0c10244.

(56) Denissen, W.; Rivero, G.; Nicolaÿ, R.; Leibler, L.; Winne, J. M.; Du Prez, F. E. Vinylogous Urethane Vitrimers. *Adv. Funct. Mater.* **2015**, *25* (16), 2451–2457. https://doi.org/10.1002/adfm.201404553.

(57) Denissen, W.; De Baere, I.; Van Paepegem, W.; Leibler, L.; Winne, J.; Du Prez, F. E. Vinylogous Urea Vitrimers and Their Application in Fiber Reinforced Composites. *Macromolecules* **2018**, *51* (5), 2054–2064. https://doi.org/10.1021/acs.macromol.7b02407.

(58) Haida, P.; Signorato, G.; Abetz, V. Blended Vinylogous Urethane/Urea Vitrimers Derived from Aromatic Alcohols. *Polym. Chem.* **2022**, *13* (7), 946–958. https://doi.org/10.1039/d1py01237a.

(59) Rekondo, A.; Martin, R.; Ruiz De Luzuriaga, A.; Cabañero, G.; Grande, H. J.; Odriozola, I. Catalyst-Free Room-Temperature Self-Healing Elastomers Based on Aromatic Disulfide Metathesis. *Mater. Horizons* **2014**, *1* (2), 237–240. https://doi.org/10.1039/c3mh00061c.

(60) Li, T.; Zheng, T.; Han, J.; Liu, Z.; Guo, Z. X.; Zhuang, Z.; Xu, J.; Guo, B. H. Effects of Diisocyanate Structure and Disulfide Chain Extender on Hard Segmental Packing and Self-Healing Property of Polyurea Elastomers. *Polymers (Basel).* **2019**, *11* (5). https://doi.org/10.3390/polym11050838.

(61) Xu, W. M.; Rong, M. Z.; Zhang, M. Q. Sunlight Driven Self-Healing, Reshaping and Recycling of a Robust, Transparent and Yellowing-Resistant Polymer. *J. Mater. Chem. A* **2016**, *4* (27), 10683–10690. https://doi.org/10.1039/c6ta02662a.

(62) Yan, C.; Yang, F.; Wu, M.; Yuan, Y.; Chen, F.; Chen, Y. Phase-Locked Dynamic and Mechanoresponsive Bonds Design toward Robust and Mechanoluminescent Self-Healing Polyurethanes: A Microscopic View of Self-Healing Behaviors. *Macromolecules* **2019**, *52* (23), 9376–9382. https://doi.org/10.1021/acs.macromol.9b02089.

(63) Azcune, I.; Odriozola, I. Aromatic Disulfide Crosslinks in Polymer Systems: Self-Healing,

Reprocessability, Recyclability and More. *Eur. Polym. J.* **2016**, *84*, 147–160. https://doi.org/10.1016/j.eurpolymj.2016.09.023.

(64) Nevejans, S.; Ballard, N.; Miranda, J. I.; Reck, B.; Asua, J. M. The Underlying Mechanisms for Self-Healing of Poly(Disulfide)S. *Phys. Chem. Chem. Phys.* **2016**, *18* (39), 27577–27583. https://doi.org/10.1039/c6cp04028d.

(65) Lei, Z. Q.; Xiang, H. P.; Yuan, Y. J.; Rong, M. Z.; Zhang, M. Q. Room-Temperature Self-Healable and Remoldable Cross-Linked Polymer Based on the Dynamic Exchange of Disulfide Bonds. *Chem. Mater.* **2014**, *26* (6), 2038–2046. https://doi.org/10.1021/cm4040616.

(66) Nellepalli, P.; Patel, T.; Oh, J. K. Dynamic Covalent Polyurethane Network Materials: Synthesis and Self-Healability. *Macromol. Rapid Commun.* **2021**, *42* (20), 1–33. https://doi.org/10.1002/marc.202100391.

(67) An, X.; Aguirresarobe, R. H.; Irusta, L.; Ruipérez, F.; Matxain, J. M.; Pan, X.; Aramburu, N.; Mecerreyes, D.; Sardon, H.; Zhu, J. Aromatic Diselenide Crosslinkers to Enhance the Reprocessability and Self-Healing of Polyurethane Thermosets. *Polym. Chem.* **2017**, *8* (23), 3641–3646. https://doi.org/10.1039/c7py00448f.

(68) Dyre, J. C. Colloquium: The Glass Transition and Elastic Models of Glass-Forming Liquids. *Rev. Mod. Phys.* **2006**, *78* (3), 953–972. https://doi.org/10.1103/RevModPhys.78.953.

(69) Montarnal, D.; Capelot, M.; Tournilhac, F.; Leibler, L. Silica-like Malleable Materials from Permanent Organic Networks. *Science (80-.).* **2011**, *334* (6058), 965–968. https://doi.org/10.1126/science.1212648.

(70) Van Zee, N. J.; Nicolaÿ, R. Vitrimers: Permanently Crosslinked Polymers with Dynamic Network Topology. *Prog. Polym. Sci.* **2020**, *104*, 101233. https://doi.org/10.1016/j.progpolymsci.2020.101233.

(71) Willocq, B.; Odent, J.; Dubois, P.; Raquez, J. M. Advances in Intrinsic Self-Healing Polyurethanes and Related Composites. *RSC Adv.* **2020**, *10* (23), 13766–13782. https://doi.org/10.1039/d0ra01394c.

(72) Fortman, D. J.; Sheppard, D. T.; Dichtel, W. R. Reprocessing Cross-Linked Polyurethanes by Catalyzing Carbamate Exchange. *Macromolecules* **2019**, *52* (16), 6330–6335. https://doi.org/10.1021/acs.macromol.9b01134.

(73) Alabiso, W.; Schlögl, S. The Impact of Vitrimers on the Industry of the Future: Chemistry, Properties and Sustainable Forward-Looking Applications. *Polymers (Basel).* **2020**, *12* (8). https://doi.org/10.3390/POLYM12081660.

(74) Da Silva, M. A.; Dos Santos, A. S. S.; Dos Santos, T. V.; Meneghetti, M. R.; Meneghetti, S. M. P. Organotin(IV) Compounds with High Catalytic ActIVities and SelectIVities in the Glycerolysis of Triacylglycerides. *Catal. Sci. Technol.* **2017**, *7* (23), 5750–5757. https://doi.org/10.1039/c7cy01559c.

(75) Davletbaev, R.; Davletbaeva, I.; Gumerov, O. The Modification of Polyurethanes by Highly Ordered Coordination Compounds of Transition Metals. *Polyurethane* **2012**, *9* (July), 330–333.

https://doi.org/10.5772/47990.

(76) Nunes, R. S.; Altino, F. M.; Meneghetti, M. R.; Meneghetti, S. M. P. New Mechanistic Approaches for Fatty Acid Methyl Ester Production Reactions in the Presence of Sn(IV) Catalysts. *Catal. Today* **2017**, *289*, 121–126. https://doi.org/10.1016/j.cattod.2016.09.016.

(77) Ayrey, G.; Hsu, S. Y.; Poller, R. C. The Use of Organotin Compounds in the Thermal Stabilization of Poly(Viny1 Chloride). VI. An Assessment. *J. Polym. Sci.* **1984**, *22*, 2871–2886.

(78) Gwon, J. G.; Kim, S. K.; Kim, J. H. Development of Cell Morphologies in Manufacturing Flexible Polyurethane Urea Foams as Sound Absorption Materials. *J. Porous Mater.* **2016**, *23* (2), 465–473. https://doi.org/10.1007/s10934-015-0100-0.

(79) Meneghetti, M. R.; Meneghetti, S. M. P. Sn(Iv)-Based Organometallics as Catalysts for the Production of Fatty Acid Alkyl Esters. *Catal. Sci. Technol.* **2015**, *5* (2), 765–771. https://doi.org/10.1039/c4cy01535e.

(80) Brutman, J. P.; Delgado, P. A.; Hillmyer, M. A. Polylactide Vitrimers. *ACS Macro Lett.* **2014**, *3* (7), 607–610. https://doi.org/10.1021/mz500269w.

(81) Yan, P.; Zhao, W.; Fu, X.; Liu, Z.; Kong, W.; Zhou, C.; Lei, J. Multifunctional Polyurethane-Vitrimers Completely Based on Transcarbamoylation of Carbamates: Thermally-Induced Dual-Shape Memory Effect and Self-Welding. *RSC Adv.* **2017**, *7* (43), 26858–26866. https://doi.org/10.1039/c7ra01711a.

(82) Zheng, N.; Fang, Z.; Zou, W.; Zhao, Q.; Xie, T. Thermoset Shape-Memory Polyurethane with Intrinsic Plasticity Enabled by Transcarbamoylation. *Angew. Chemie - Int. Ed.* **2016**, *55* (38), 11421–11425. https://doi.org/10.1002/anie.201602847.

(83) Poller, R. C.; Retout, S. P. Organotin Compounds as Transesterification Catalysts. *J. Organomet. Chem.* **1979**, *173* (3). https://doi.org/10.1016/S0022-328X(00)84794-4.

(84) Ferreira, A. B.; Lemos Cardoso, A.; da Silva, M. J. Tin-Catalyzed Esterification and Transesterification Reactions: A Review. *ISRN Renew. Energy* **2012**, *2012*, 1–13. https://doi.org/10.5402/2012/142857.

(85) Capelot, M.; Unterlass, M. M.; Tournilhac, F.; Leibler, L. Catalytic Control of the Vitrimer Glass Transition. *ACS Macro Lett.* **2012**, *1* (7), 789–792. https://doi.org/10.1021/mz300239f.

(86) Demongeot, A.; Mougnier, S. J.; Okada, S.; Soulié-Ziakovic, C.; Tournilhac, F. Coordination and Catalysis of Zn2+ in Epoxy-Based Vitrimers. *Polym. Chem.* **2016**, *7* (27), 4486–4493. https://doi.org/10.1039/c6py00752j.

(87) Altuna, F. I.; Hoppe, C. E.; Williams, R. J. J. Epoxy Vitrimers with a Covalently Bonded Tertiary Amine as Catalyst of the Transesterification Reaction. *Eur. Polym. J.* **2019**, *113*, 297–304. https://doi.org/10.1016/j.eurpolymj.2019.01.045.

(88) Hernández, A.; Houck, H. A.; Elizalde, F.; Guerre, M.; Sardon, H.; Du Prez, F. E. Internal Catalysis on the Opposite Side of the Fence in Non-Isocyanate Polyurethane Covalent Adaptable Networks. *Eur. Polym. J.* **2022**, *168* (October 2021).

https://doi.org/10.1016/j.eurpolymj.2022.111100.

(89) Podgórski, M.; Fairbanks, B. D.; Kirkpatrick, B. E.; McBride, M.; Martinez, A.; Dobson, A.; Bongiardina, N. J.; Bowman, C. N. Toward Stimuli-Responsive Dynamic Thermosets through Continuous Development and Improvements in Covalent Adaptable Networks (CANs). *Adv. Mater.* **2020**, *32* (20), 1–26. https://doi.org/10.1002/adma.201906876.

(90) Gai, Y.; Li, H.; Li, Z. Self-Healing Functional Electronic Devices. *Small* **2021**, *17* (41), 1–19. https://doi.org/10.1002/smll.202101383.

(91) Mai, W.; Yu, Q.; Han, C.; Kang, F.; Li, B. Self-Healing Materials for Energy-Storage Devices. *Adv. Funct. Mater.* **2020**, *30* (24). https://doi.org/10.1002/adfm.201909912.

(92) Qiu, J.; Ma, S.; Wang, S.; Tang, Z.; Li, Q.; Tian, A.; Xu, X.; Wang, B.; Lu, N.; Zhu, J. Upcycling of Polyethylene Terephthalate to Continuously Reprocessable Vitrimers through Reactive Extrusion. *Macromolecules* **2021**, *54* (2), 703–712. https://doi.org/10.1021/acs.macromol.0c02359.

(93) Zych, A.; Pinalli, R.; Soliman, M.; Vachon, J.; Dalcanale, E. Polyethylene Vitrimers via Silyl Ether Exchange Reaction. *Polymer (Guildf).* **2020**, *199* (April). https://doi.org/10.1016/j.polymer.2020.122567.

(94) Sun, S.; Gan, X.; Wang, Z.; Fu, D.; Pu, W.; Xia, H. Dynamic Healable Polyurethane for Selective Laser Sintering. *Addit. Manuf.* **2020**, *33* (March), 101176. https://doi.org/10.1016/j.addma.2020.101176.

(95) Chen, D.; Wang, D.; Yang, Y.; Huang, Q.; Zhu, S.; Zheng, Z. Self-Healing Materials for next-Generation Energy Harvesting and Storage Devices. *Adv. Energy Mater.* **2017**, *7* (23), 27–31. https://doi.org/10.1002/aenm.201700890.

(96) Ezeigwe, E. R.; Dong, L.; Manjunatha, R.; Tan, M.; Yan, W.; Zhang, J. A Review of Self-Healing Electrode and Electrolyte Materials and Their Mitigating Degradation of Lithium Batteries. *Nano Energy* **2021**, *84*, 105907. https://doi.org/10.1016/j.nanoen.2021.105907.

(97) Ding, P.; Lin, Z.; Guo, X.; Wu, L.; Wang, Y.; Guo, H.; Li, L.; Yu, H. Polymer Electrolytes and Interfaces in Solid-State Lithium Metal Batteries. *Mater. Today* **2021**, *51*, 449–474. https://doi.org/10.1016/j.mattod.2021.08.005.

Chapter 2

Chapter 2. Influence of catalysts in the dynamicity of polyurethane networks

2.1. Introduction

As explained in Chapter 1, thermosets are cross-linked polymer networks suitable for applications that demand high dimensional stability, mechanical strength and high solvent-resistance[1]. However, due to their static cross-linked structure, their ability to be reprocessed, recycled or reshaped is strongly hindered and once these materials suffer any damage, they are usually discarded[2]. Taking into account that the thermoset market is in a constant upward trend[3], and due to growing environmental concerns, there is a need to find alternatives with the aim to reuse, reshape or even recycle thermosets.

An attractive chemical strategy to provide a second life in cross-linked polymer networks is offered by the introduction of exchangeable chemical bonds[4]. However, the introduction of additional functional groups containing exchangeable bonds into polymers that are already produced commercially is not an easy step as these new polymers have to be investigated in terms of price, processability and market demands. In this regard, the control of the dynamic nature of linkages already existing in commodity polymers is potentially an easier pathway from academia to the industry.

Thus, in 2011 Leibler and co-workers[5], introduced dynamic character to an epoxy resin, allowing their reprocessability. In this work, they promoted internal transesterification reactions by using a catalyst, thereby enabling the exchange of functional groups already present in these polymers. Following this strategy, several authors have taken advantage of exchangeable groups[6–9] to create dynamic character to thermoset formulations already present in our daily life.

Analyzing the thermoset market by class of polymer, polyurethanes are the most employed polymer among epoxies, unsaturated polyesters and phenolic resins[10]. Looking at their chemical structure, these materials are based on urethane linkages that are susceptible to undergo transcarbamoylation reactions. These exchange reactions have been studied in different polyurethane networks in order to facilitate their reprocessability. One of the unique characteristics of urethane linkages is that the exchange reaction can be given by two different mechanisms, associative or dissociative. While in conventional polyurethanes it has been postulated that the most predominant mechanism is the dissociative one (Figure 2.1 A), in the case of polyhydroxyurethanes, where plenty of free alcohol groups are present, the associative mechanism has greater impact (Figure 2.1 B).

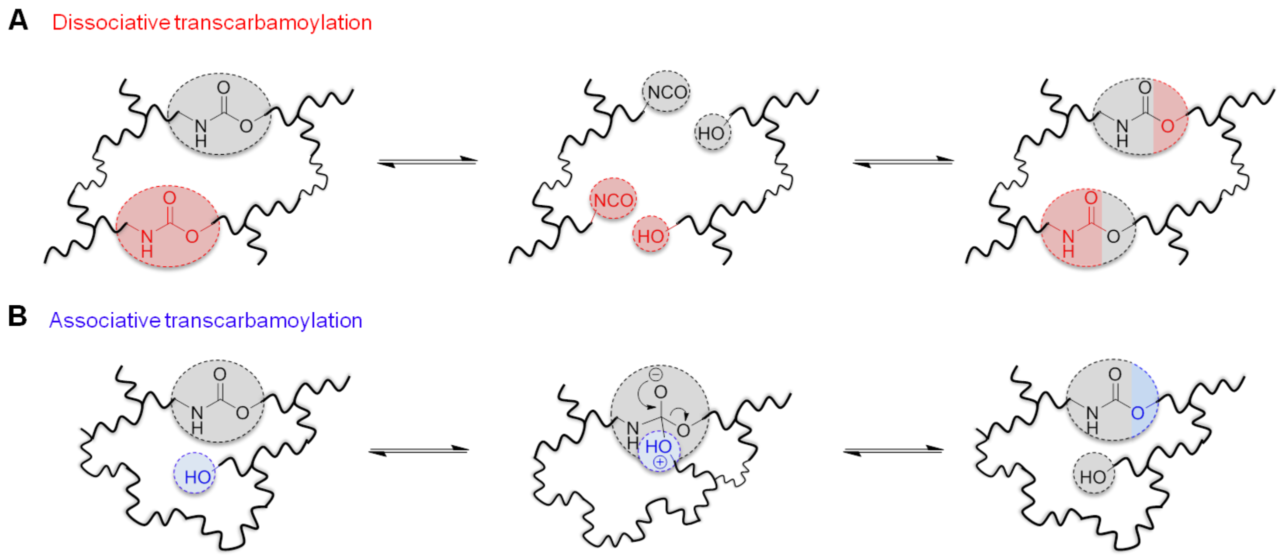
A
Dissociative transcarbamoylation
O
N
H
O
NCO
HO
NCO
HO
B
Associative transcarbamoylation
HO

Figure 2.1. A) Dissociative (non free alcohol mediated) and B) Associative (free alcohol mediated) transcarbamoylation exchange reactions.

Although both mechanisms can provide dynamic character to the final polymer network, they imply different challenges for its potential application. Theoretically, the dissociative mechanism leads to a rapid drop in viscosity, which can enable its reprocessing more effectively[11–13]. However, the dissociation mechanism implies the formation of isocyanate groups, that can lead to secondary reactions and stable byproducts that can reduce the dynamic character of the network[14–16]. In addition, the dynamic reaction should be precisely controlled to promote limited dissociation and to avoid compromising the material integrity during the dynamic process. In contrast, the associative approach avoids the formation of free isocyanate but it requires high amounts of catalyst to be dynamic, as it is a kinetically controlled process[17].

Several publications suggest that transcarbamoylation reactions can enable the reprocessability and recyclability of polyurethane thermosets, especially in the presence of an appropriate catalyst[18]. For instance, Xie and co-workers[19] demonstrated fast relaxation in aliphatic thermosets by loading between 0.5, 1 and 2 wt % of tin catalyst at 130 °C. However, such metal loadings can be harmful for the environment and health[20,21]. In order to mitigate these issues coming from the tin based catalyst Dichtel *et al.*[22] studied the effect of different Lewis acid catalysts and compared them to tin catalysts in MDI based polyurethanes, showing fast stress relaxation at 140 °C and that these materials are capable of stress relaxation on extremely short timescales compared to many dynamic covalent networks.

While these catalysts enable the synthesis of high molecular weight polymers, there are a number of issues that arise with the use of metal catalysts and therefore recent efforts in polyurethane synthesis have been oriented towards the design and synthesis of novel organocatalysts that can perform as effectively as tin-based catalysts. Our group has demonstrated high catalytic activity in PU synthesis of several organic bases and acids and their potential to replace tin based catalysts in certain formulations[20]. In addition, some of these catalysts have been shown to greatly impact in the dynamic character of vinylogous urethanes[8].

Taking into account that the dynamic behavior of polyurethanes can be affected by the nature of the catalyst, the objective of the work presented in this chapter is to gain an insight into the structural parameters, such as the nature of the isocyanate, the urethane/alcohol ratio and specifically the effect that the catalyst has on the dynamic behavior of polyurethane thermosets. In addition, we investigated the exchange mechanism in the presence of different catalyst families.

2.2. Results and discussion

2.2.1. Dynamic behavior of polyurethane thermosets

In order to understand the effect of different catalysts on the dynamic behavior of polyurethane thermosets we synthesized a reference polyurethane structure that allowed us to systematically change the most relevant parameters (Figure 2.2. A). First, a tris-isocyanate terminated pre-polymer was obtained by reacting commercially available poly(propylene glycol) (PPG) with an average molecular weight of 3.7 kDa, with 4,4'-methylenediphenyl diisocyanate (MDI) or hexamethylene diisocyanate (HDI). The selection of the polyether diol was based on their common use industrially as well as their lack of ester bonds that can enhance exchange rates in polyurethane formulations. The selection of the isocyanates was based on their commercial interest but also allowed us to study the effect of the catalyst in aromatic and aliphatic polyurethanes. After the synthesis of the NCO terminated prepolymer, 1,6-Hexanediol was added to the pre-polymer to get a cross-linked material and aromatic or aliphatic polyurethane films were acquired when the curing process was completed. This last step was also carried out without any catalyst. In order to create a material able to proceed through dissociative or associate exchange mechanism, a small excess of 1,6-Hexanediol was added (0.1 equiv. excess). To follow both steps (pre-polymer formation and the subsequent curing process) FTIR spectroscopy was employed (Figure 2.2.B). As can be seen in the synthesis of aliphatic polyurethane networks, the isocyanate stretching band at 2268 cm^{-1} completely disappeared and new bands corresponding to formation of the urethane group appeared at 1719 and 1682 cm^{-1}. A representative example of the appearance of the cross-linked polyurethane films is shown in Figure 2.2 C. More information about the polyurethane preparation (yields and reaction conditions) is given in the experimental section. Moreover, FTIR characterization and the physical appearance of the aromatic materials can be found in Figure S2.1 and Figure S2.2 respectively.

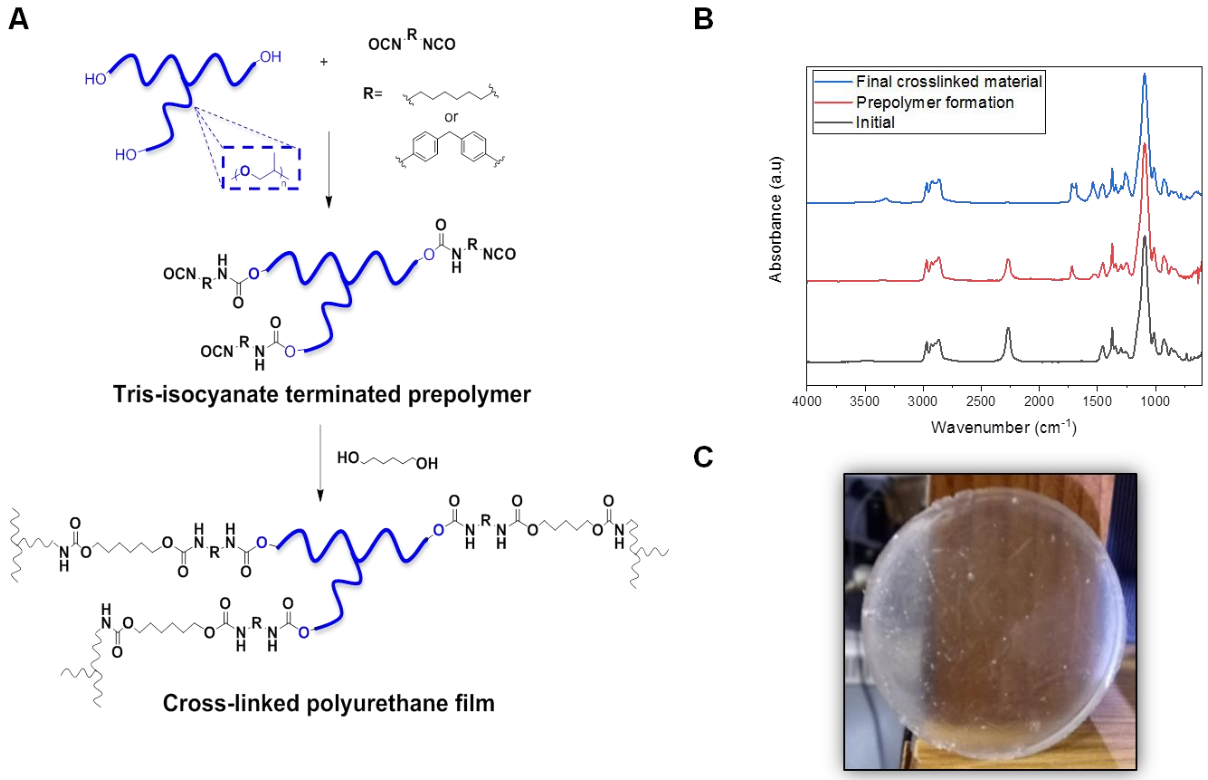
A
HO
OH
HO
OCN R NCO
R=
or
Tris-isocyanate terminated prepolymer
HO OH
Cross-linked polyurethane film
B
Final crosslinked material
Prepolymer formation
Initial
Absorbance (a.u)
4000
3500
3000
2500
2000
1500
1000
Wavenumber (cm-1)
C

Figure 2.2. A) Synthetic procedure for obtaining aromatic (MDI) or aliphatic (HDI) cross-linked polyurethanes. B) Representative FTIR spectra of the reaction of PPG triol (Mn=3740 g/mol) with HDI at t=0min (black trace) and t=420 min (pre-polymer formation, red trace). The blue trace corresponds to the final polyurethane film cross-linked for 24h at 70°C with 1,6-Hexanediol. C) Aliphatic polyurethane film cross-linked without catalyst.

2.2.2. Exchange in catalyst free polyurethanes

In order to investigate the relaxation of both polyurethanes, a rheological investigations as well as DMTA analysis were performed. For the rheological study of the dynamic behavior of synthesized aromatic and aliphatic polyurethane reference materials, stress-relaxation measurements were carried out at 100, 120 and 140°C (Figure 2.3A,B) in the absence of any type of catalyst. Johannsmann and co-workers found that in spite of the benefits of running the reaction at high temperatures to increase the rate of the dissociative exchange reactions for HDI and MDI based polyurethanes, secondary products (allophanates) could be produced during the annealing[23]. In order to avoid the undesirable formation of these new bonds we investigated the exchange in mild conditions.

As can be seen, samples showed decay in the relaxation moduli with significant temperature dependence. At high temperatures (140°C) relaxations in both systems were relatively fast (less than 600 seconds). When comparing the aromatic and aliphatic polyurethanes we found that the decay in aromatic polyurethanes was faster and the decay difference increased when decreasing the measurement temperature. This suggests that the exchange reaction is significantly more favored in aromatic systems in comparison to aliphatic ones, as has previously been reported.

In order to clarify if this relaxation at high temperature was due to dynamic exchange reactions or, alternatively, due to topological changes in the network caused by degradation of the thermoset, the relaxation curves were compared with results obtained by dynamic mechanical thermal analysis (DMTA) measurements carried out at similar measurement temperatures (100, 120 and 140°C). In the absence of degradation the isothermal experiment should give a constant value while if degradation occurs there will be an onset of degradation after a given time. If we compare the results for the aliphatic (Figure 2.3C) and aromatic polyurethanes (Figure

2.3D) it can be concluded that in both systems degradation takes place, even at the lowest temperature, but that this degradation is significantly affected by the temperature. While at 140°C and 120°C the degradation is significant and occurs relatively rapidly, at 100°C degradation occurs over very long times in both polyurethane networks. In all the catalyst-free systems investigated, the onset time for degradation in DMTA experiments occurs before the stress relaxation time, indicating that the observed behavior in stress relaxation measurements is not due to any exchange reaction but rather due to an irreversible degradation process. It may therefore be concluded that even if the degradation of aromatic polyurethanes is not as fast as in the aliphatic materials, in the absence of a catalyst polyurethane thermosets suffer this drop in moduli due to the degradation of the polymer network.

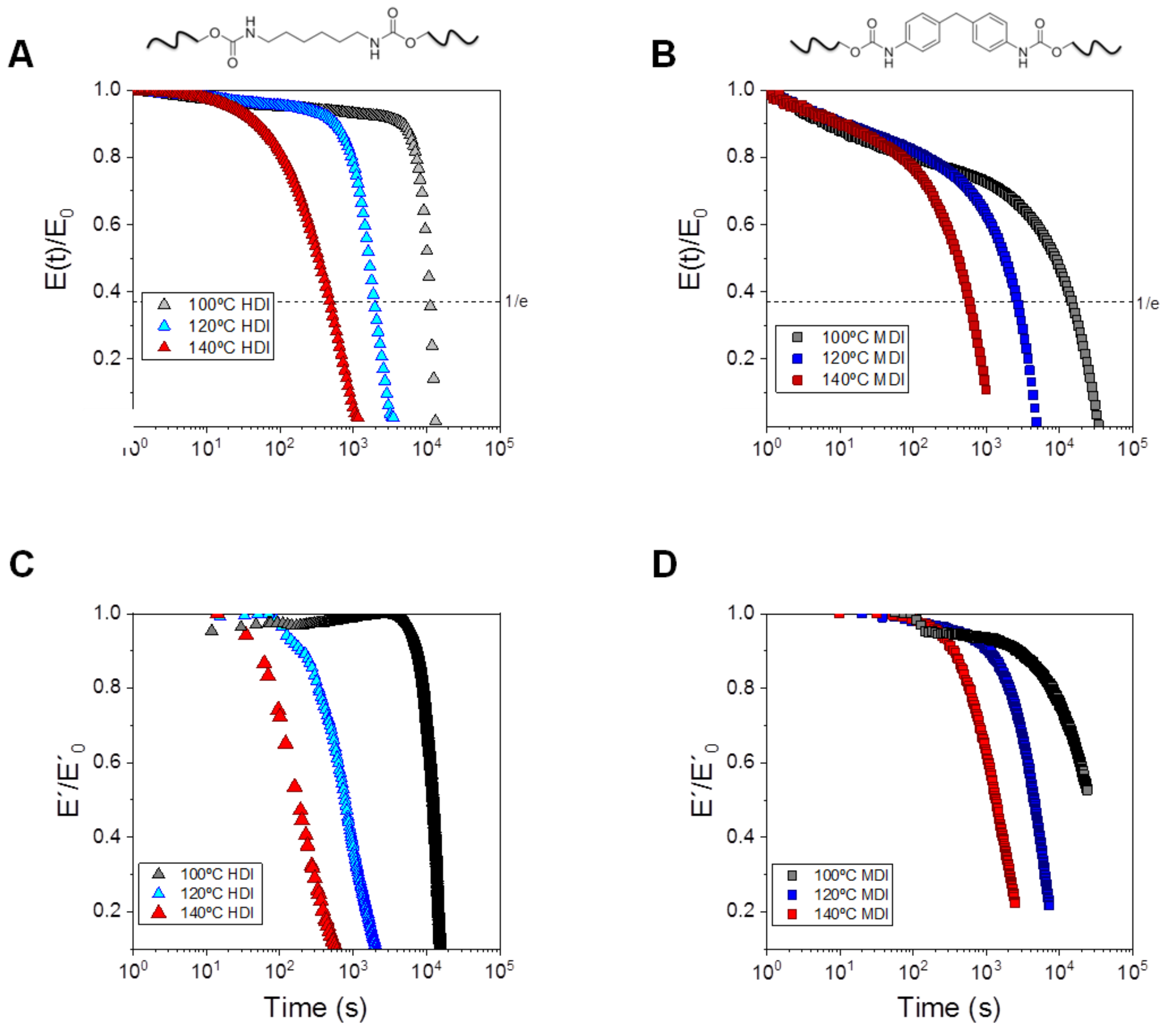

Figure 2.3. A) Stress-relaxation measurements for aliphatic (HDI) cross-linked polyurethanes performed at 100 °C, 120 °C and 140 °C. B) Stress-relaxation measurements for aromatic (MDI) cross-linked polyurethanes performed at 100 °C, 120 °C and 140 °C. C) Dynamic Mechanical Thermal Analysis (DMTA) experiments by means of isothermal time sweeps for aliphatic (HDI) crosslinked polyurethanes performed at 100 °C, 120 °C and 140 °C. D) Dynamic Mechanical Thermal Analysis (DMTA) experiments by means of isothermal time sweeps for aromatic (MDI) crosslinked polyurethanes performed at 100 °C, 120 °C and 140 °C.

2.2.3. Effect of the catalyst in the exchange reaction of aromatic and aliphatic polyurethanes

With the objective of increasing the rate of exchange reactions in polyurethane networks, several catalysts were introduced into the polymer network. 3 different catalysts were selected, organometallic, dibutyltin dilaurate (DBTDL) acid, p-toluensulfonic acid (PTSA), and basic, triazabicyclodecene (TBD). Dibutyltin dilaurate (DBTDL) is the most commonly employed organotin catalyst for the industrial synthesis of polyurethanes and the most studied one for novel dynamic polyurethane thermosets based on non-hydroxyl mediated transcarbamoylation reactions[24,25,26]. With the aim of investigating alternatives to DBTDL,[20] PTSA and TBD organocatalysts, which have shown to be effective catalyst for polyurethane preparation, were also selected.

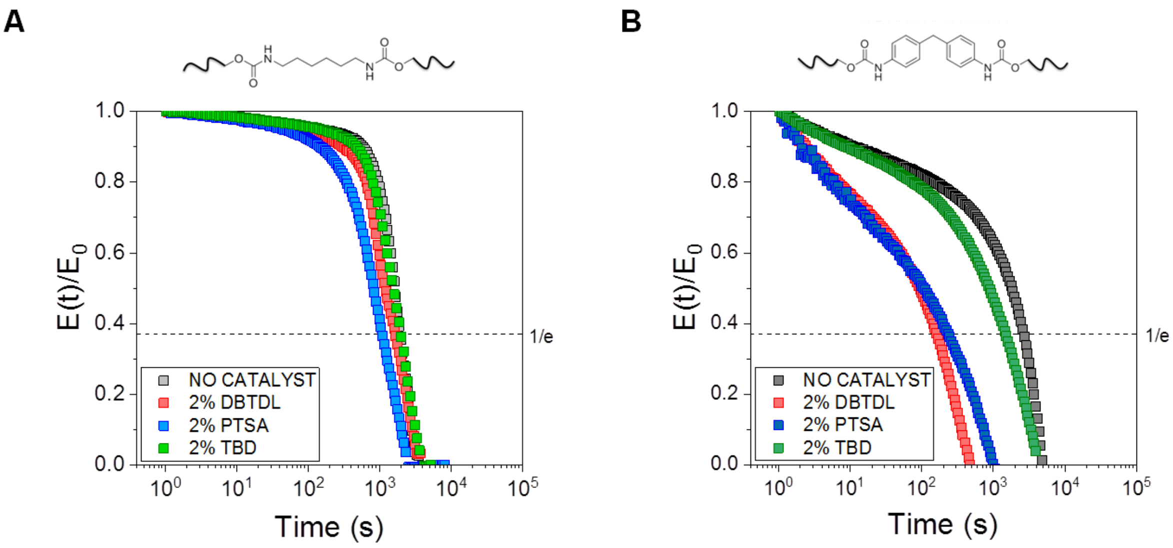

Figure 2.4. A) Stress-relaxation measurements for cross-linked aliphatic polyurethanes (A) and aromatic polyurthanes (B) measured at 120 °C.

For the introduction of these catalysts into the polymer networks, polyurethanes were synthesized as before but prior to curing in the oven, 2 mol % of DBTDL, PTSA or TBD were added to the pre-polymer (1 equiv.) and 1,6-Hexanediol (1.1 equiv) mixture.

The relaxation curves obtained for the aliphatic polyurethanes are shown in Figure 2.4A and demonstrate that the introduction of catalysts does not show any enhancement in the dynamic behavior of the aliphatic cross-linked polyurethanes. Similar to the case in the absence of catalyst, we can therefore relate this drop to the degradation of the material. Surprisingly, the network containing DBTDL did not show any improvement in the dynamic behavior, contrary to what we expected on the basis of previous studies at high temperatures[19]. To further explore this behavior, we prepared another polyurethane network introducing three times the amount of DBTDL (6 mol %). Stress relaxation measurements showed the same behavior as before (Figure S2.3), and it can therefore be concluded that even at higher contents of catalyst, the dynamic behavior does not change significantly.

The effect of catalyst was explored for the aromatic polyurethanes. In this case the addition of different catalysts clearly changed the behavior of the urethane network (Figure 2.4B). Aromatic cross-linked polyurethanes with PTSA and DBTDL catalysts showed much shorter relaxation times of close to 200 seconds. In order to study whether an increase of DBTDL could increase the speed of network relaxation, 6 mol % of DBTDL was introduced into the aromatic network, but we did not observe any difference in the stress relaxation behavior (Figure S2.4). Finally, while TBD showed a small increase of the dynamic behavior, this change in the network behavior was negligible in comparison to the impact of DBTDL and PTSA.

To ensure that the fast relaxation was not due to the degradation of the network, DMTA measurements were performed (Figure S2.5) which showed that the networks remain unaffected.

As previously described, the exchange reaction in polyurethane networks can arise either via an associative exchange mechanism, enabled by free alcohol groups that remain in the network, or via a dissociative exchange mechanism, by means of the reversible dissociation of the urethane group into an isocyanate and an alcohol (Figure 2.1 A & B).

In order to confirm the predominant mechanism for bond exchange, aromatic polyurethane networks without free alcohol groups were synthesized by decreasing the content of 1,6-Hexanediol to 1.0 equivalent. These new aromatic polyurethane materials were compared with the previously synthesized aromatic polyurethane networks containing free alcohol groups (1.1 equivalents of 1,6-Hexanediol). If polyurethane thermosets undergo predominantly associative exchange, samples without free alcohols available in the network will not speed up the relaxation time, showing the same behavior as non catalyzed samples. The performance of PTSA and DBTDL was evaluated as stress relaxation measurements demonstrated that both these catalysts were active in enhancing the relaxation of aromatic polyurethane networks (Figure 2.4).

As can be seen in Figure 2.5. A, the catalytic effect of PTSA was only noticeable when free alcohol groups were present in the network, and there was no enhancement of the dynamic activity of the aromatic polyurethanes when the network was only constituted by urethane linkages. This result confirms that PTSA catalyzes the associative transcarbamoylation mechanism. On the other hand, DBTDL showed enhancement of the dynamic behavior for all cases as can be seen in Figure 2.5. B. This result suggests that although DBTDL is known to enhance the transcarbamoylation reaction via the free hydroxyl groups, it is also able to enhance dissociative exchange in MDI based PU networks. Characteristic Arrhenius plots and activation energies for PTSA catalyzed (free OH network) and DBTDL catalyzed (free and not free OH) networks are shown in Figure 2.5. C. As shown, the activation energies for DBTDL containing formulations present activations energies in the range of 150-160 kJ/mol, very similar to those presented in literature[22]. In addition, the activation energy for the free OH containing sample is slightly lower. In our opinion, it is due to both associative and dissociative processes can take place simultaneously. In comparison, PTSA containing samples present two different trends. At low temperatures, the activation energy is similar to those of DBTDL based systems (158 kJ/mol). However, above 120 °C the relaxation processes slowdown in comparison to DBTDL references, resulting in lower Ea values. It is to know that these temperatures are near the boiling temperature of PTSA (140 °C) so we assign this efficiency loss to the evaporation of the catalyst.

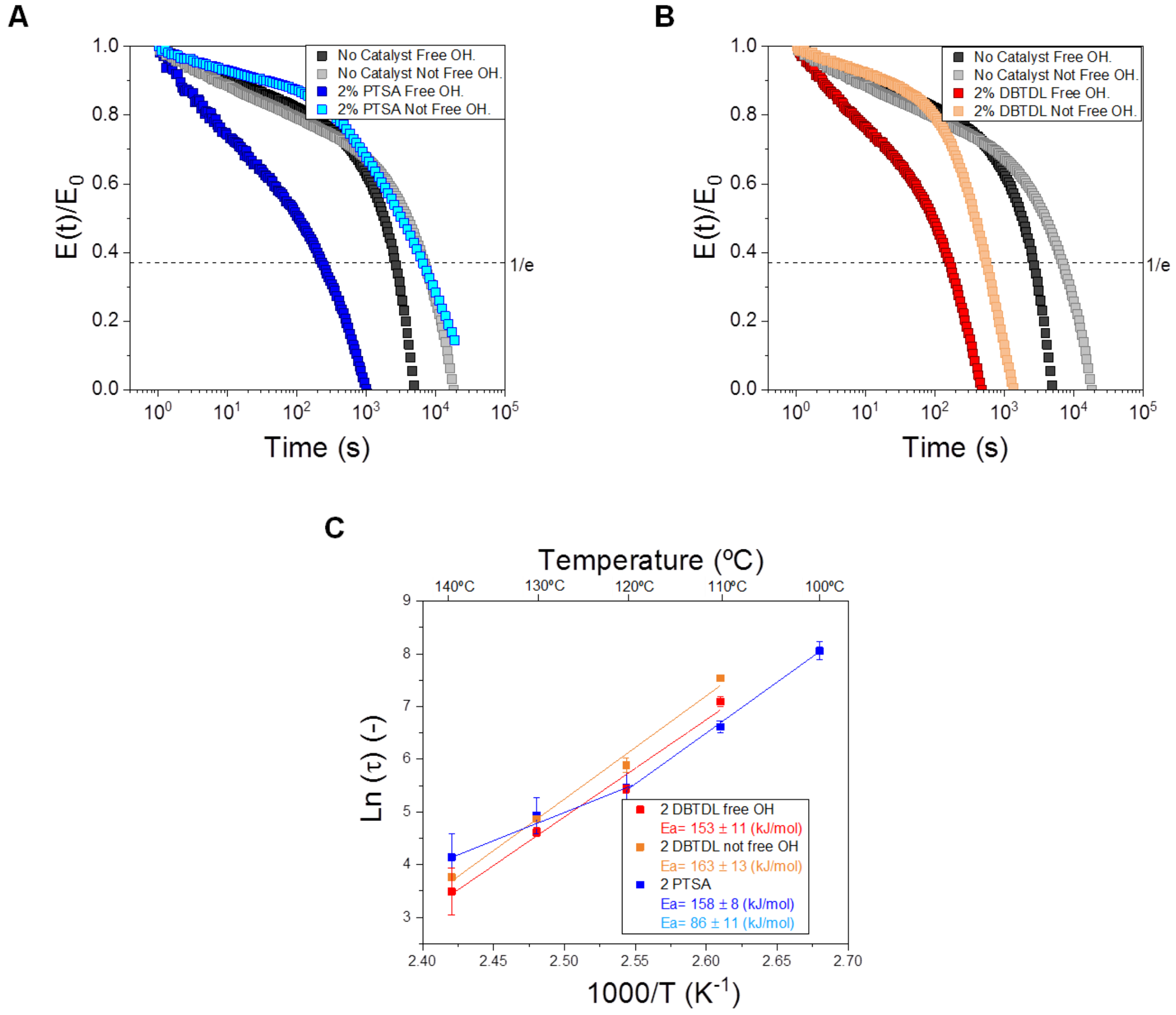

Figure 2.5. A) Stress relaxation analysis for no catalyst and 2 mol % PTSA catalyzed aromatic PU samples, free alcohol and without performed at 120°C B) Stress-relaxation analysis for no catalyst and 2 mol % DBTDL catalyzed aromatic PU samples, with excess of free alcohol and without performed at 120 °C. C) Arrhenius plots of characteristic relaxation times of catalyzed aromatic PU samples.

2.2.4. Model study of associative and dissociative exchange mechanisms in presence of PTSA and DBTDL catalysts

As it was demonstrated that PTSA and DBTDL were the most effective catalysts to enhance the dynamic behavior of cross-linked aromatic polyurethanes, their performance was evaluated using low molecular weight molecules as model reactions. For the study of the associative exchange mechanism, aromatic and aliphatic urethane model compounds were synthesized and mixed with equimolar content of 3-methyl 1-butanol (Figure 2.6 A). The model reactions without a catalyst were used as a benchmark and for the catalyst evaluation 2 mol % of PTSA or DBTDL was added to the reaction mixture. Model reactions were characterized by ^{1}H-NMR.

Regardless of the aromatic or aliphatic nature, in the absence of catalyst urethane model compounds did not react with 3-methyl 1-butanol and only the starting compounds were observed in both cases, in agreement with the data of polyurethane networks. In the case of the aromatic polyurethanes, in the presence of the catalysts (Figure 2.6 B), the exchange reaction was observed with both catalysts, consistent with the fast stress relaxation given in cross-linked aromatic polyurethanes. In the case of aliphatic polyurethanes the presence of PTSA did not show any enhancement of the exchange reactions, in agreement with the observations for polyurethane thermosets. In contrast, DBTDL was shown to be able to promote the exchange reaction in the aliphatic model compound. This observation differs from the stress relaxation curves obtained for the polymer network as it was not able to speed up the exchange before the degradation took place. It should be noted however that this exchange is much less pronounced in the case of aliphatic urethanes in comparison to aromatic urethanes. These results confirm that both PTSA and DBTDL are able to enhance associative exchange in aromatic urethanes. This behavior has been further investigated between 110 °C and 140 °C. Has can be seen in the supporting information (Figure S2.6 and Figure S2.7), DBTDL has been proved to be more reactive in this range of temperatures than PTSA but it has to be mention that at 130 °C and 140 °C secondary products can be observed. We believe that the formation of these secondary compounds is due to the ability of DBTDL to enhance the dissociation of aromatic urethanes, forming reactive free isocyanates. PTSA catalyzed reactions presented very low conversions, in contrast to the rheological performance of PTSA containing networks. These differences between chemical model experiments and dynamic polymer networks have been properly explained in one of the last perspective about dynamic materials by Du Prez *et al.*[27] In addition, it is to consider the boiling point of the catalyst and the difficulty to be well integrated in the reaction mixture, unlike in polymers, where the acid catalyst has been well dissolved, dispersed and introduced into the network during the curing step at 70 °C.

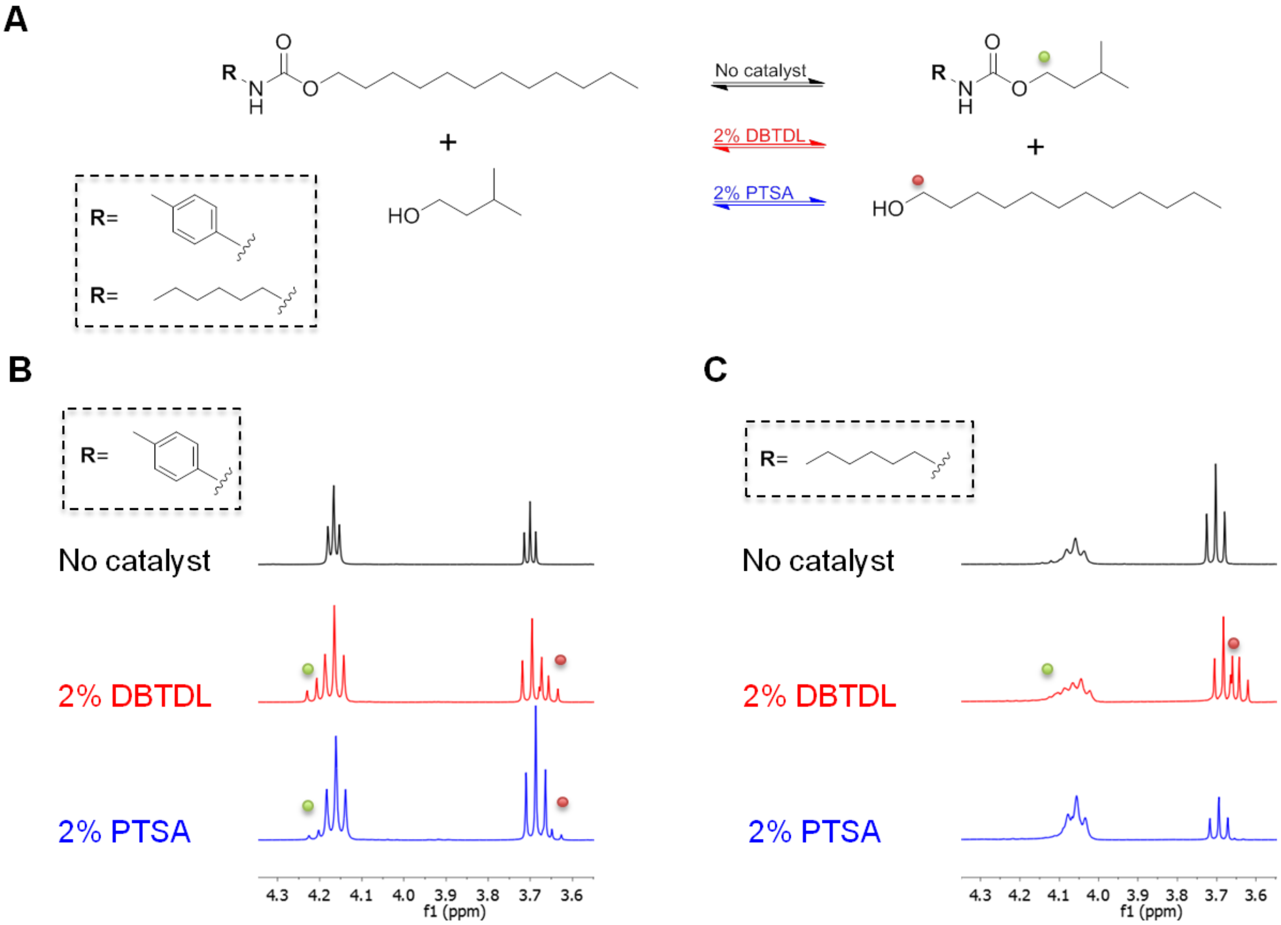
A
R
N
H
O
O
+
HO
R=
R=
No catalyst
2% DBTDL
2% PTSA
B
R=
No catalyst
2% DBTDL
2% PTSA
4.3 4.2 4.1 4.0 3.9 3.8 3.7 3.6
f1 (ppm)
C
R=
No catalyst
2% DBTDL
2% PTSA
4.3 4.2 4.1 4.0 3.9 3.8 3.7 3.6
f1 (ppm)

Figure 2.6 A) Alcohol mediated transcarbamoylation reaction between N-tolyl-O-dodecyl urethane or N-hexyl-O-dodecyl urethane with 3-methyl-1-butanol to give the corresponding model exchange compounds. ^{1}H-NMR of the reaction mixture of the aromatic model compound (B) and the aliphatic model compound (C) taken after heating at 120 °C for 48h.

Besides associative exchange, in order to investigate whether there is any dissociative exchange further model reactions were performed. As shown in Figure 2.7 A HDI and MDI were end-capped with either 1-dodecanol (D-R-D) or 1-hexanol (H-R-H).

Equimolar mixtures of model compounds with different molecular weights were reacted at 120 °C for 48h under air and analyzed by MALDI-TOF. The spectra for aromatic diurethane compounds without catalyst (black spectra), with 2% of DBTDL (red spectra) and 2% of PTSA (blue spectra) are shown in Figure 2.7 B and C for aromatic and aliphatic urethanes respectively. Peaks labeled with numbers correspond to products in the reactive mixture plus the Na cation. The characterization of H-R-H and D-R-D aliphatic and aromatic model compounds and of the employed matrix can be found from Figure S2.8 to Figure S2.18.

Analyzing both sections (Figure 2.7 B and C), it can be observed that in the absence of catalyst and in the presence of PTSA no exchange product was found for MDI and HDI based model compounds. This is in agreement with the results obtained in polyurethane thermosets where PTSA was observed to only catalyze the associative exchange mechanism. In contrast, in the presence of DBTDL the exchange product can be observed in the spectra. While in the aliphatic model reaction the exchange product was observed at relatively low intensity, in the aromatic model reaction the signal from exchange product was higher than that of the starting compounds. These results are consistent with the results obtained in the polymer networks as DBTDL was shown to catalyze both associative and dissociative exchange in the aromatic polyurethanes.

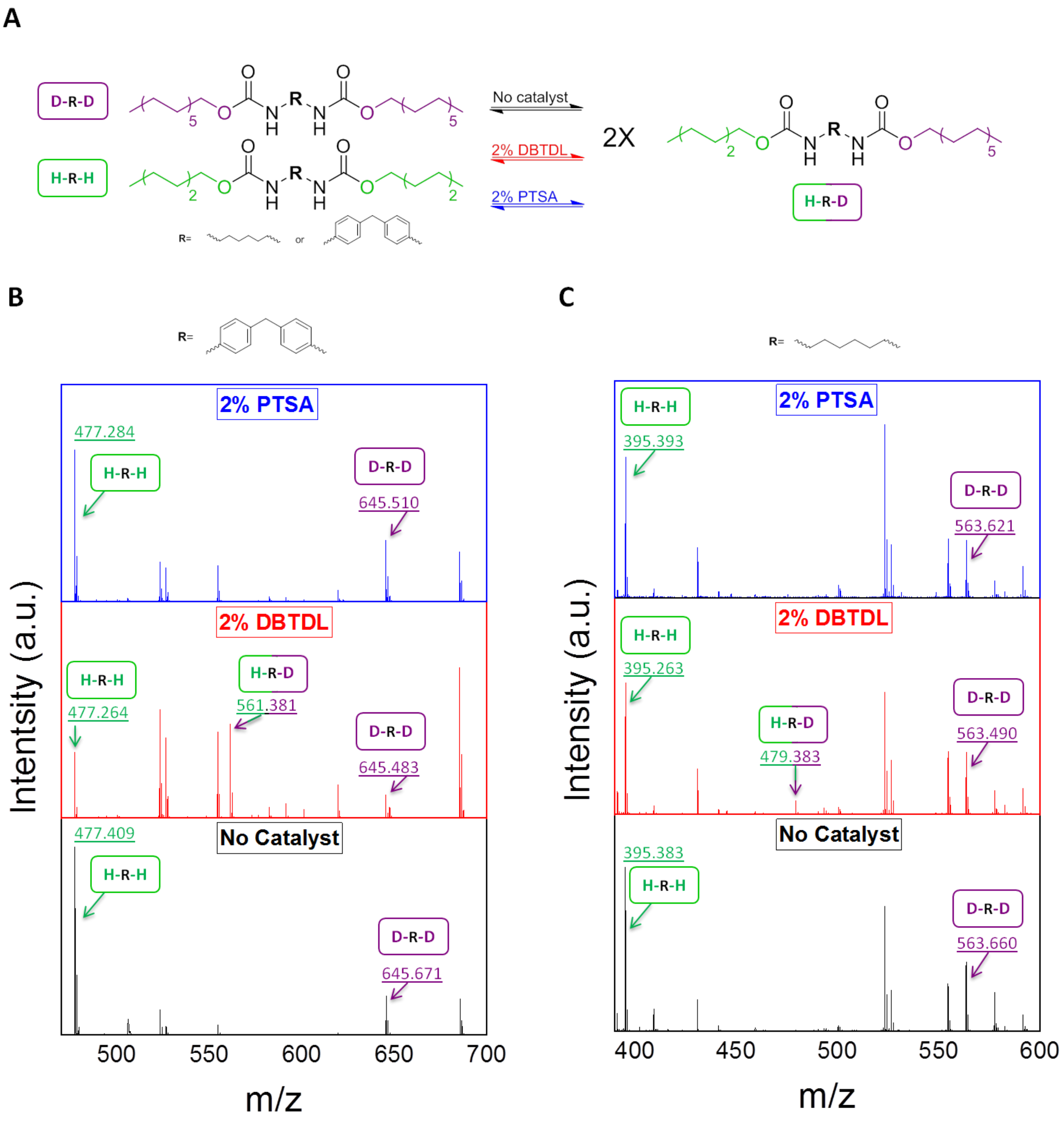

Figure 2.7 A) Non-hydroxyl mediated transcarbamoylation reaction for aliphatic and aromatic diurethane model compounds at 120 °C for 48 hours. Characterization by MALDI-TOF for aromatic (B) and aliphatic (C) model reactions. The characterization of H-R-H and D-R-D aliphatic and aromatic model compounds and of the employed matrix can be found from Figure S2.8 to Figure S2.18.

2.3. Conclusion

In summary, it has been demonstrated that the dynamic nature of polyurethanes is strongly dependent on both the characteristics of the polyurethane network (type of isocyanate and the NCO/OH ratio) and the presence of catalyst. Thus, PTSA and DBTDL were both shown to be effective catalysts for enhancing the dynamics of exchange in aromatic polyurethane thermosets at mild conditions, whereas TBD was not observed to have a significant effect. In addition, the nature of the catalyst was shown to influence the mechanism of bond exchange with PTSA catalyzing the transcarbamoylation reaction only the in presence of free alcohol groups *via* associative exchange, while DBTDL was shown to catalyze both *via* associative and dissociative mechanisms. Overall, this chapter offers an insight into the influence of structural parameters and catalyst effects in the dynamic nature of polyurethanes and could enhance the reusability and recyclability of commercial polyurethane thermosets.

2.5. References

(1) Jehanno, C.; Sardon, H. Dynamic Polymer Network Points the Way to Truly Recyclable Plastics. *Nature* **2019**, *568* (7753), 467–468. https://doi.org/10.1038/d41586-019-01209-3.

(2) Fortman, D. J.; Brutman, J. P.; Cramer, C. J.; Hillmyer, M. A.; Dichtel, W. R. Mechanically Activated, Catalyst-Free Polyhydroxyurethane Vitrimers. *J. Am. Chem. Soc.* **2015**, *137* (44), 14019–14022. https://doi.org/10.1021/jacs.5b08084.

(3) Occams Business Research and Consulting. *Global Polyurethane Market, Forecast 2014-2020*; Vol. 5699.

(4) Denissen, W.; Winne, J. M.; Du Prez, F. E. Vitrimers: Permanent Organic Networks with Glass-like Fluidity. *Chem. Sci.* **2016**, *7* (1), 30–38. https://doi.org/10.1039/c5sc02223a.

(5) Montarnal, D.; Capelot, M.; Tournilhac, F.; Leibler, L. Silica-like Malleable Materials from Permanent Organic Networks. *Science (80-.).* **2011**, *334* (6058), 965–968. https://doi.org/10.1126/science.1212648.

(6) Erice, A.; Ruiz de Luzuriaga, A.; Matxain, J. M.; Ruipérez, F.; Asua, J. M.; Grande, H. J.; Rekondo, A. Reprocessable and Recyclable Crosslinked Poly(Urea-Urethane)s Based on Dynamic Amine/Urea Exchange. *Polymer (Guildf).* **2018**, *145*, 127–136. https://doi.org/10.1016/j.polymer.2018.04.076.

(7) Denissen, W.; Droesbeke, M.; Nicola, R.; Leibler, L.; Winne, J. M.; Du Prez, F. E. Chemical Control of the Viscoelastic Properties of Vinylogous Urethane Vitrimers. *Nat. Commun.* **2017**, *8*. https://doi.org/10.1038/ncomms14857.

(8) Denissen, W.; Rivero, G.; Nicolaÿ, R.; Leibler, L.; Winne, J. M.; Du Prez, F. E. Vinylogous Urethane Vitrimers. *Adv. Funct. Mater.* **2015**, *25* (16), 2451–2457. https://doi.org/10.1002/adfm.201404553.

(9) Obadia, M. M.; Jourdain, A.; Cassagnau, P.; Montarnal, D.; Drockenmuller, E. Tuning the Viscosity Profile of Ionic Vitrimers Incorporating 1,2,3-Triazolium Cross-Links. *Adv. Funct. Mater.* **2017**, *27* (45), 1–10. https://doi.org/10.1002/adfm.201703258.

(10) Bobade, S. K.; Paluvai, N. R.; Mohanty, S.; Nayak, S. K. Bio-Based Thermosetting Resins for Future Generation: A Review. *Polym. - Plast. Technol. Eng.* **2016**, *55* (17), 1863–1896. https://doi.org/10.1080/03602559.2016.1185624.

(11) McBride, M. K.; Worrell, B. T.; Brown, T.; Cox, L. M.; Sowan, N.; Wang, C.; Podgorski, M.; Martinez, A. M.; Bowman, C. N. Enabling Applications of Covalent Adaptable Networks. *Annu. Rev. Chem. Biomol. Eng.* **2019**, *10* (1), 175–198. https://doi.org/10.1146/annurev-chembioeng-060718-030217.

(12) Gu, Y.; Zhao, J.; Johnson, J. A. A Unifying Review of Polymer Networks: From Rubbers and Gels to Porous Frameworks. *Angew. Chemie Int. Ed.* **2019**, 2–30. https://doi.org/10.1002/anie.201902900.

(13) Post, W.; Susa, A.; Blaauw, R.; Molenveld, K.; Knoop, R. J. I. A Review on the Potential and Limitations of Recyclable Thermosets for Structural Applications. *Polym. Rev.* **2019**, *60* (2), 359–388. https://doi.org/10.1080/15583724.2019.1673406.

(14) Aguirresarobe, R. H.; Irusta, L.; Fernandez-Berridi, M. J. Application of TGA/FTIR to the Study of the Thermal Degradation Mechanism of Silanized Poly(Ether-Urethanes). *Polym. Degrad. Stab.* **2012**. https://doi.org/10.1016/j.polymdegradstab.2012.06.019.

(15) Cherng, J. Y.; Hou, T. Y.; Shih, M. F.; Talsma, H.; Hennink, W. E. Polyurethane-Based Drug Delivery Systems. *Int. J. Pharm.* **2013**, *450* (1–2), 145–162. https://doi.org/10.1016/j.ijpharm.2013.04.063.

(16) Chattopadhyay, D. K.; Webster, D. C. Thermal Stability and Flame Retardancy of Polyurethanes. *Prog. Polym. Sci.* **2009**, *34* (10), 1068–1133. https://doi.org/10.1016/j.progpolymsci.2009.06.002.

(17) Herck, V. N.; Maes, D.; Unal, K.; Guerre, M.; Winne, J. M.; Du Prez, F. E. Covalent Adaptable Networks with Tunable Exchange Rates Based on Reversible Thiol–Yne Cross-Linking. *Adv. Mater.* **2020**, *59* (9), 3637–3646. https://doi.org/10.1002/ANGE.201912902.

(18) Yan, P.; Zhao, W.; Fu, X.; Liu, Z.; Kong, W.; Zhou, C.; Lei, J. Multifunctional Polyurethane-Vitrimers Completely Based on Transcarbamoylation of Carbamates: Thermally-Induced Dual-

Shape Memory Effect and Self-Welding. *RSC Adv.* **2017**, *7* (43), 26858–26866. https://doi.org/10.1039/c7ra01711a.

(19) Zheng, N.; Fang, Z.; Zou, W.; Zhao, Q.; Xie, T. Thermoset Shape-Memory Polyurethane with Intrinsic Plasticity Enabled by Transcarbamoylation. *Angew. Chemie - Int. Ed.* **2016**, *55* (38), 11421–11425. https://doi.org/10.1002/anie.201602847.

(20) Sardon, H.; Pascual, A.; Mecerreyes, D.; Taton, D.; Cramail, H.; Hedrick, J. L. Synthesis of Polyurethanes Using Organocatalysis: A Perspective. *Macromolecules* **2015**, *48* (10), 3153–3165. https://doi.org/10.1021/acs.macromol.5b00384.

(21) Bossion, A.; Heifferon, K. V.; Meabe, L.; Zivic, N.; Taton, D.; Hedrick, J. L.; Long, T. E.; Sardon, H. Opportunities for Organocatalysis in Polymer Synthesis via Step-Growth Methods. *Prog. Polym. Sci.* **2019**, *90*, 164–210. https://doi.org/10.1016/j.progpolymsci.2018.11.003.

(22) Fortman, D. J.; Sheppard, D. T.; Dichtel, W. R. Reprocessing Cross-Linked Polyurethanes by Catalyzing Carbamate Exchange. *Macromolecules* **2019**, *52* (16), 6330–6335. https://doi.org/10.1021/acs.macromol.9b01134.

(23) Prenveille, T.; Garreau, C.; Matner, M.; Dijkstra, D.; Oppermann, W.; Johannsmann, D. Reactivity of Urethanes at High Temperature: Transurethanization and Side Reactions. *J. Polym. Sci. Part A Polym. Chem.* **2019**, *57* (5), 621–629. https://doi.org/10.1002/pola.29301.

(24) Guan, G.; Kusakabe, K.; Sakurai, N.; Moriyama, K. Transesterification of Vegetable Oil to Biodiesel Fuel Using Acid Catalysts in the Presence of Dimethyl Ether. *Fuel* **2009**, *88* (1), 81–86. https://doi.org/10.1016/j.fuel.2008.07.021.

(25) Schenzel, A.; Hufendiek, A.; Barner-Kowollik, C.; Meier, M. A. R. Catalytic Transesterification of Cellulose in Ionic Liquids: Sustainable Access to Cellulose Esters. *Green Chem.* **2014**, *16* (6), 3266–3271. https://doi.org/10.1039/c4gc00312h.

(26) Nath, M. Toxicity and the Cardiovascular Activity of Organotin Compounds: A Review. *Appl. Organomet. Chem.* **2008**, *22* (10), 598–612. https://doi.org/10.1002/aoc.1436.

(27) Winne, J. M.; Leibler, L.; Prez, F. E. Du. Dynamic Covalent Chemistry in Polymer Networks: A Mechanistic Perspective. **2019**, *10*, 6091–6108. https://doi.org/10.1039/c9py01260e.

Chapter 3

Chapter 3. Introduction of alkoxyamine based diols to tune the dynamic behavior of aliphatic polyurethanes

3.1. Introduction

In the previous chapter, we explored the dynamic behavior of aliphatic and aromatic polyurethanes. The aliphatic PUs did not show any faster stress-relaxation in presence of different catalyst, thus, the dynamicity of these materials should be triggered by the introduction of other fast and interesting exchange chemistries.

For this reason, orthogonal chemistries have been selected and introduced in order to trigger dynamic behavior following other functional alternatives[1]. Several examples have emerged recently, such as aromatic disulfur[2] and diseleinides[3], alkoxyamines[4], Diels-Alder exchange reactions[5] and so. In fact the development of new chemistries for producing exchangeable bonds is an intense research field.

Among these available dynamic chemistries, radical chemistry allows the fastest exchange. As explained in the section *1.6.1 Introduction of dynamic bonds into polyurethane networks* of the first chapter, different radical mediated recombination can be classified in two groups according to the following exchange mechanism. On the one hand, thiuram disulfides, aromatic and aliphatic disulfides and diseleinides bonds are classified inside the group that follows associative-dissociative exchange mechanism[6]. By implementing so in CANs, Matijaszewski and coworkers create self-healing polymers by reshuffling thiuram disulfide bonds at ambient temperatures under visible light[7]. Aromatic and aliphatic disulfides have been widely employed in polyurethane based CANs[2,8] and in our group their performance it has been also compared to diseleinide bearing polyurethane dynamic networks[3]. On the other hand, according to the radical exchanges that just recombine following the dissociative path, alkoxyamine chemistry is the predominant group and has emerged as one of the most promising dynamic linkages. In this alternative, much more radical species are created comparing to the abovementioned mechanism[9].This aspect is directly related to the bond dissociation energy (BDE) and the stability of the formed radical. As explained by Audran and coworkers, the BDE of alkoxyamines is given by the sum of thermodynamic and polar terms[10]. The first term (thermodynamics), takes into account the steric strain and the stability of the released radical species. On the other hand, polar term describes the electronegativity difference between O and C groups in these compounds. Equal electron sharing between abovementioned atoms gives the lowest BDE and thus, the equilibrium is more shifted to the open scenario.

This fast recombination of thermally reversible C-ON bonds has been proved for self-healing materials in previous works[11–13] proving repeated crosslinking and de-crosslinking. Finally the crack healing of polyurethanes has been proved due to the introduction of 4-hydroxy-1-(20-hydroxy-10-phenyl-10-methyl)ethyl-TEMPO (diol)[14]. Recently, the abovementioned TEMPO structure has been modified to delete NO-C bond and insert and N-S-S-S-N (TEMPO-trisulfide) dynamic bond and compare with its performance with N-S-S-N (TEMPO-disulfide) analog. Eventhough the synthetic knowledge of these groups was set up for the first time[15] decades ago, these bonds have not been applied until Otsuka and coworkers synthesized and explored acrylate moieties bearing these groups to create thermally healable crosslinked polymers[16].

Alkoxyamines are very interesting structures due to to the potential modification of neighbor groups that can tune bond dissociation kineticks. This concept has been particularly investigated for the field of controlled radical polymerization where it is essential to understand the reactivity of C–ON[17,18].

Nevertheless, there has not been studied the key role that different alkoxyamine structures could play in order to tune the reprocessing temperature in polyurethane networks. In this work, two novel alkoxyamine based diols named as PV1 and PV2 have been designed and synthesized in our search for a dynamic bond with tunable dissociation temperatures (Scheme 3.8.). We target to obtain different dissociation temperature ranges just by small variation in their molecular structures. After the evaluation of their dissociation behavior, these novel alkoxyamine-based diols have been introduced as chain extenders in the conventional aliphatic PU formulation studied in Chapter 2, to subsequently enhance the dynamicity of crosslinked polyurethane materials at different temperatures. This concept has been proved for aliphatic polyurethane thermosets, in order to give dynamic behavior at low temperatures, as in previous work has been demonstrated that introducing several catalysts does not enhance transcarbamoylation reactions for this type of polyurethanes even at mild- high temperatures[19].

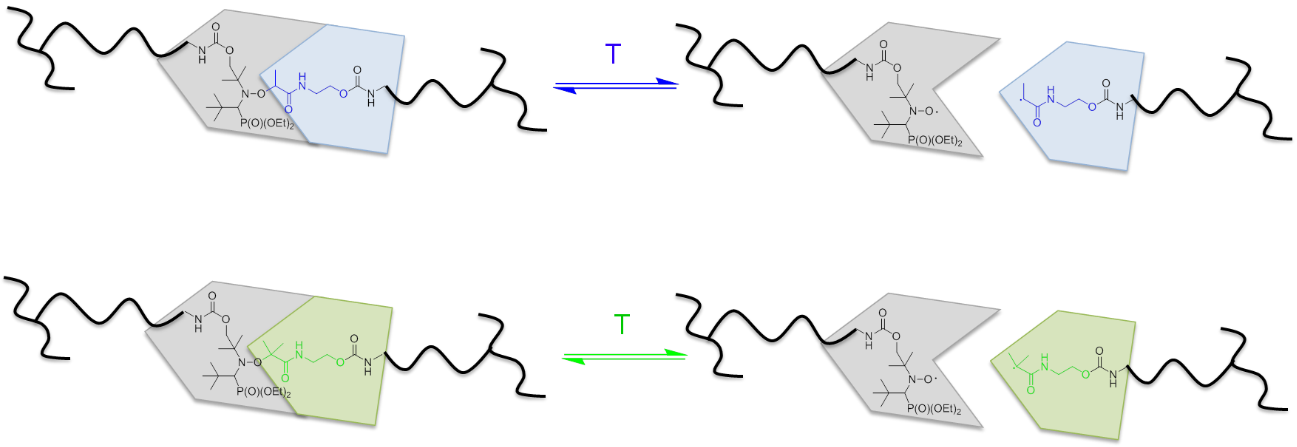

Scheme 3.8. Dissociation equilibrium of PV1 (blue, top) and PV2 (green, bottom) alkoxyamine based diols on nitroxide and alkyl group.

3.2. Results and discussion

3.2.1. Synthesis and characterization of different alkoxyamine based diols

The molecular structures of the two different alkoxyamines employed in this chapter are shown in Scheme 3.2. From now on, and looking for an easier manner to name these molecules, they will be named as PV1 and PV2 respectively as shown in Scheme 3.2 A and B.

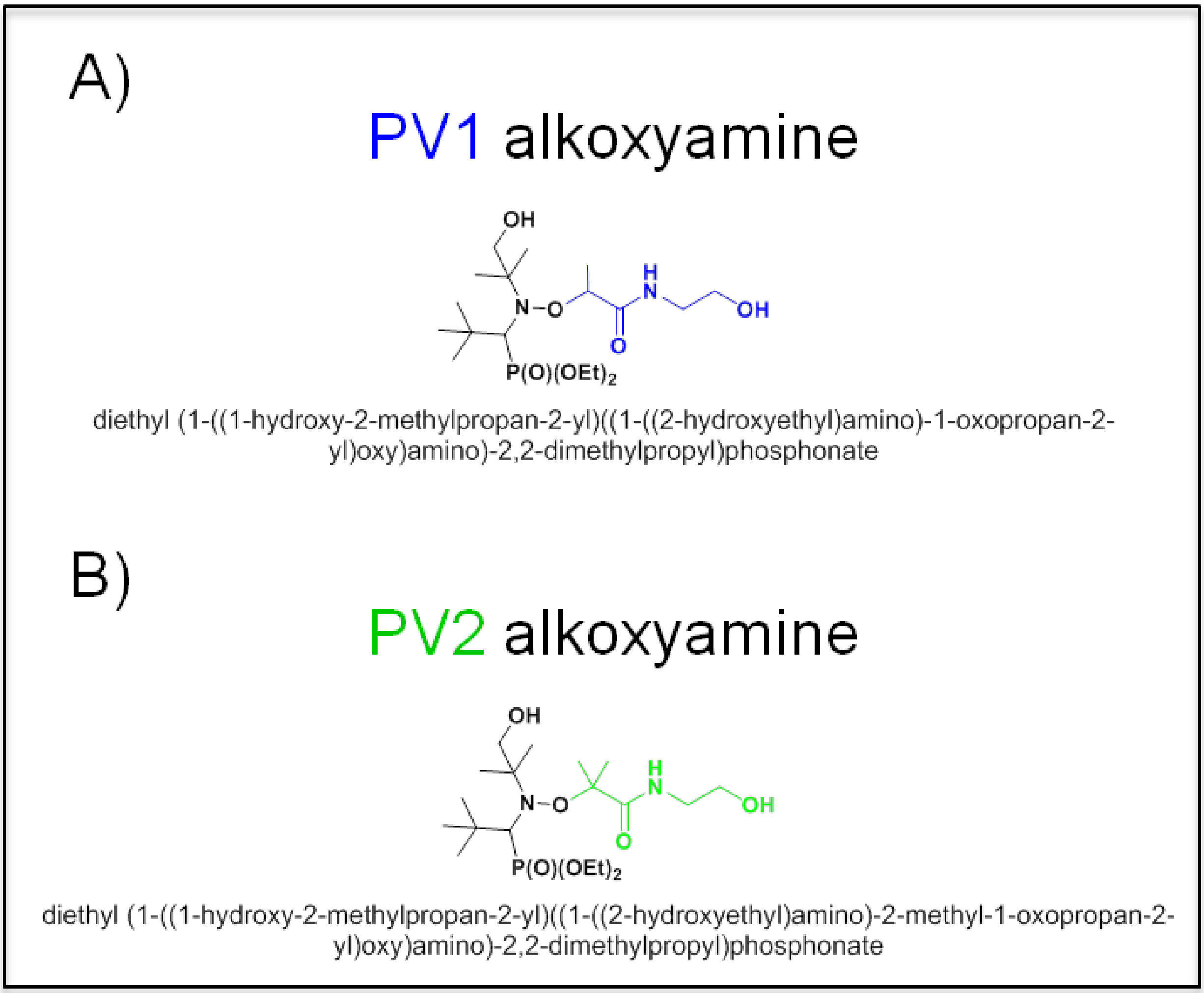
A)
PV1 alkoxyamine
OH
H
N
N–O
OH
O
P(O)(OEt)2
diethyl (1-((1-hydroxy-2-methylpropan-2-yl)((1-((2-hydroxyethyl)amino)-1-oxopropan-2-yl)oxy)amino)-2,2-dimethylpropyl)phosphonate
B)
PV2 alkoxyamine
OH
H
N
N–O
OH
O
P(O)(OEt)2
diethyl (1-((1-hydroxy-2-methylpropan-2-yl)((1-((2-hydroxyethyl)amino)-2-methyl-1-oxopropan-2-yl)oxy)amino)-2,2-dimethylpropyl)phosphonate

Scheme 3.9. Molecular structures and chemical nomenclatures of PV1 alkoxyamine (A) and PV2 alkoxyamine (B) respectively.

In order to understand how small modifications in molecular structure of alkoxyamines affect to the fast radical exchange ability of these species, PV1 (R=H) and PV2 (R=CH_3) alkoxyamine based diols have been synthesized.

The alkoxyamines were designed in a two step process were the nitroxide part and the alkyl group were synthesized separately and coupled afterwards. The nitroxide was synthesized based on the previously published pathway of Acerbis *et al.*[20] (

Figure 3.1 A). The alkyl group (2-bromo-N-(2-hydroxyethyl)-propanamide in case of PV1 and 2-bromo-N-(2-hydroxyethyl)-2-methylpropanamide for PV2) were synthesized based on a procedure described by Huang and Chang[21] (

Figure 3.1 B). Afterwards, an atom-transfer radical addition (ATRA) was performed between the nitroxide and the alkyl group to obtain the final product (

Figure 3.1 C).

A) Synthesis of nitroxide radical

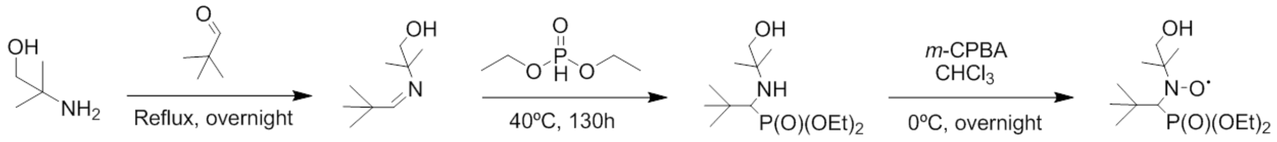
OH
NH2
O
Reflux, overnight
OH
N
O
P
H
O
O
40ºC, 130h
OH
NH
P(O)(OEt)2
m-CPBA
CHCl3
0ºC, overnight
OH
N-O˙
P(O)(OEt)2

B) Synthesis of alkyl parts

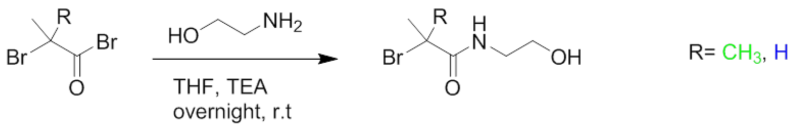
R
Br
Br
O
HO
NH2
THF, TEA
overnight, r.t
R
Br
H
N
OH
O
R= CH3, H

C) Atom transfer radical addition to obtain alkoxyamines

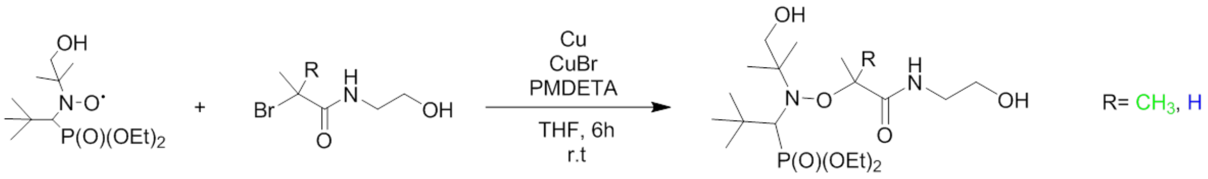
OH
N-O˙
P(O)(OEt)2
+
R
Br
H
N
OH
O
Cu
CuBr
PMDETA
THF, 6h
r.t
OH
N-O
R
H
N
OH
O
P(O)(OEt)2
R= CH3, H

Figure 3.1. Synthetic procedure employed to obtain PV1 and PV2 alkoxyamines. First a three step reaction pathway has been followed to obtain a nitroxide radical (A). Concurrently, the aliphatic part of each alkoxyamine has been synthesized (B). Finally, an atom transfer radical addition was carried out to acquire alkoxyamine based diols (C).

These molecular structures have been characterized by ^{1}H-NMR, as can be seen in Figure 3.2.1H-NMR spectra of PV1 (R=H) (A) and PV2 (R=CH3) (B) alkoxyamine based diols.Figure 3.2 A and B. Attending to the ^{1}H-NMR spectras of both alkoxyamines several similarities can be found. Thus, signals corresponding to the methyl protons appear between 1 and 1.5 ppm. At higher ppm values (3.0- 3.5 ppm) we find the signals corresponding to $C\underline{H}_2$ protons adjacent to OH and NH groups. Signal number 12 corresponding to the proton of the carbon bonded to N and P atoms appear at 3.65 ppm in both cases. Multiplets 13 and 14 (3.9-4.1 ppm) correspond to the $C\underline{H}_2$ protons of the diethylphosphite group. To conclude with the similarities, protons bonded to alcohol groups ($O\underline{H}$, 4.6-4.8 ppm) and amide groups ($CON\underline{H}$, 8.2 ppm) appear at highest values.

Certainly two big differences can be found analyzing both spectra. Attending to the signal number 8, relative to the R group, it is noticeable the integration difference in both alkoxyamines. In the spectra of PV1 alkoxyamine the integration value of signal number 8 gives 3, as expected for the methyl group. In PV2 alkoxyamine, this signal value is close to 6, as expected due to the 2 methyl substituents. As a consecuence of this different structure, also in PV1 alkoxyamine the corresponding peak (number 15) for the proton boned to the carbon atom adjacent to the oxygen can be found. The absence of this peak in PV2 spectra also confirms the molecular structure of this alkoxyamine. These characterizations were corroborated by COSY experiments (Figure S3.1and Figure S3.2 for PV1 and PV2 respectively).

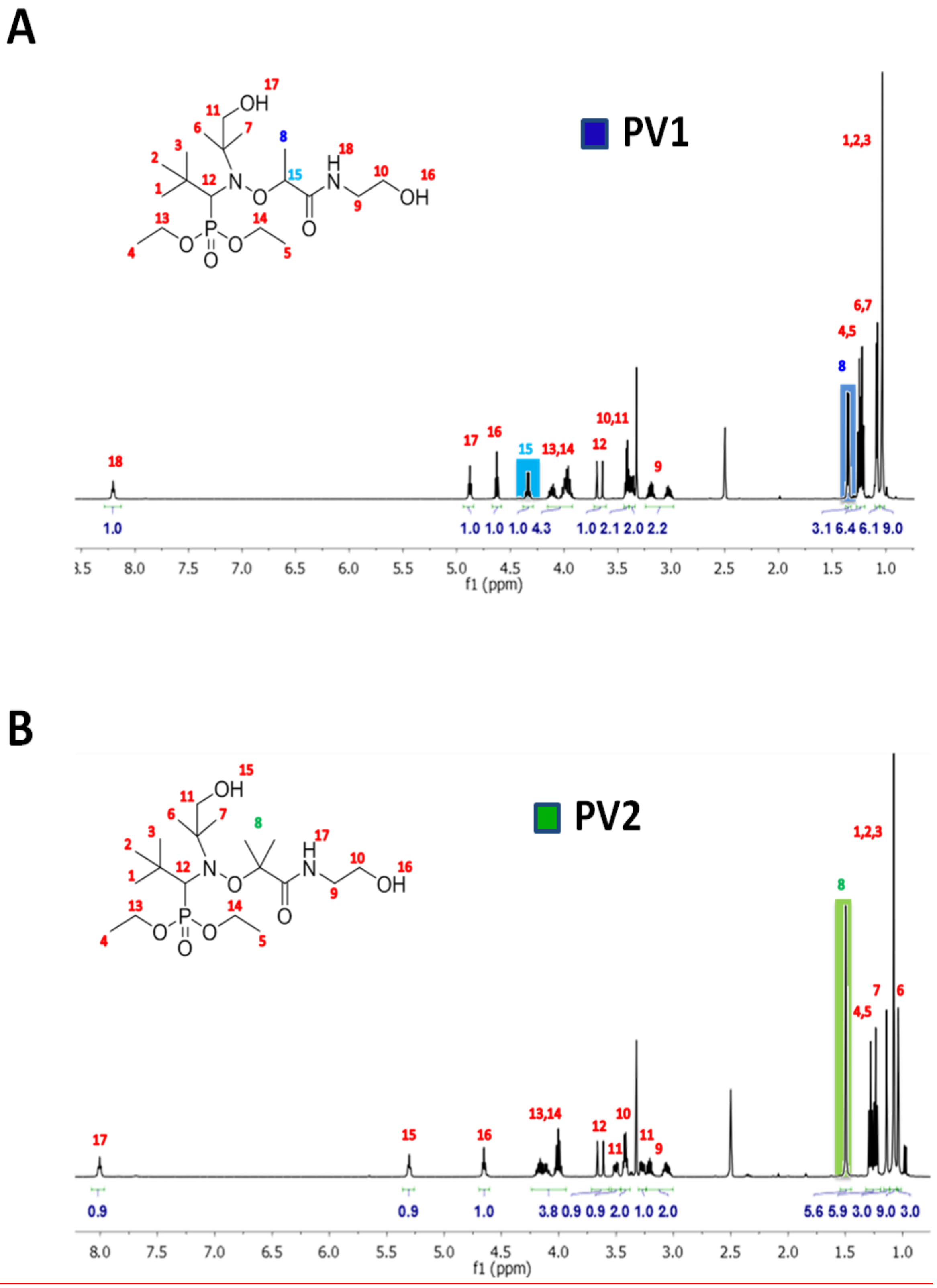

Figure 3.2. ^{1}H-NMR spectra of PV1 (R=H) (A) and PV2 (R=CH_3) (B) alkoxyamine based diols.

The radical excision and recombination of the alkoxyamine moieties can potentially provide a dynamic character to synthesized films (Scheme 3.8).

The dissociation ability of the alkoxyamine has been further evaluated using computational chemistry and compared to aromatic disulfide a well reported fast exchange dynamic bond. To do so density functional theory (DFT) calculations have been performed to evaluate the bond dissociation energy (BDE) of the NO-C bond. The calculated BDEs for the NO-C bond in PV1 (33.08 kcal·mol^{-1}) and in PV2 (26.13 kcal·mol^{-1}) are lower than those observed for aromatic disulfides (around 48 kcal·mol^{-1}) a well-known moiety used in self-healing polymers, which supports the potential of these two alkoxylamines to provide a fast exchange in mild conditions[6].

Electron paramagnetic resonance (EPR) measurements have been carried out in order to understand and compare the temperature dependence of the radical concentration formed upon heating both PV1 and PV2 alkoxyamines (Figure 3.3 A and B). Both EPR measurements showed an increasing signal associated to the appearance of radical species associated to the N-O-C bond. Interestingly, it is a strong dependence of the formed radicals with the chemical structure. PV2 alkoxyamine shows higher dissociative ability in all the range of temperatures studies. This effect is more clearly seen in the EPR signal *vs.* temperature plot (Figure 3.3 C). PV2 alkoxyamine is able to produce a radical excision in mild conditions, as it shows a noticeable increase of the signal near 80 ^{o}C. In contrast, PV1 alkoxyamine dissociates much slower. This effect is related to both the higher stabilization of the generated alkyl radical and the higher steric hindrance within the starting alkoxyamine [22]. However, PV2 show a remarkable drop in the EPR signal at high temperatures, which will be discussed more in detail in a later section.

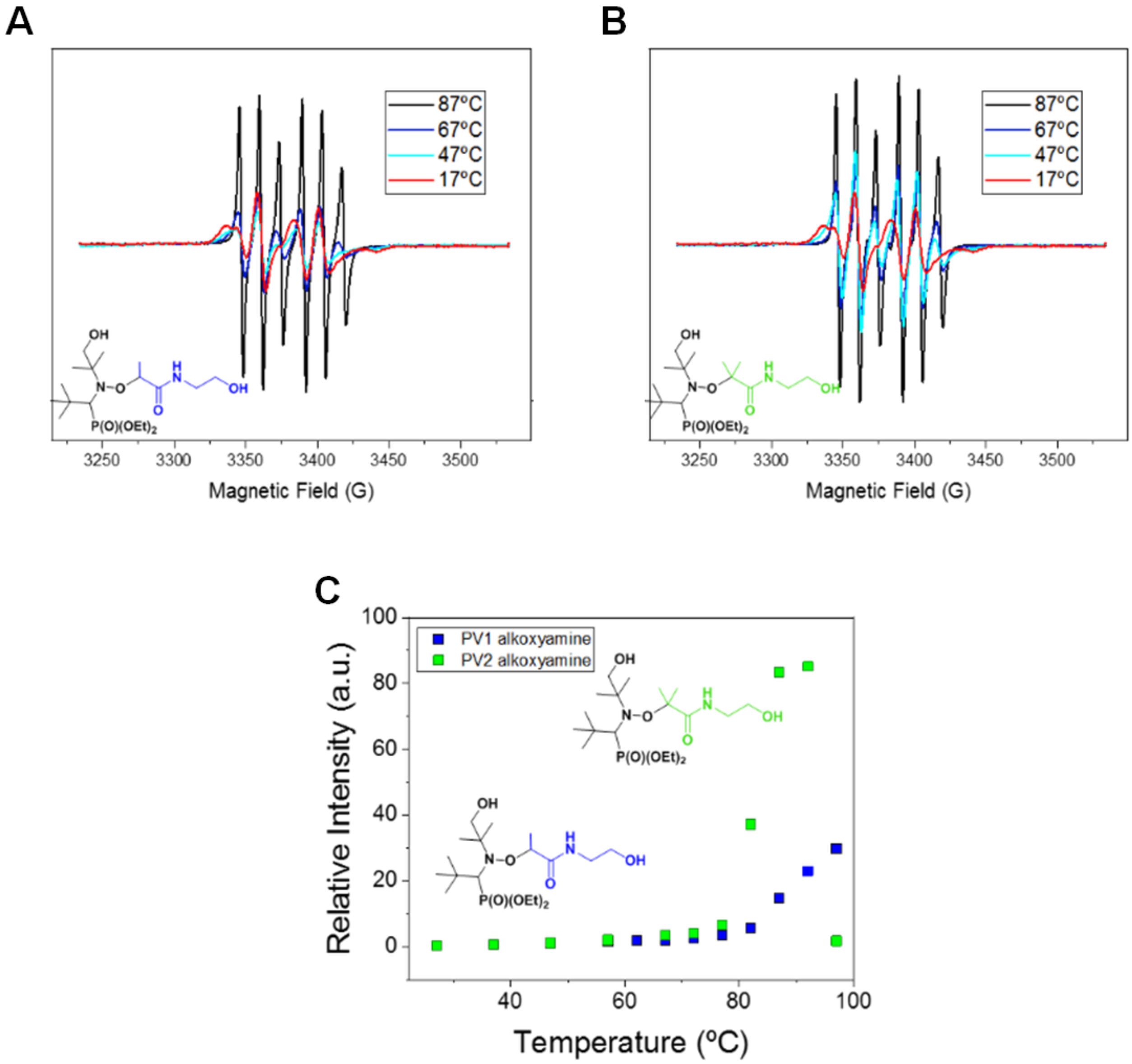

Figure 3.3. Free radical intensities versus temperature obtained by electron paramagnetic resonance (EPR) for both PV1 (A) and PV2 alkoxyamines (B), respectively. The values of the signal integration vs temperature are shown for both alkoxyamines (C).

3.2.2. Synthesis of aliphatic polyurethane network containing PV2 alkoxyamine

In order to confirm the capabilities of synthesized alkoxyamines to develop dynamic thermosets, we introduced PV1 or PV2 in a reference polyurethane thermoset structure, as shown in Figure 3.4 A. The proposed structure allowed us to easily tune the dynamic structure by introducing different chain extenders such as previously mentioned alkoxyamine and the non-dynamic 1,6-Hexanediol (HDO).To do so, the pre-polymer strategy was followed. First, we synthesized a tris-isocyanate terminated pre-polymer by reacting commercially available poly(propylene glycol) (PPG) with an average molecular weight of 3.7 kDa, with hexamethylene diisocyanate (HDI). The isocyanate selection was based on taking into account our previous research where has been demonstrated that aliphatic polyurethane thermosets do not undergo transcarbamoylation exchange reactions that could allow these materials to stress relax at temperatures as low as 120 ^{o}C[19]. The reference material was obtained in a second step by adding 1,6-Hexanediol to the pre-polymer. After a complete curing (60 ^{o}C, overnight), a cross-linked material and aliphatic polyurethane film was acquired. Dynamic thermoset films were synthesized by replacing different amounts of the aforementioned chain extender equivalents by PV1 or PV2 alkoxyamine. For all cases 2 mol % of DBTDL was added before the curing step. This catalyst was employed first of all because it has fast catalytic activity for the synthesis of polyurethanes and moreover it has been proved that does not promote any dynamic behavior in aliphatic polyurethane thermosets synthesized with HDI[19].

To follow both steps (pre-polymer formation and the subsequent curing process) FTIR spectroscopy was employed (Figure 3.4 B). As can be seen in the synthesis of dynamic aliphatic polyurethane networks with 1,6-Hexanediol (Figure S3.3) and alkoxyamines, the isocyanate stretching band at 2271 cm^{-1} completely disappeared and new bands corresponding to formation of the urethane group appeared at 1718 cm^{-1}. The band at 1654 cm^{-1} appeared due to the stretching of the NH-CO group of alkoxyamines. In all of the cases, the proposed synthetic pathway led to homogeneous transparent polymers for alkoxyamine based polyurethanes (Figure 3.4 C).

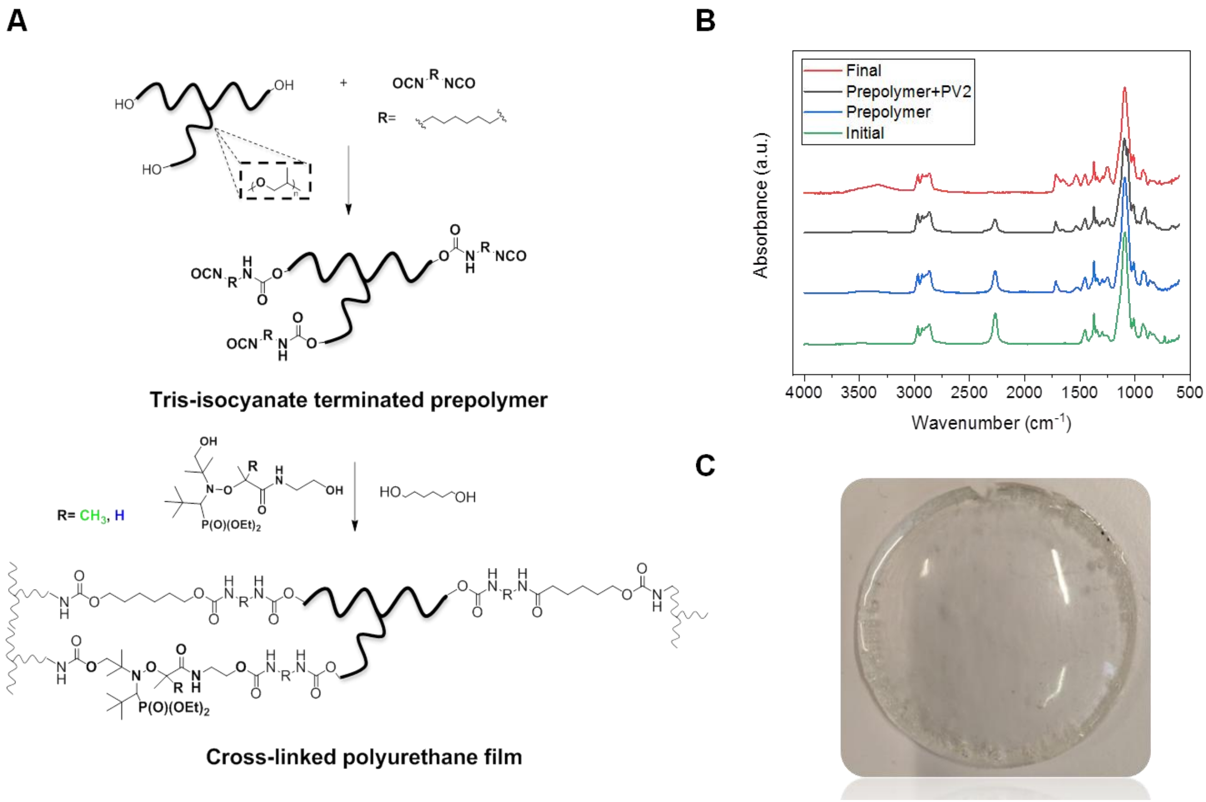
A
HO
OH
HO
+
OCN R NCO
R=
Tris-isocyanate terminated prepolymer
R= CH3, H
P(O)(OEt)2
HO OH
Cross-linked polyurethane film
B
Final
Prepolymer+PV2
Prepolymer
Initial
Absorbance (a.u.)
4000
3500
3000
2500
2000
1500
1000
500
Wavenumber (cm-1)
C

Figure 3.4. A) Synthetic procedure for obtaining aliphatic (HDI) cross-linked polyurethanes with different contents of PV2 alkoxyamine and 1,6-Hexanediol (HDO) has chain-extenders following the pre-polymer strategy. B) Representative FTIR spectra of synthesized pre-polymer with HDI (blue trace) and after the addition of PV2 alkoxyamine and 1,6-Hexanediol (black trace). Red trace corresponds to the final polyurethane film crosslinked for 1h at 70 ^{o}C. C) Representative film of the obtained materials.

3.2.3. Effect of chemical structure and concentration of alkoxyamines in the dynamic behavior of aliphatic polyurethane thermosets

After characterizing the films, the dynamic behavior of the different films has been analyzed by stress-relaxation measurements in tension mode at different temperatures and compared with the blank polyurethane without any dynamic bond. In both cases 50 mol % on 1,6-Hexanediol has been exchanged by the corresponding alkoxyamine. As expected, the increase in temperature fastened the relaxation of the material (Figure 3.5 A and B). Materials containing alkoxyamines showed a fast relaxation of the relaxation modulus E(t) on time even at temperatures below 100 ºC. However, it is important to remark that at room temperature we did not observe any relaxation of the crosslinked polyurethane film. At this condition, the dissociation equilibrium of alkoxyamine/nitroxide is shifted totally to the alkoxyamine state.

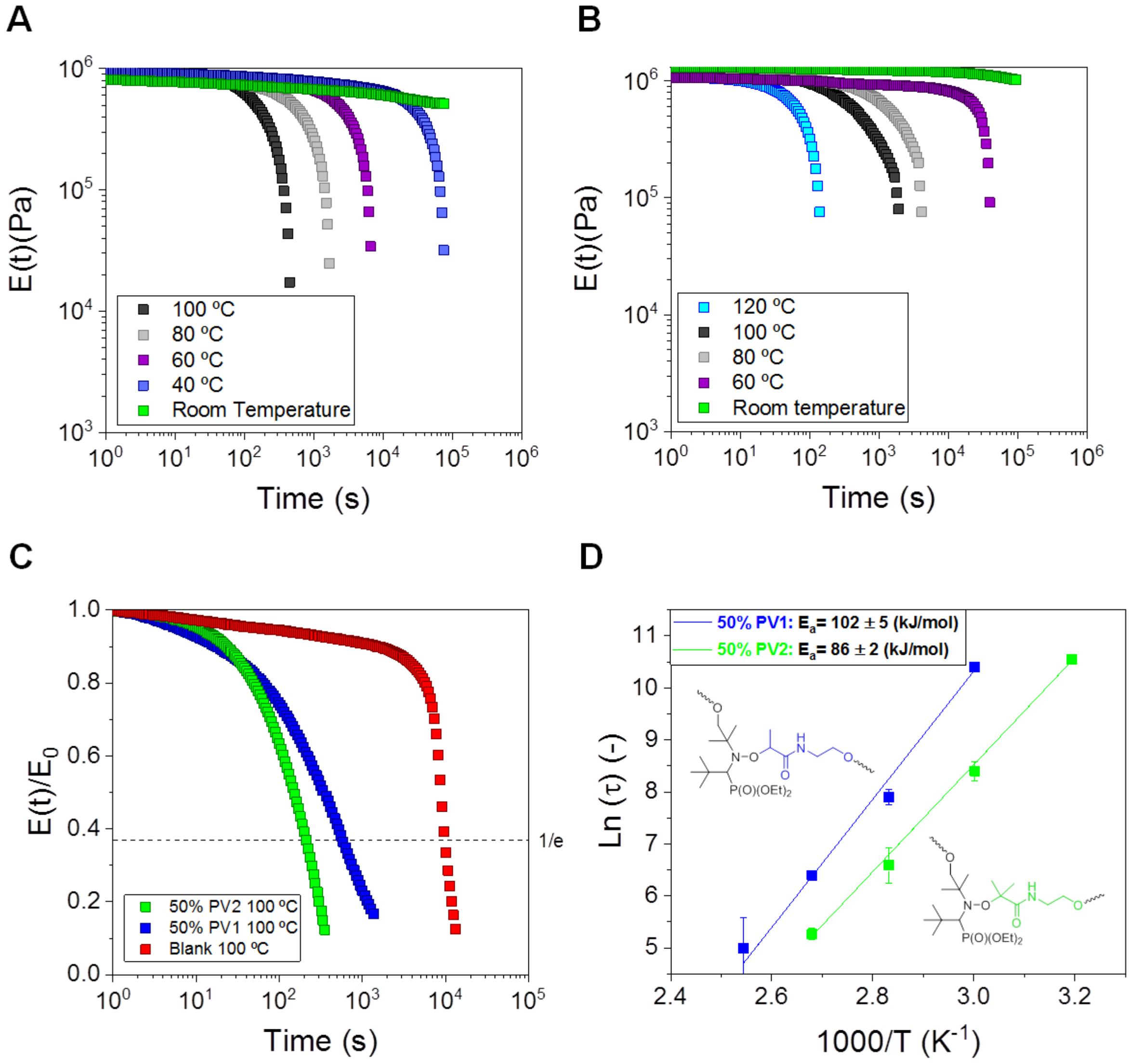

Figure 3.5 A) Stress-relaxation measurements for a representative network 50/50 (PV2/HDO) performed at 100 °C, 80 °C, 60 ºC, 40 ºC and room temperature B) Stress-relaxation measurements for a representative network 50/50 (PV1/HDO) performed at 120 °C,100 °C 80 °C, 60 ºC and room temperature C) Influence of the alkoxyamine concentration in the relaxation time. D) Arrhenius plot of characteristic relaxation time of cross-linked polyurethanes and their respective activation energies (E_a).

As can be seen in Figure 3.5 C, the relaxation is highly alkoxyamine nature dependent. Fast relaxation times have been obtained at 100 ^{o}C, temperatures above the estimated dissociation temperature of both PV1 and PV2 alkoxyamines. As expected from EPR measurements, the higher dissociative character of PV2 leads to a faster relaxation in the synthesized PU network. This effect is also reflected in the Arrhenius activation energy (Figure 3.5 D), that shows a higher value for PV1 (102 kJ/mol) than for PV2 (86 kJ/mol). It is to note that the un-functionalized sample shows a decay in the relaxation modulus a very long times (10^4 s), caused by partial degradation of the network, as we recently reported[19].

Additionally, the effect of the concentration of alkoxyamine in the dynamic character of polyurethane thermosets was analyzed using PV2 as reference (Figure S3.4). As shown in Figure S3.5A, the fast excision of alkoxyamine can produce the relaxation of the polymer network by just replacing a 25 mol% of the total chain extenders in the material. Even at this low concentration, the relaxation occurs below 1000 s at 100 ^{o}C. In addition, as can be seen in Figure S3.5 B, the activation energy shows a slightly dependence with the alkoxyamine concentration (from 100 to 80 kJ/mol). The difference in the activation energy can be related to the different mechanical performance of the polymer network ($E(t)_0$ values) when changing the alkoxyamine concentration.

3.2.4. Reprocessing capabilities of alkoxyamine based polyurethanes

Based on the results, the reprocessing capabilities of materials were tested (Figure 3.6). Thus, abovementioned dynamic networks were powder and placed in a thin metal layer mold and introduced in a hot press to reprocess them at 80 ^{o}C or 100 ^{o}C for 60 minute with a pressure of 200 bars. As can be seen in Figure 3.6 A, material is introduced as a white powder and after the reprocessing, discs with a diameter around 8 mm were obtained.

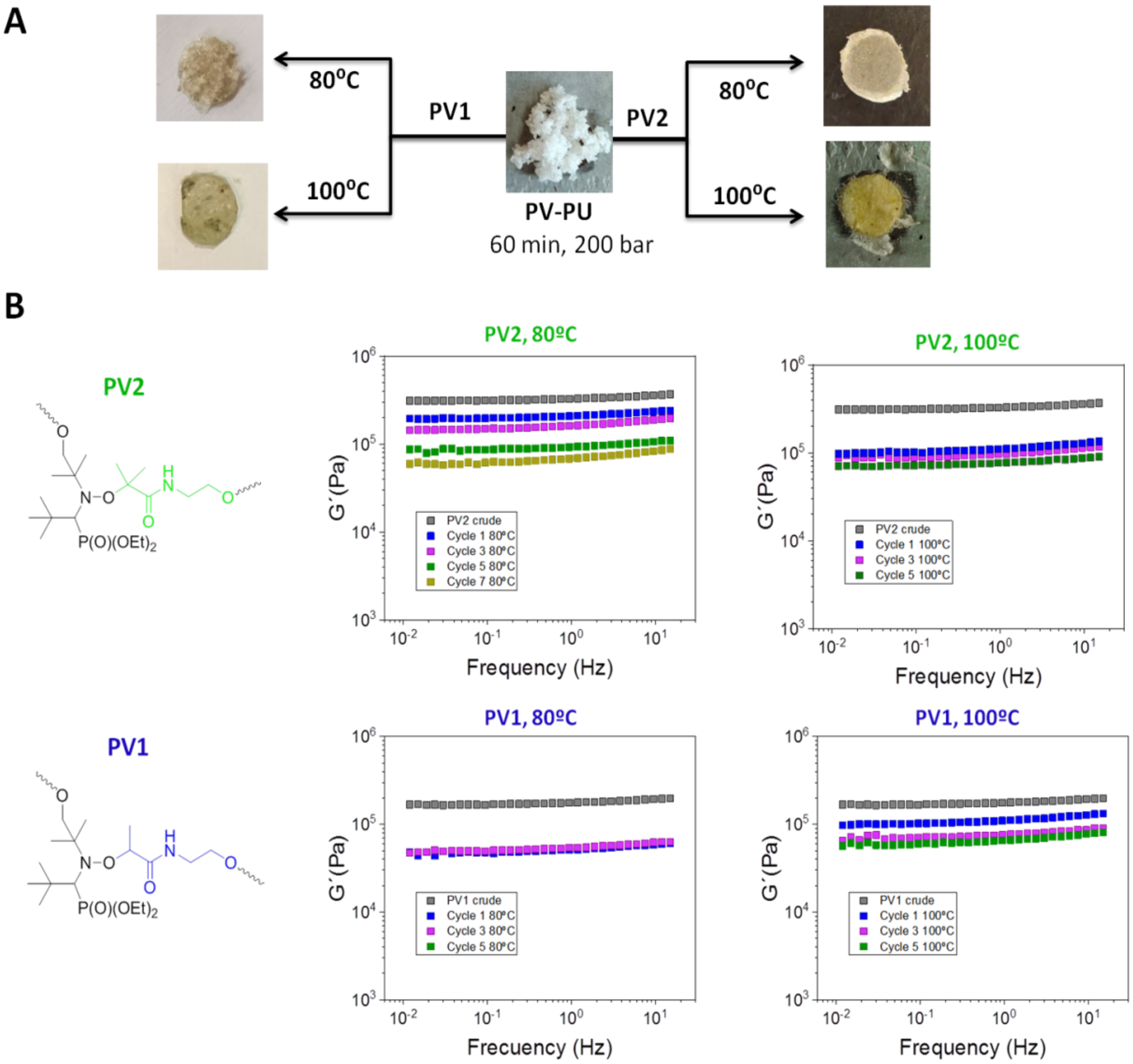

Figure 3.6. A) Reprocessing characteristics for the aforementioned 50/50 (PV/HDO) samples. B) Frequency sweeps after several reprocessing cycles at 80 °C or 100 °C for PV1 and PV2 based systems.

The mechanical characteristics of the polymer network were analyzed by small amplitude oscillatory shear experiments in frequency sweeps (Figure 3.6 B). In the case of PV2-PU network, the best reprocessed material was obtained at 80 °C as the obtained plateau modulus is close to the one of virgin material. However, as the number of cycles increases, the obtained plateau modulus for the material decays. This behavior is more noticeable for 100 °C and the drop in modulus is observed even for the first reprocessing cycle. A similar behavior is observed for PV1 at 100 °C. This behavior is attributed to degradation processes that will be discussed later on. It is to note that in the case of PV1-PU network, at 80 ^{o}C the temperature is still too low to effectively open the majority of the alkoxyamine linkages leading to inhomogeneous films with very low moduli.

3.2.5. Limitations of synthesized alkoxyamine based polyurethane thermosets

As observed in the reprocessing experiments, the mechanical properties of films decay as the number of cycles increases. In addition, according to EPR measurements, PV2 alkoxyamine suffers a sudden drop of radical concentration at 100 ^{o}C (Figure 3.3 C). In order to better understand this behavior, we performed ^{1}H-NMR for both alkoxyamines at different temperatures (Figure 3.1).

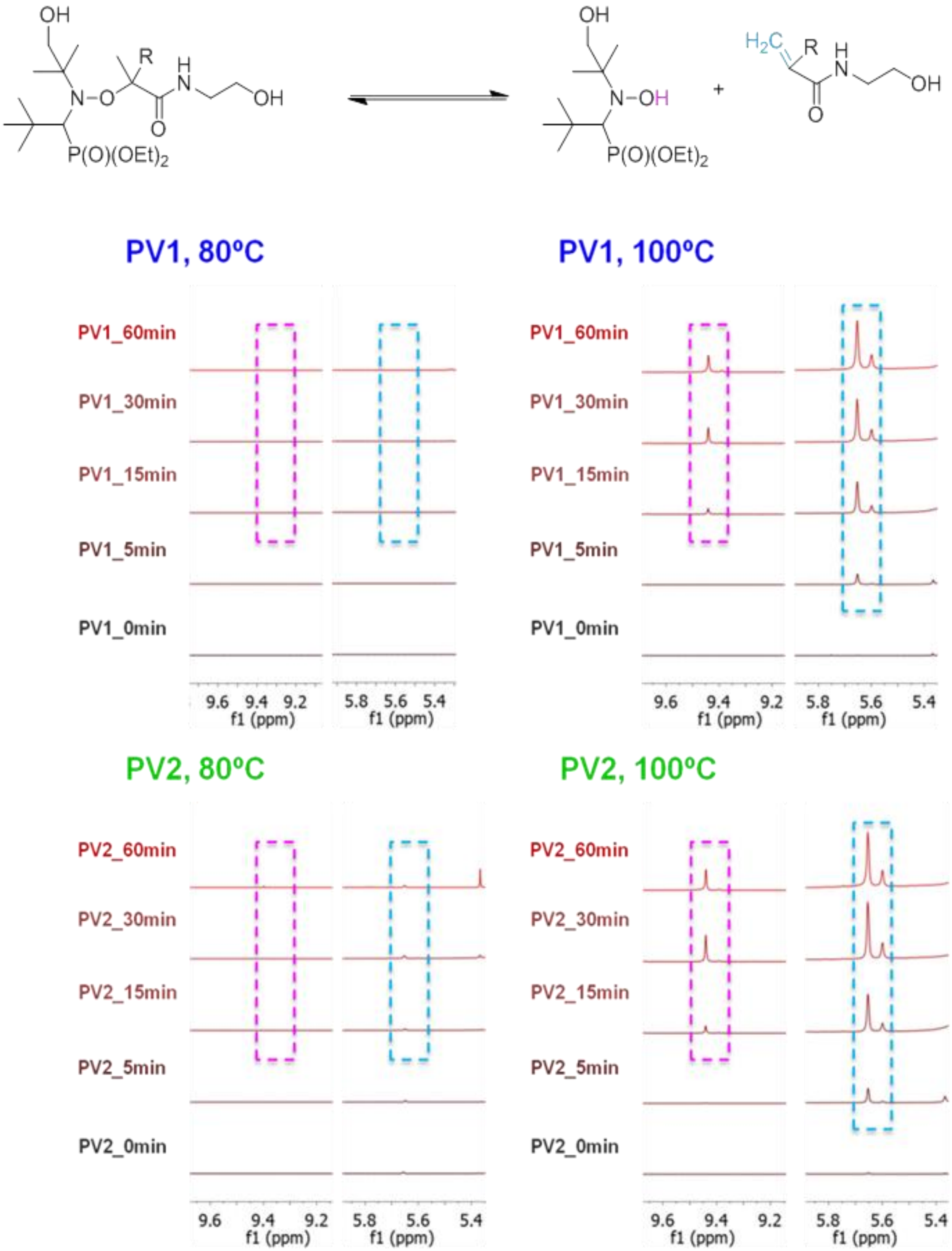

Figure 3.1. A) ^{1}H-NMR of PV1 (BLUE) and PV2 (GREEN) alkoxyamines pre-heated for 5, 15, 30 and 60 minutes at 80 ^oC and 100 ^oC

Several samples (5, 15, 30 and 60 minutes) of the heated solutions at 80 ^{o}C and 100 ^{o}C have been taken in order to understand the degradation behavior of each alkoxyamine-diol. Besides this, other signals have been observed in the ^{1}H NMR. The reduced nitroxide moiety can be easily characterize in both alkoxyamines. The increase of the pick at 9.5 ppm is noticeable at 100 ^{o}C. At 80 ^{o}C, these signals do not appear. These secondary reactions can be characterized also analyzing the vynil $C\underline{H}_2$ protons of the other undesired product. These signals are clearly present at 5.6 ppm, at 100 ^{o}C, for both alkoxyamines. At 80 ^{o}C, just some small signals can be seen at the longest times for the PV2 alkoxyamine.

It has to be taken into account also that at these molecular levels, solvent effect[23,24] and inter and intra molecular hydrogen bonding[10,25] can affect to the radical stability and bond dissociation equilibrium constant (k_d). However it clearly shows the possibility of side reactions at high temperatures.

3.3. Conclusion

In summary, in this chapter it has been demonstrated that the introduction of different alkoxyamines can tune the stress-relaxation of aliphatic polyurethane networks and therefore, become a key factor for the reprocessing of these materials at low temperatures.

Although, both alkoxyamine based diols have shown high dissociative behavior at 100 ^{o}C, its stability is compromised as shown by EPR and ^{1}H-NMR measurements, becoming PV2 alkoxyamine the most interesting and stable one for the final reprocessing of these materials at 80 ^{o}C. Overall, this work has proved the effective introduction of novel alkoxyamine based diols for the reprocessing of aliphatic polyurethane networks at temperatures as low as 80 ^{o}C, avoiding undesired secondary reactions that could occur from dissociative transcarbamoylation reactions at higher temperatures.

3.4. References

(1) Nellepalli, P.; Patel, T.; Oh, J. K. Dynamic Covalent Polyurethane Network Materials: Synthesis and Self-Healability. *Macromol. Rapid Commun.* **2021**, *42* (20), 1–33. https://doi.org/10.1002/marc.202100391.

(2) Rekondo, A.; Martin, R.; Ruiz De Luzuriaga, A.; Cabañero, G.; Grande, H. J.; Odriozola, I. Catalyst-Free Room-Temperature Self-Healing Elastomers Based on Aromatic Disulfide Metathesis. *Mater. Horizons* **2014**, *1* (2), 237–240. https://doi.org/10.1039/c3mh00061c.

(3) An, X.; Aguirresarobe, R. H.; Irusta, L.; Ruipérez, F.; Matxain, J. M.; Pan, X.; Aramburu, N.; Mecerreyes, D.; Sardon, H.; Zhu, J. Aromatic Diselenide Crosslinkers to Enhance the Reprocessability and Self-Healing of Polyurethane Thermosets. *Polym. Chem.* **2017**, *8* (23), 3641–3646. https://doi.org/10.1039/c7py00448f.

(4) Otsuka, H.; Aotani, K.; Higaki, Y.; Amamoto, Y.; Takahara, A. Thermal Reorganization and Molecular Weight Control of Dynamic Covalent Polymers Containing Alkoxyamines in Their Main Chains. *Macromolecules* **2007**, *40* (5), 1429–1434. https://doi.org/10.1021/ma061667u.

(5) Liu, Y. L.; Chuo, T. W. Self-Healing Polymers Based on Thermally Reversible Diels-Alder Chemistry. *Polym. Chem.* **2013**, *4* (7), 2194–2205. https://doi.org/10.1039/c2py20957h.

(6) Matxain, J. M.; Asua, J. M.; Ruiperez, F. Design of New Disulfide-Based Organic Compounds for the Improvement of Self-Healing Materials. *Phys. Chem. Chem. Phys.* **2016**, *18*, 1758–1770. https://doi.org/10.1039/C5CP06660C.

(7) Amamoto, Y.; Otsuka, H.; Takahara, A.; Matyjaszewski, K. Self-Healing of Covalently Cross-Linked Polymers by Reshuffling Thiuram Disulfide Moieties in Air under Visible Light. *Adv. Mater.* **2012**, *24* (29), 3975–3980. https://doi.org/10.1002/adma.201201928.

(8) Li, T.; Zheng, T.; Han, J.; Liu, Z.; Guo, Z. X.; Zhuang, Z.; Xu, J.; Guo, B. H. Effects of Diisocyanate Structure and Disulfide Chain Extender on Hard Segmental Packing and Self-Healing Property

of Polyurea Elastomers. *Polymers (Basel).* **2019**, *11* (5). https://doi.org/10.3390/polym11050838.

(9) Aguirresarobe, R. H.; Nevejans, S.; Reck, B.; Irusta, L.; Sardon, H.; Asua, J. M.; Ballard, N. Healable and Self-Healing Polyurethanes Using Dynamic Chemistry. *Prog. Polym. Sci.* **2021**, *114*. https://doi.org/10.1016/j.progpolymsci.2021.101362.

(10) Audran, G.; Marque, S. R. A.; Mellet, P. Smart Alkoxyamines: A New Tool for Smart Applications. *Acc. Chem. Res.* **2020**, *53* (12), 2828–2840. https://doi.org/10.1021/acs.accounts.0c00457.

(11) Zhang, Z. P.; Rong, M. Z.; Zhang, M. Q.; Yuan, C. Alkoxyamine with Reduced Homolysis Temperature and Its Application in Repeated Autonomous Self-Healing of Stiff Polymers. *Polym. Chem.* **2013**, *4* (17), 4648–4654. https://doi.org/10.1039/c3py00679d.

(12) Otsuka, H. Reorganization of Polymer Structures Based on Dynamic Covalent Chemistry: Polymer Reactions by Dynamic Covalent Exchanges of Alkoxyamine Units. *Polym. J.* **2013**, *45* (9), 879–891. https://doi.org/10.1038/pj.2013.17.

(13) Higaki, Y.; Otsuka, H.; Takahara, A. A Thermodynamic Polymer Cross-Linking System Based on Radically Exchangeable Covalent Bonds. *Macromolecules* **2006**, *39* (6), 2121–2125. https://doi.org/10.1021/ma052093g.

(14) Yuan, C.; Rong, M. Z.; Zhang, M. Q. Self-Healing Polyurethane Elastomer with Thermally Reversible Alkoxyamines as Crosslinkages. *Polymer (Guildf).* **2014**, *55* (7), 1782–1791. https://doi.org/10.1016/j.polymer.2014.02.033.

(15) Danen, W. C.; Newkirk, D. D. Nitrogen-Centered Free Radicals. IX. The Ease of Formation of Thionitroxide Radicals. *J. Am. Chem. Soc.* **1976**, *98* (2), 516–520. https://doi.org/10.1021/ja00418a031.

(16) Aiba, M.; Koizumi, T. A.; Futamura, M.; Okamoto, K.; Yamanaka, M.; Ishigaki, Y.; Oda, M.; Ooka, C.; Tsuruoka, A.; Takahashi, A.; Otsuka, H. Use of Bis(2,2,6,6-Tetramethylpiperidin-1-Yl)Trisulfide as a Dynamic Covalent Bond for Thermally Healable Cross-Linked Polymer Networks. *ACS Appl. Polym. Mater.* **2020**, *2* (9), 4054–4061.

https://doi.org/10.1021/acsapm.0c00681.

(17) Wetter, C.; Gierlich, J.; Knoop, C. A.; Müller, C.; Schulte, T.; Studer, A. Steric and Electronic Effects in Cyclic Alkoxyamines - Synthesis and Applications as Regulators for Controlled/Living Radical Polymerization. *Chem. - A Eur. J.* **2004**, *10* (5), 1156–1166. https://doi.org/10.1002/chem.200305427.

(18) Matyjaszewski, K.; Woodworth, B. E.; Zhang, X.; Gaynor, S. G.; Metzner, Z. Simple and Efficient Synthesis of Various Alkoxyamines for Stable Free Radical Polymerization. *Macromolecules* **1998**, *31* (17), 5955–5957. https://doi.org/10.1021/ma9807264.

(19) Elizalde, F.; Aguirresarobe, R. H.; Gonzalez, A.; Sardon, H. Dynamic Polyurethane Thermosets: Tuning Associative/Dissociative Behavior by Catalyst Selection. *Polym. Chem.* **2020**, *11* (33), 5386–5396. https://doi.org/10.1039/d0py00842g.

(20) Acerbis, S.; Bertin, D.; Boutevin, B.; Gigmes, D.; Lacroix-Desmazes, P.; Le Mercier, C.; Lutz, J. F.; Marque, S. R. A.; Siri, D.; Tordo, P. Intramolecular Hydrogen Bonding: The Case of β-Phosphorylated Nitroxide (=aminoxyl) Radical. *Helv. Chim. Acta* **2006**, *89* (10), 2119–2132. https://doi.org/10.1002/hlca.200690201.

(21) Huang, C. J.; Chang, F. C. Polypeptide Diblock Copolymers: Syntheses and Properties of Poly(N-Isopropylacrylamide)-b-Polylysine. *Macromolecules* **2008**, *41* (19), 7041–7052. https://doi.org/10.1021/ma801221m.

(22) Gigmes, D.; Gaudel-Siri, A.; Marque, S. R. A.; Bertin, D.; Tordo, P.; Astolfi, P.; Greci, L.; Rizzoli, C. Alkoxyamines of Stable Aromatic Nitroxides: N-O vs. C-O Bond Homolysis. *Helv. Chim. Acta* **2006**, *89* (10), 2312–2326. https://doi.org/10.1002/hlca.200690215.

(23) Audran, G.; Brémond, P.; Marque, S. R. A.; Obame, G. Chemically Triggered C-ON Bond Homolysis of Alkoxyamines. Part 4: Solvent Effect. *Polym. Chem.* **2012**, *3* (10), 2901–2908. https://doi.org/10.1039/c2py20447a.

(24) Nkolo, P.; Audran, G.; Bikanga, R.; Brémond, P.; Marque, S. R. A.; Roubaud, V. C-ON Bond Homolysis of Alkoxyamines: When Too High Polarity Is Detrimental. *Org. Biomol. Chem.* **2017**, *15* (29), 6167–6176. https://doi.org/10.1039/c7ob01312d.

(25) Audran, G.; Bikanga, R.; Brémond, P.; Edeleva, M.; Joly, J. P.; Marque, S. R. A.; Nkolo, P.; Roubaud, V. How Intramolecular Hydrogen Bonding (IHB) Controls the C-ON Bond Homolysis in Alkoxyamines. *Org. Biomol. Chem.* **2017**, *15* (39), 8425–8439. https://doi.org/10.1039/c7ob02223a.

Chapter 4

Chapter 4. Applying hindered urea bonds as self-healing poly(urea-urethane) electrolytes for Lithium Batteries

4.1. Introduction

In previous chapters, different aspects have been analyzed in order to understand and improve the dynamic behaviour of polyurethane networks. In this part, we will be focused in the final application, but, of course, assuring the dynamic properties of the final materials. For this purpose, another strategy will be used to synthesize dynamic PU networks, based in new findings reported in literature[1] and taking into consideration our previous knowledge[2].

During the past few decades, Li-ion batteries (LIBs) have enabled the development of portable electronic devices (mobile phones, laptops, digital cameras, etc.) and are also the best choice for electric vehicles[3]. This technology is based on the rocking chair concept, where Li ions shuttle between electrodes during charge and discharge cycles[4]. Unfortunately, this technology is now reaching its theoretical energy density value and therefore will probably not be able to meet the foreseen future energetic needs[5]. One strategy to enhance the energy density of these energy storage devices is to directly use Li-metal as anode material, thanks to its high theoretical capacity and low reduction potential[6,7]. Nevertheless, the practicality of Li-metal batteries is limited to the inevitable damages provoked by Li dendrite growth, which can either propagate through the separator after repetitive cycling processes, leading to the final short-circuiting of the cell or, for the thinner ones, break from the roots, forming the so-called “dead lithium”[8,9]. Mainly, aforementioned Li dendrite growth is caused by the spontaneous formation of an unstable solid electrolyte interphase, which results to be fragile and heterogeneous with variable spatial resistance, thus inducing uneven Li ions flow and random Li deposition underneath[10]. This mechanical instability and heterogeneity of the layer has become the main issue for the commercialization of batteries based on Li-metal anodes[11]. In this scenario, the scientific community is fully aware that Li-metal batteries need continuous development to reach further and more demanding applications.

Taking into account the growing awareness on global sustainability and the increasing demand of energy storage and conversion devices, one of the greatest upcoming challenges that can be found nowadays is to develop effective, safe and recyclable electrochemical devices[12]. With the aim of overcoming undesired failures, solid polymer electrolytes (SPEs) have emerged as mechanically robust materials with low flammability properties, improved safety and good thermal stability[13]. However, when unwanted scratches form in the material, these advantages disappear, resulting in catastrophic failure[14].

As shown, self-healing materials based on covalent adaptable networks (CANs) have been studied for several applications[15], but their is still a promising target for Li-metal batteries. Up to now, most published studies for this application report mainly self-healing mechanisms based on the formation of hydrogen bonds[16], and the research activity in much more related to the development of self-healing binders than SPEs[17]. Few examples can be found in literature, such as aliphatic disulfides[14] and boronic esters[18]. As previously reported, Li-metal batteries can lose efficiency and present safety problems after damaging of the electrolyte/separator component[3,19]. Indeed, as it can be seen in Figure 4.7 A, when the SPE is not able to self-repair, a simple scratch (that can occur during battery operation under real conditions) can create an easy pathway for faster dendrite grow and eventual short-circuiting the whole cell. On the contrary, self-healable polymer electrolytes can rapidly eliminate the scratch and avoid the final shorting of the device, allowing for a longer and safer cycle life (Figure 4.7 B).

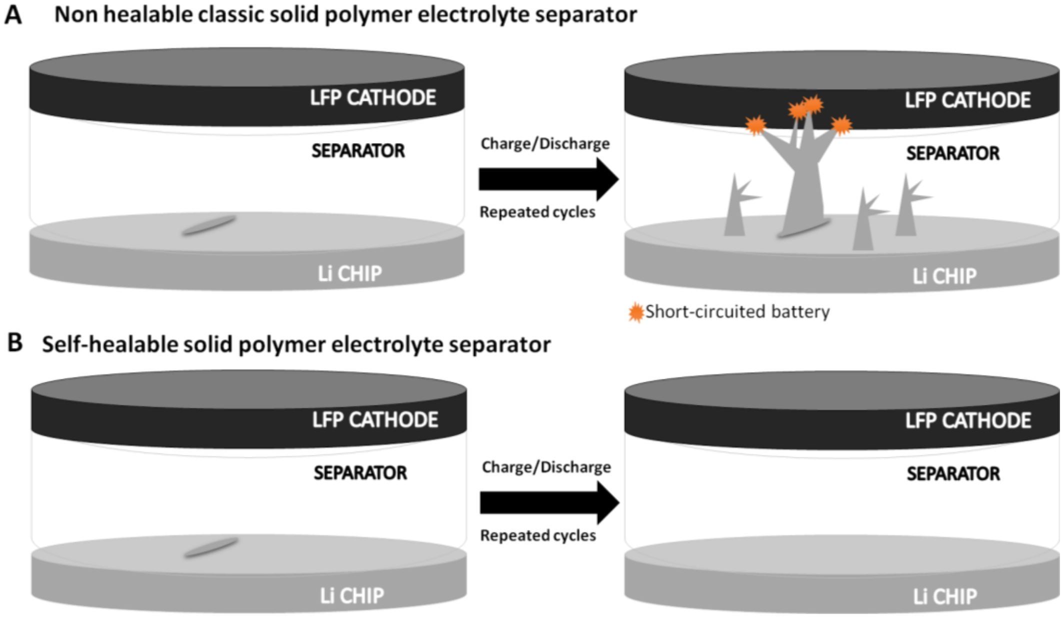
A Non healable classic solid polymer electrolyte separator
LFP CATHODE
SEPARATOR
Li CHIP
Charge/Discharge
Repeated cycles
LFP CATHODE
SEPARATOR
Li CHIP
Short-circuited battery
B Self-healable solid polymer electrolyte separator
LFP CATHODE
SEPARATOR
Li CHIP
Charge/Discharge
Repeated cycles
LFP CATHODE
SEPARATOR
Li CHIP

Figure 4.7. A) Scratched classic SPE separator before and after repeated charge and discharge cycles. B) Scratched self-healable SPE separator to avoid dendrite growth after repeated charge/discharge cycles.

As explained in previous chapters, polyurethanes are one of the most versatile families and their adaptable synthesis allows *ad hoc* material properties tailored to their final application[20,21]. Besides, most of the starting reactants (common polyols, isocyanates and small molecular weight diols/diamines) are well known and have been employed industrially since several decades; polyurethanes still offer an open door for the introduction of more sophisticated compounds that could play a key role in advanced energy storage applications. As an example, single-ion conducting polyurethane electrolytes were studied by Porcarelli *et al.*[22], while a review article on polyurethane-based polymer electrolytes for LIBs has recently summarized the main advantages[23].

Regarding self-healing dynamic polyurethanes, Cheng *et al.* reported the first dynamic polyurea thermosets based on hindered urea bonds (HUBs)[24]. They concluded that the introduction of bulky substituents on the nitrogen atom weakens the planarity of the amide bond, reducing the stability of the urea bonds and resulting in the dissociation of isocyanate and amine under mild conditions. In comparison with other exchangeable bonds, HUBs significantly weakened the bonding energy of amide bond and reduced the reverse reaction conditions. They showed intrinsically dynamic reaction without catalyst under room temperature, thus allowing the self-healing of HUBs-based thermosets under ambient conditions. Since this discovery, these dynamic bonds have gained an incredible attention due to the excellent self-healing, recycling and shape-memory properties that they exhibit[1]. However, to the best of our knowledge this successful chemistry has not yet been considered by the scientific community operating in the electrochemical energy storage field.

For this reason, in this chapter the implementation of HUB-s will be studied in Li-ion batteries.

The strategy relies on the synthesis of dynamic HUB crosslinking points to subsequently create self-healable crosslinked poly(urea-urethane) network by the addition of polyethylene glycol 2000 (PEG2000); this matrix will be referred, from now on, as HUB-PU network. After checking the effective self-healing behavior of the newly proposed membrane, a complete electrochemical characterization was carried out to assess its potential application as gel-polymer electrolyte in Li-metal batteries, and the outputs were compared to those obtained for a Celgard® 2500 separator embedded with liquid electrolyte. Galvanostatic cycling demonstrated – just after cells assembly – similar performances between the newly proposed SPE and Celgard® 2500. The final goal is to investigate the self-healing ability of the HUB-PU membrane and its performance in batteries after cutting and healing cycles as compared to the commonly used porous separators.

4.2. Results and discussion

4.2.1. Synthesis of self-healable crosslinked poly(urea-urethane) network: HUB-PU network

The synthetic route to obtain cross-linked poly(urea-urethane) networks is describe in Figure 4.8 A. This synthesis is carried out in two steps. First, a trifunctional bulky secondary amine is reacted with a diisocyanate in order to prepare a functional urethane polyurea precursor. In the second step, the HUB-PU network is formed by reacting with PEG2000. Every step of the reported procedure was followed by FTIR spectroscopy, as shown in Figure 4.8 B. As it can be seen in the spectra, during the synthesis of the HUB-PU network, the isocyanate stretching band at 2256 cm^{-1} completely disappeared and a new band, corresponding to the formation of urea group, appeared at 1618 cm^{-1}, followed by the corresponding band of urethane group at 1717 cm^{-1}. A representative picture of the crosslinked HUB-PU film is also shown in Figure 4.8 C.

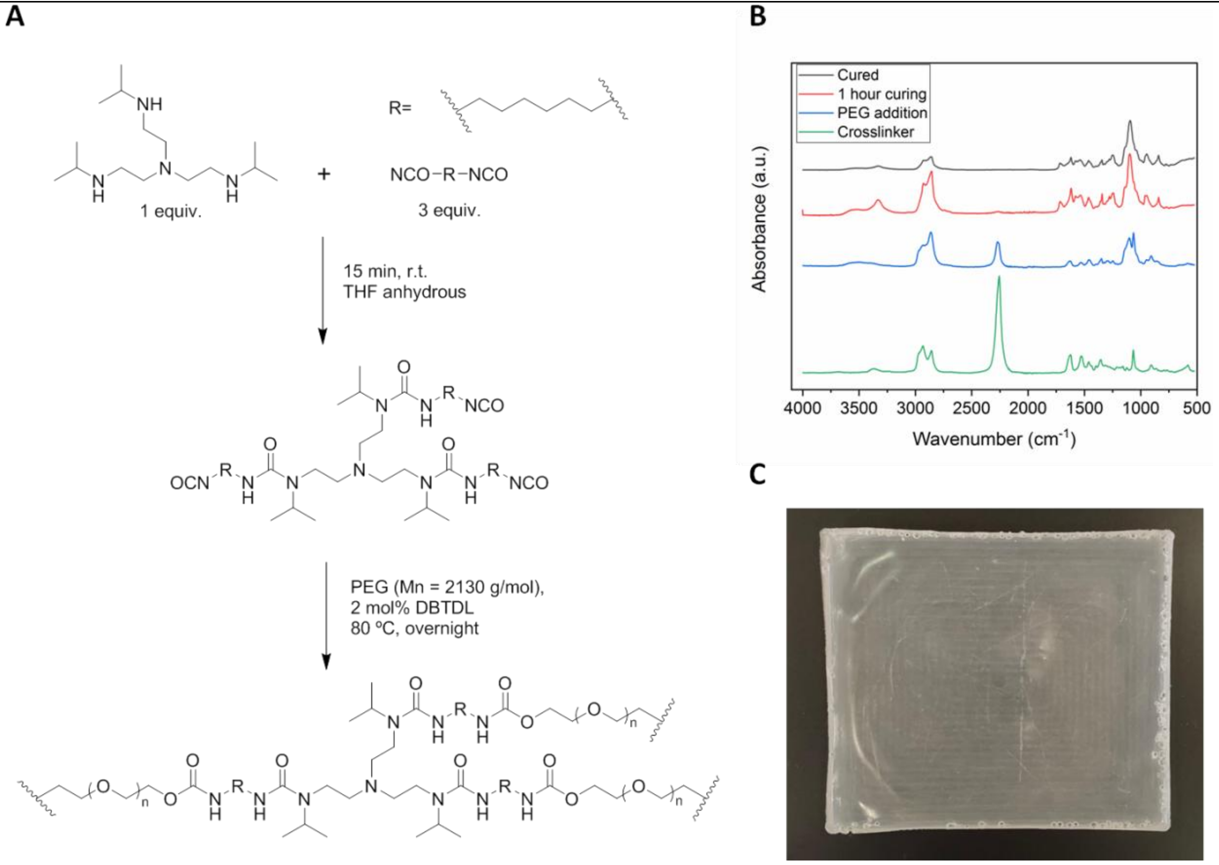
A
B
C
R=
NCO−R−NCO
1 equiv.
3 equiv.
15 min, r.t.
THF anhydrous
PEG (Mn = 2130 g/mol),
2 mol% DBTDL
80 °C, overnight
Cured
1 hour curing
PEG addition
Crosslinker
Absorbance (a.u.)
Wavenumber (cm-1)
4000
3500
3000
2500
2000
1500
1000
500

Figure 4.8. A) Synthetic procedure for obtaining cross-linked aliphatic polyurethanes with dynamic crosslinking points based on HUBs. B) Representative FTIR spectra of the reaction between tris[2-(isopropylamino)ethyl]amine and hexamethylene diisocyanate (green spectrum). The addition of PEG2000 to the mixture (blue spectrum) and the spectrum obtained after 1 h curing (red spectrum) are also shown. Finally, the black spectrum corresponds to the final poly(urea-urethane) film crosslinked for 12 h at 80 °C. C) Representative image of one of the synthesized HUB-PU networks.

4.2.2. Self-healing ability of HUB-PU network

The self-healing ability of synthesized dynamic network was characterized by optical microscopy. Firstly, the self-healing behavior of the HUB-PU network (before being activated with Li salt) was analyzed under pressure and heating up to 80 °C. This temperature was applied in order to be above the melting temperature of PEG2000, thus increasing chain mobility within the membrane. We noticed that, depending on the pressure applied, the self-healing time could vary between 4 h (with a squeezer clamp, Figure S4.1) and 12 h (sampled placed between two glass pieces and closed with paper clips). A representative image is given in Figure 4.9 A.

As regards the rheological study of the dynamic behavior of HUB-PU network, stress-relaxation measurements were carried out at 80, 100, 120, 140 and 160 °C (Figure 4.9 B). As it can be seen, samples showed a decay in the relaxation moduli with significant temperature dependence. The relaxation curves showed fast relaxation under mild conditions and the material did not show any degradation sign even at 160 °C. Characteristic Arrhenius' plot and activation energy for HUB-PU network is shown in Figure 4.9 C. This plot was obtained from stress relaxation measurements carried out between 80 °C and 160 °C. It can be concluded that the obtained characteristic low activation energy value is common for dissociative CANs.

In order to properly understand the dynamic behavior of the sample when used in real conditions, the swollen membrane (*i.e.*, the HUB-PU network activated with a typical Li-metal battery electrolyte) was also analyzed, under pressure, to properly see the scratch disappearance (Figure S4.2 A). Clearly, the swelling of the membrane with liquid electrolyte decreased its crystallinity (*i.e.*, the membrane became translucent), thus enhancing chain mobility and allowing the self-healing of the scratch even at room temperature. Such an achievement demonstrated the very promising features of the newly designed SPE for application in Li-metal batteries. Stress-relaxation measurements of the swollen membrane also confirmed the dynamicity of the material at room temperature (Figure S4.2 B).

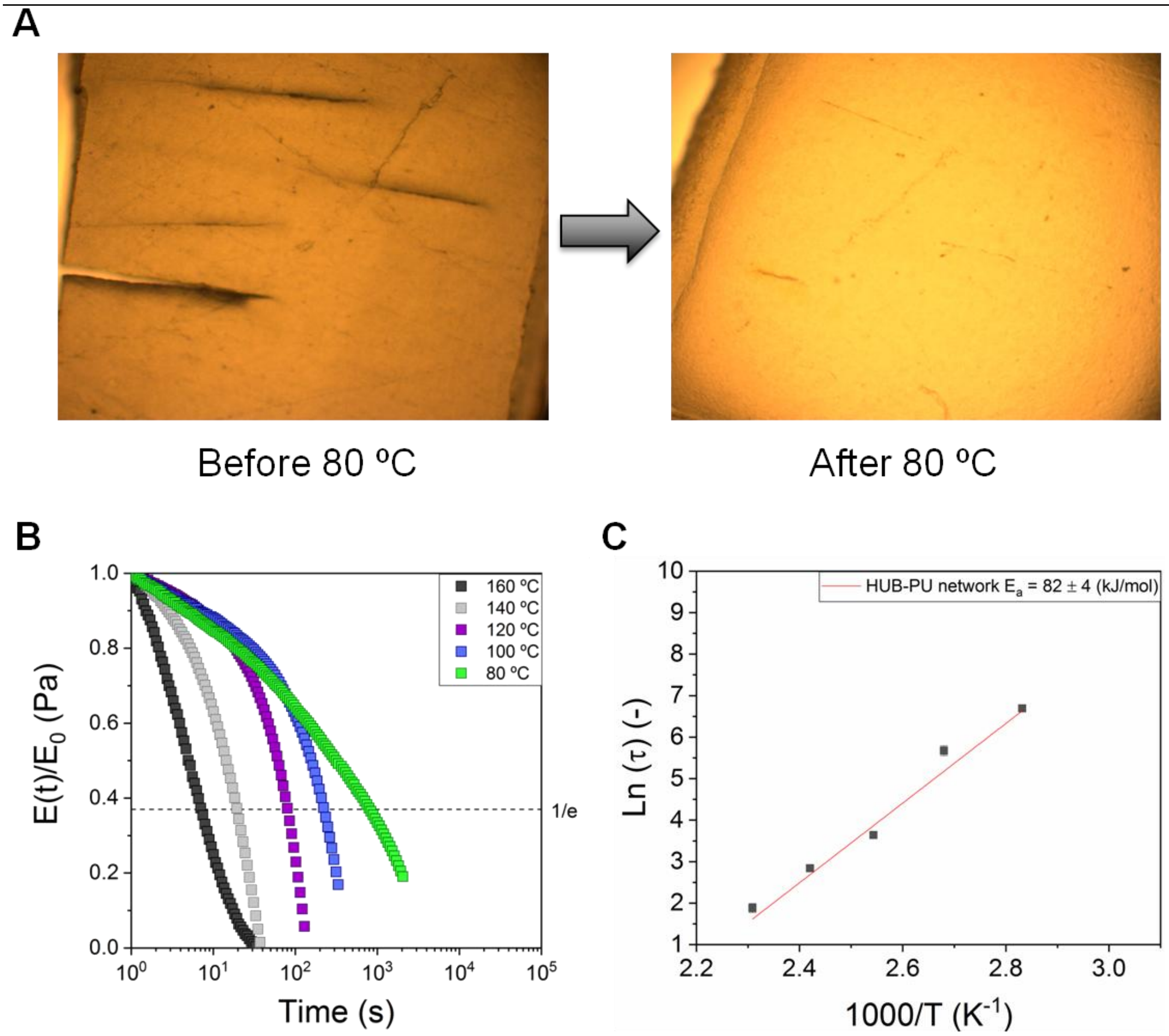

Figure 4.9. A) Scratch disappearance in raw dynamic poly(urea-urethane) network membrane after being kept overnight at 80 °C with pressure (applied by closing two glass pieces with paper clips). B) Stress-relaxation analysis for HUB-PU network, performed between 80 and 160 °C. C) Arrhenius' plot of characteristic relaxation times of the HUB-PU network.

4.2.3. Electrochemical characterization of gel-polymer electrolyte based on swollen HUB-PU network

A thorough electrochemical characterization was carried out in order to understand and analyze the most important electrochemical characteristics of the HUB-PU network, also comparing them to those featured by the commercial separator Celgard® 2500.

A mandatory step to activate the proposed polymer electrolyte is to soak the membrane into a standard liquid electrolyte, *i.e.* $LiPF_6$ 1.0 M in a mixture of ethylene carbonate and diethyl carbonate (EC:DEC 1:1, v:v), for at least 30 min; such a step permits the uptake of the solvated Li ions and the liquid phase, thus ensuring a good ionic mobility within the polymeric network. As a result of this process, a self-standing polymer electrolyte membrane was obtained, that was subsequently cut and used in lab-scale Li-metal cells (ECC-Std geometry). The electrolyte uptake was measured upon time (Figure S4.3) and, overall, it was observed that the membrane was able to swell up to 590% of its initial weight.

Ionic conductivity represents the first key parameter to evaluate electrolytes performance. Arrhenius' plots of ionic conductivity obtained in a temperature range from 20 to 60 °C for both the HUB-PU network and Celgard® 2500 are shown in Figure 4.10 A. Noteworthy, HUB-PU network presented a higher ionic conductivity than the commercial separator over the whole temperature range. A possible explanation could be that the activation of the newly proposed membrane with the liquid electrolyte resulted in multidirectional swelling of the polymer molecular chains, forming more amorphous regions and, therefore, providing effective channels for Li ions migration[25].

The electrochemical stability window (ESW) of the electrolyte, *i.e.* the figure of merit that defines the voltage range in which the electrolyte can work safely, was the second feature we investigated for the HUB-PU membrane. This assessment is very important for a new polymeric matrix proposed for Li-metal batteries, since if the electrochemical potential of the anode is above the electrolyte reduction potential, this could lead to the reduction of the electrolyte. Similarly, if the electrochemical potential of the cathode is below the electrolyte oxidation potential, this could lead to the oxidation of the electrolyte[26]. Taking into account that the charge and discharge cycles of cells based on the Li/membrane/$LiFePO_4$ cathode architecture are usually performed between 2.5 and 4.2 V, the ESW of our HUB-PU electrolyte must be wider than this potential range. According to Figure 4.10 B, the HUB-PU network showed a stability window that fully satisfies the operation conditions of a Li-metal cell. As regards Celgard® 2500, it showed an even wider ESW; overall, both materials demonstrated to be perfectly stable in the range of interest and were subsequently subjected to further electrochemical characterization.

Galvanostatic cycling measurements were initially carried out on symmetric Li/Li cells to study the plating and stripping behavior of Li, which may determine Li dendrites nucleation and growth[27]. Potential profiles of Li stripping and plating at various current densities (*i.e.*, 0.1, 0.5 and 1 mA cm^{-2}) at 25 °C were reported for HUB-PU network and Celgard® 2500 samples in Figure 4.10 C and D, respectively. When the current densities were increased from 0.1 to 0.5 and 1 mA cm^{-2}, a great change of overpotential was noticed in both materials, being this increase much more noticeable for Celgard® 2500. These electrochemical tests assured that both materials were quite efficient against dendrite growth at low current densities (0.1 mA cm^{-2}). At higher values, visible changes appeared on the voltage profiles. In particular, the cell with Celgard® 2500 showed a peaking shape, which has already been reported in literature as the result of different (and unfavored) kinetic pathways for reactions at the electrode/electrolyte interface[28]. Such shape change was not detected in the cell assembled with the HUB-PU network. Overall, these observations demonstrated a much easier plating/stripping process and stabilized interface for the HUB-PU network, indicating restrained Li dendrite growth and highly stable Li plating/stripping reversibility[29].

To further study and compare the performance of HUB-PU network and Celgard® 2500, Li-metal cells with a $LiFePO_4$ (LFP) cathode were assembled and tested at room temperature. Figure 4.10 E and Figure 4.10 F presents the cell performances at different charge and discharge rates (from C/10 to 1C) in the presence of the HUB-PU network or Celgard® 2500, respectively. The newly proposed polymer electrolyte showed high capacity values at every C-rate, even if slightly lower than those shown by Celgard® 2500 (121 mAh g^{-1} and 131 mAh g^{-1} at 1C, respectively). Even though, the cell capacities obtained remain rather impressive for a polymer electrolyte obtained by a new synthetic process, never explored before by the electrochemistry community and able to work at room temperature (especially at 1C). Nevertheless, it is also noteworthy to highlight the more stable specific capacities provided by the HUB-PU network, when compared to Celgard® 2500 counterpart, after 200 cycles at constant C/10 current (Figure S4.4) with 93.35% of 10th cycle capacity retained for the HUB-PU network, against 89.78% for Celgard® 2500.

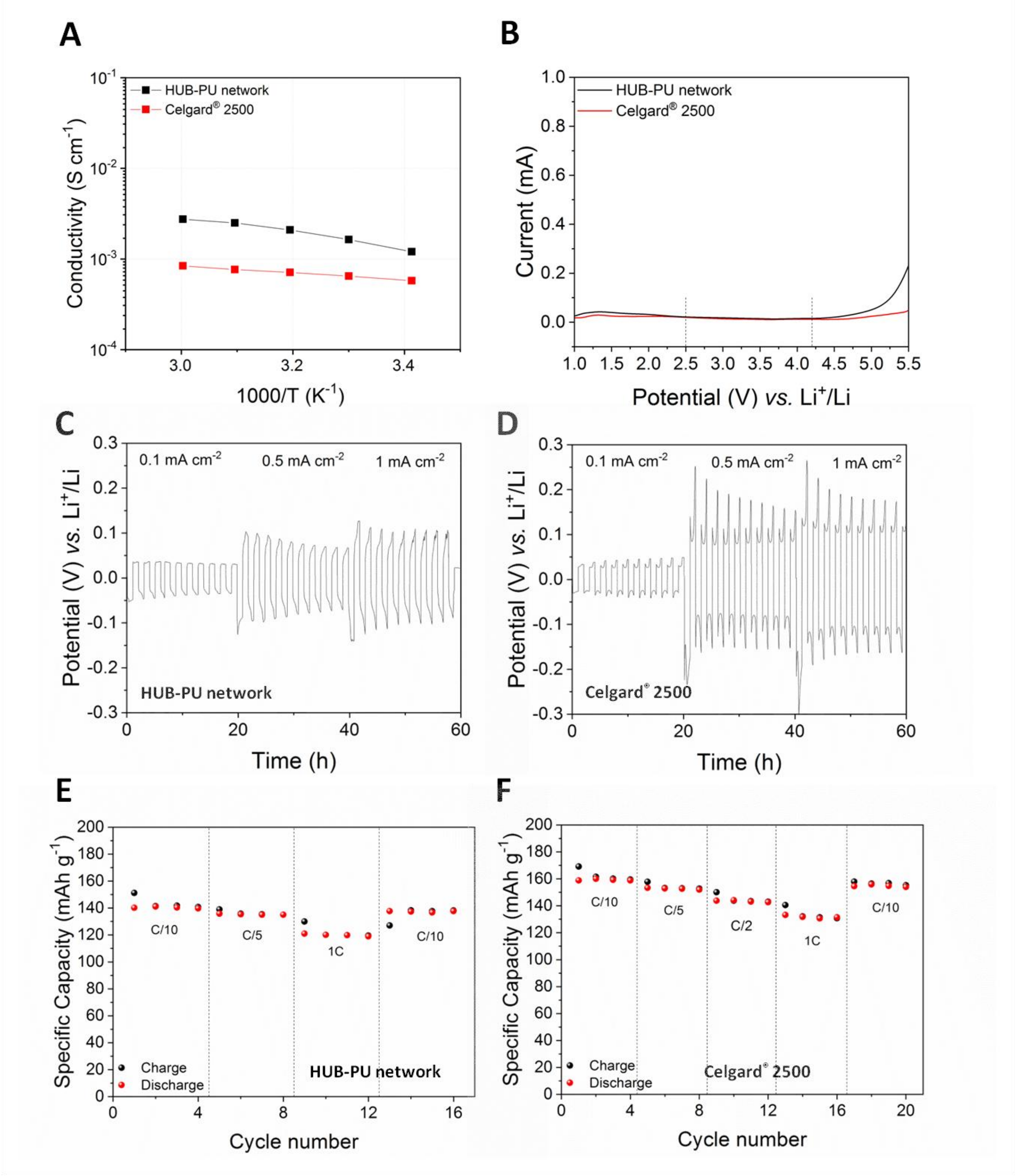

Figure 4.10. A) Ionic conductivity values at different temperatures for HUB-PU network and Celgard® 2500 electrolytes. B) ESW of HUB-PU network and Celgard® 2500. C-D) Potential *vs.* test time of Li stripping and plating for a symmetrical Li/Li cell at various current densities and at room temperature, for HUB-PU network and Celgard® 2500 samples, respectively. E-F) Charge/discharge

performances of Li/electrolyte/$LiFePO_4$ cells at various C-rates in the presence of HUB-PU network and Celgard® 2500 electrolytes, respectively.

4.2.4. Li-metal cells performance after mechanical damage and healing of the HUB-PU gel polymer electrolyte

The charge/discharge capacity comparison at C/5 rate was performed between HUB-PU network and Celgard® 2500 samples in order to analyze how each membrane was able to recover after cut, *i.e.* a mechanical damage. To properly carry out this characterization, first each membrane was cycled at the abovementioned rate for 10 cycles. Right after, both cells were put into the glovebox and were disassembled. Carefully, the LFP cathode was removed and, with a surgeon knife, each membrane got a similar cut (see Figure 4.11 A and B). Successively, the electrochemical cells were reassembled and cycling test was resumed at the same C/5 rate. The obtained results were very different. As shown in Figure 4.11 C and D, the self-healable membrane was able to charge and discharge again, giving capacity values very close to the ones obtained during the first 10 cycles. In particular, the capacity just before the cut was around 161 mAh g^{-1}, while just after the cut 159 mAh g^{-1} were recovered. Indeed, after the cut, the HUB-PU network showed really good performance for other 50 cycles, with 94.78% of capacity retention at the 50th cycle with respect to the 10th cycle. Later, this capacity decreases slowly to lower values (as typical for non-optimized lab-scale cells), but still worked even after 100 cycles (Figure S4.5), retaining 79.68% the 10th cycle capacity. Of note, from our literature research (see Table S4.1), no previous studies were carried out with polymer electrolytes directly cut in the electrochemical cell and cycled when still damaged.

On the other hand, in the case of the commercial Celgard® 2500 membrane, Figure 4.11 D clearly shows its incapacity to recover from the cut (further confirmed by its potential profiles in Figure S4.6). After the scratch, the cell worked with lower capacity values compared to the first ten cycles. Indeed, the charge capacity of the first cycle after cut is 27% of the one before the cut and the corresponding discharge capacity is only 39 mAh g^{-1}. Moreover, the subsequent charge capacity values seemed quite random, clearly showing the ongoing failure of the cell.

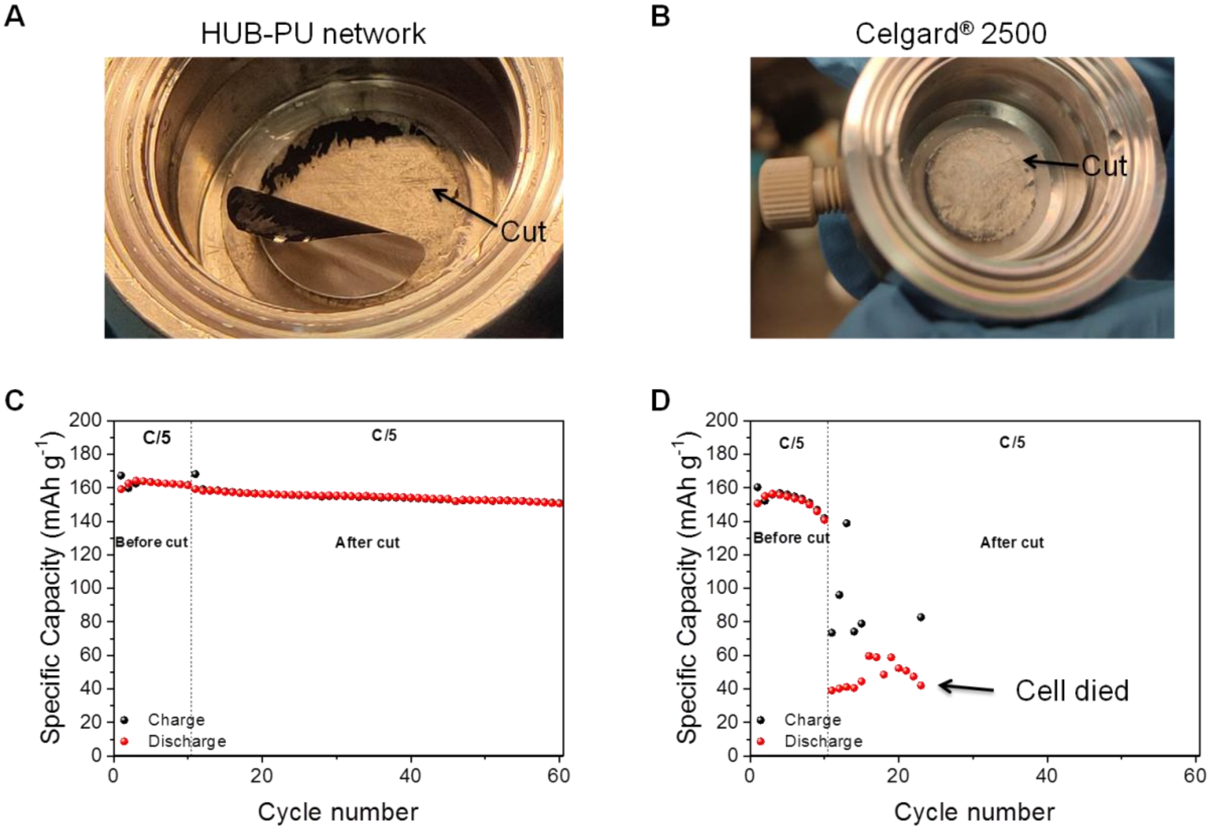

Figure 4.11. A-B) Optical proof of the cut carried out inside the glove box on both the self-healable HUB-PU network and Celgard® 2500 membrane after 10 cycles at C/5 rate. C-D) Specific capacity (mAh g^{-1}) *vs.* cycle number at C/5 rate for HUB-PU network and Celgard® 2500 membrane, respectively. First 10 cycles are carried out before cut, while the subsequent cycles refer to the period after cut.

4.3. Conclusion

In summary, in this chapter polyurethane network containing dynamic crosslinking points based on HUBs has been synthesized and effectively used for the first time as self-healable polymer electrolyte in Li-metal batteries. Noteworthy, this novel membrane has shown superior ionic conductivity than the typical liquid electrolyte embedded in commercial porous Celgard® 2500 separators. Furthermore, to the best of our knowledge, self-healing electrolyte have never been electrochemically cycled while still damaged, only when already healed. In this paper, the self-healing efficiency of HUB-PU membranes has been compared after cutting the materials and cycling them in lab-scale prototypes at C/5 rate. In the case of the reference commercial membrane, after the scratch the capacity value dropped to half of the previous values and the electrochemical performances rapidly deteriorated. On the contrary, the novel HUB-PU membrane showed good recovery after mechanical damage and the capacity values remained constant and similar to the initial ones with 161 mAh g^{-1} before the cut and 159 mAh g^{-1} just after. The HUB-PU polymer electrolyte with self-healing feature has been able to cycle for more than 100 cycles after damage/healing. Overall, we believe that the findings of this work contribute to optimize and enhance the implementation of covalent adaptable linkages (more specifically, HUBs) in the growing technology transfer of safe, solid-state and self-repairing materials for electrochemical energy storage.

4.4 References

(1) Zhang, Q.; Wang, S.; Rao, B.; Chen, X.; Ma, L.; Cui, C.; Zhong, Q.; Li, Z.; Cheng, Y.; Zhang, Y. Hindered Urea Bonds for Dynamic Polymers: An Overview. *React. Funct. Polym.* **2021**, *159* (November 2020). https://doi.org/10.1016/j.reactfunctpolym.2020.104807.

(2) Elizalde, F.; Aguirresarobe, R. H.; Gonzalez, A.; Sardon, H. Dynamic Polyurethane Thermosets: Tuning Associative/Dissociative Behavior by Catalyst Selection. *Polym. Chem.* **2020**, *11* (33), 5386–5396. https://doi.org/10.1039/d0py00842g.

(3) Xie, J.; Lu, Y. C. A Retrospective on Lithium-Ion Batteries. *Nat. Commun.* **2020**, *11* (1), 9–12. https://doi.org/10.1038/s41467-020-16259-9.

(4) Hundekar, P.; Basu, S.; Pan, J.; Bartolucci, S. F.; Narayanan, S.; Yang, Z.; Koratkar, N. Exploiting Self-Heat in a Lithium Metal Battery for Dendrite Healing. *Energy Storage Mater.* **2019**, *20* (April), 291–298. https://doi.org/10.1016/j.ensm.2019.04.013.

(5) Liu, Y.; Zhang, R.; Wang, J.; Wang, Y. Current and Future Lithium-Ion Battery Manufacturing. *iScience* **2021**, *24* (4), 102332. https://doi.org/10.1016/j.isci.2021.102332.

(6) Wu, N.; Shi, Y. R.; Lang, S. Y.; Zhou, J. M.; Liang, J. Y.; Wang, W.; Tan, S. J.; Yin, Y. X.; Wen, R.; Guo, Y. G. Self-Healable Solid Polymeric Electrolytes for Stable and Flexible Lithium Metal Batteries. *Angew. Chemie - Int. Ed.* **2019**, *58* (50), 18146–18149. https://doi.org/10.1002/anie.201910478.

(7) Yu, Y.; Yin, Y. Bin; Ma, J. L.; Chang, Z. W.; Sun, T.; Zhu, Y. H.; Yang, X. Y.; Liu, T.; Zhang, X. B. Designing a Self-Healing Protective Film on a Lithium Metal Anode for Long-Cycle-Life Lithium-Oxygen Batteries. *Energy Storage Mater.* **2019**, *18* (December 2018), 382–388. https://doi.org/10.1016/j.ensm.2019.01.009.

(8) Chen, K. H.; Wood, K. N.; Kazyak, E.; Lepage, W. S.; Davis, A. L.; Sanchez, A. J.; Dasgupta, N. P. Dead Lithium: Mass Transport Effects on Voltage, Capacity, and Failure of Lithium Metal Anodes. *J. Mater. Chem. A* **2017**, *5* (23), 11671–11681. https://doi.org/10.1039/c7ta00371d.

(9) Zhang, X. Q.; Cheng, X. B.; Zhang, Q. Advances in Interfaces between Li Metal Anode and Electrolyte. *Adv. Mater. Interfaces* **2018**, *5* (2), 1–19.

https://doi.org/10.1002/admi.201701097.

(10) Chen, K.; Yang, D. Y.; Huang, G.; Zhang, X. B. Lithium-Air Batteries: Air-Electrochemistry and Anode Stabilization. *Acc. Chem. Res.* **2021**, *54* (3), 632–641. https://doi.org/10.1021/acs.accounts.0c00772.

(11) Ding, P.; Lin, Z.; Guo, X.; Wu, L.; Wang, Y.; Guo, H.; Li, L.; Yu, H. Polymer Electrolytes and Interfaces in Solid-State Lithium Metal Batteries. *Mater. Today* **2021**, *51*, 449–474. https://doi.org/10.1016/j.mattod.2021.08.005.

(12) Verdier, N.; Foran, G.; Lepage, D.; Prébé, A.; Aymé-Perrot, D.; Dollé, M. Challenges in Solvent-Free Methods for Manufacturing Electrodes and Electrolytes for Lithium-Based Batteries. *Polymers (Basel).* **2021**, *13* (3), 1–26. https://doi.org/10.3390/polym13030323.

(13) Chen, Y.; Xu, G.; Liu, X.; Pan, Q.; Zhang, Y.; Zeng, D.; Sun, Y.; Ke, H.; Cheng, H. A Gel Single Ion Conducting Polymer Electrolyte Enables Durable and Safe Lithium Ion Batteries via Graft Polymerization. *RSC Adv.* **2018**, *8* (70), 39967–39975. https://doi.org/10.1039/C8RA07557C.

(14) Jo, Y. H.; Li, S.; Zuo, C.; Zhang, Y.; Gan, H.; Li, S.; Yu, L.; He, D.; Xie, X.; Xue, Z. Self-Healing Solid Polymer Electrolyte Facilitated by a Dynamic Cross-Linked Polymer Matrix for Lithium-Ion Batteries. *Macromolecules* **2020**, *53* (3), 1024–1032. https://doi.org/10.1021/acs.macromol.9b02305.

(15) Lindenmeyer, K. M.; Johnson, R. D.; Miller, K. M. Self-Healing Behaviour of Furan-Maleimide Poly(Ionic Liquid) Covalent Adaptable Networks. *Polym. Chem.* **2020**, *11* (33), 5321–5326. https://doi.org/10.1039/d0py00016g.

(16) Cheng, Y.; Xiao, X.; Pan, K.; Pang, H. Development and Application of Self-Healing Materials in Smart Batteries and Supercapacitors. *Chem. Eng. J.* **2020**, *380*, 122565. https://doi.org/10.1016/j.cej.2019.122565.

(17) Munaoka, T.; Yan, X.; Lopez, J.; To, J. W. F.; Park, J.; Tok, J. B. H.; Cui, Y.; Bao, Z. Ionically Conductive Self-Healing Binder for Low Cost Si Microparticles Anodes in Li-Ion Batteries. *Adv. Energy Mater.* **2018**, *8* (14), 1–11. https://doi.org/10.1002/aenm.201703138.

(18) Jing, B. B.; Evans, C. M. Catalyst-Free Dynamic Networks for Recyclable, Self-Healing Solid

Polymer Electrolytes. *J. Am. Chem. Soc.* **2019**, *141* (48), 18932–18937. https://doi.org/10.1021/jacs.9b09811.

(19) Chang, C.; Yao, Y.; Li, R.; Guo, Z. H.; Li, L.; Pan, C.; Hu, W.; Pu, X. Self-Healing Single-Ion-Conductive Artificial Polymeric Solid Electrolyte Interphases for Stable Lithium Metal Anodes. *Nano Energy* **2022**, *93*, 106871. https://doi.org/10.1016/j.nanoen.2021.106871.

(20) Lopez De Pariza, X.; Erdmann, T.; Arrechea, P. L.; Perez, L.; Dausse, C.; Park, N. H.; Hedrick, J. L.; Sardon, H. Synthesis of Tailored Segmented Polyurethanes Utilizing Continuous-Flow Reactors and Real-Time Process Monitoring. *Chem. Mater.* **2021**, *33* (20), 7986–7993. https://doi.org/10.1021/acs.chemmater.1c01919.

(21) Aguirresarobe, R. H.; Nevejans, S.; Reck, B.; Irusta, L.; Sardon, H.; Asua, J. M.; Ballard, N. Healable and Self-Healing Polyurethanes Using Dynamic Chemistry. *Prog. Polym. Sci.* **2021**, *114*. https://doi.org/10.1016/j.progpolymsci.2021.101362.

(22) Porcarelli, L.; Manojkumar, K.; Sardon, H.; Llorente, O.; Shaplov, A. S.; Vijayakrishna, K.; Gerbaldi, C.; Mecerreyes, D. Single Ion Conducting Polymer Electrolytes Based On Versatile Polyurethanes. *Electrochim. Acta* **2017**, *241*, 526–534. https://doi.org/10.1016/j.electacta.2017.04.132.

(23) Lv, Z.; Tang, Y.; Dong, S.; Zhou, Q.; Cui, G. Polyurethane-Based Polymer Electrolytes for Lithium Batteries: Advances and Perspectives. *Chem. Eng. J.* **2022**, *430*, 132659. https://doi.org/10.1016/j.cej.2021.132659.

(24) Ying, H.; Zhang, Y.; Cheng, J. Dynamic Urea Bond for the Design of Reversible and Self-Healing Polymers. *Nat. Commun.* **2014**, *5*. https://doi.org/10.1038/ncomms4218.

(25) Guo, Q.; Han, Y.; Wang, H.; Xiong, S.; Li, Y.; Liu, S.; Xie, K. New Class of LAGP-Based Solid Polymer Composite Electrolyte for Efficient and Safe Solid-State Lithium Batteries. *ACS Appl. Mater. Interfaces* **2017**, *9* (48), 41837–41844. https://doi.org/10.1021/acsami.7b12092.

(26) Marchiori, C. F. N.; Carvalho, R. P.; Ebadi, M.; Brandell, D.; Araujo, C. M. Understanding the Electrochemical Stability Window of Polymer Electrolytes in Solid-State Batteries from Atomic-Scale Modeling: The Role of Li-Ion Salts. *Chem. Mater.* **2020**, *32* (17), 7237–7246.

https://doi.org/10.1021/acs.chemmater.0c01489.

(27) Porcarelli, L.; Gerbaldi, C.; Bella, F.; Nair, J. R. Super Soft All-Ethylene Oxide Polymer Electrolyte for Safe All-Solid Lithium Batteries. *Sci. Rep.* **2016**, *6* (January). https://doi.org/10.1038/srep19892.

(28) Wood, K. N.; Kazyak, E.; Chadwick, A. F.; Chen, K. H.; Zhang, J. G.; Thornton, K.; Dasgupta, N. P. Dendrites and Pits: Untangling the Complex Behavior of Lithium Metal Anodes through Operando Video Microscopy. *ACS Cent. Sci.* **2016**, *2* (11), 790–801. https://doi.org/10.1021/acscentsci.6b00260.

(29) Calderón, C. A.; Vizintin, A.; Bobnar, J.; Barraco, D. E.; Leiva, E. P. M.; Visintin, A.; Fantini, S.; Fischer, F.; Dominko, R. Lithium Metal Protection by a Cross-Linked Polymer Ionic Liquid and Its Application in Lithium Battery. *ACS Appl. Energy Mater.* **2020**, *3* (2), 2020–2027. https://doi.org/10.1021/acsaem.9b02309.

Chapter 5

Chapter 5: Conclusions and perspective

In this section, the most relevant conclusions and perspectives of this thesis will be explained.

As highlighted in the introduction of this thesis, thermosets and elastomers offer great solvent resistance and mechanical properties, but due to their crosslinked structure, their recycling and reprocessing has become a big issue. For this reason, to trigger the dynamicity of already preexisting functional groups or the introduction of other dynamic chemistries along polymer chains are tottaly necessary for the generation of new materials that conbine the abovementioned properties and recycling opportunities.

Nevertheless, to understand a crosslinked material as a dynamic network, not only the attention should be focused in the exchangeable bond nature but in the whole material properties, including the network dynamics and the presence or absence of catalysts. In order to ensure sufficient mobility and assure exchanges between dynamic linkages, all the proposed systems have been synthesized as elastomers.

The potential strategy to enhance the dynamicity by introducing different kind of catalysts has been explored in Chapter 2. Thus, tin based catalyst, acid and basic organocatalysts have been incorporated into polyurethane networks. It has been proved that catalysts are able to trigger transcarbamoylation reactions in aromatic polyurethanes following different pathways. Selecting the appropriate catalyst, it is possible to activate the associative or dissociative mechanism. More interstingly, organocatalysts appear as a real alternative to industrially relevant organotin catalysts for the activation of transcarbamoylation reactions.

To end up, it is worthy to mention that degradation of the materials is a key factor when high temperatures are used in CANs. Mostly, researchers have looked for the shortest relaxation times and fastest reprocessing conditions that imply high temperatures, but degradation can be present in this scenario. This hypothesis has been checked in PU networks, and from the materials analyzed in Chapter 2, it is concluded that temperatures above 120 °C should not be used to trigger transcarbamoylation reactions as degradation is more notorious. Therefore, catalysts are necessary to activate transurethanizations exchanges before the degradation happens. This statement is fulfilled only for aromatic polyurethanes, and other strategies are necessary for the case of aliphatic polyurethanes.

Keeping in mind the findings of the previous chapter, in Chapter 3, radical chemistry has been introduced in order to transform aliphatic polyurethane networks into CANs. Alkoxyamine based diols have been synthesized for this purposed, and as expected, they have fastened the relaxation times. Furthermore, little changes in the structure of these novel molecules has resulted crutial in the overall dynamic behavior of the samples. Thanks to these alkoxyamines, we have been able to reprocess these materials at temperatures as low as 80 °C, depending on the alkoxyamine load and nature.

Unfortunately, these molecules can give secondary reactions, and for this reason, more research about reprocessing conditions and alkoxyamine structure designs is needed.

These conclusions are derived from the data obtained in small molecular model reactions and rheological characterization of PU networks. Actually, this strategy of correlating polymer characterization and small molecular models is an interesting option, but several ideas should be mentioned. Model compounds, offer cualitative information about exchange possibilities, but are not close to simulate the behavior of polymer networks. Thus, they can be used as complementary information, but the activation energies (E_a) of this kind of experiments should not be directlycompared with the ones acquired from stress-relaxation measurements.

Finally, in the last chapter, polyurethane CANs have been applied as self-healing electrolytes. Specifically, hindered urea bonds have been introduced as crosslinking points, and its recovery after damage has been tested and compared to a commercial porous membrane, Celgard® 2500. After physically scratching both gel electrolytes, only HUB-PU network was able to recover, showing regular capacity values very close to the initial ones. Interestingly, even more than 100 cycles have been reached after cutting the self-healable separator. For this reason, hindered urea bonds are a good choice for self-healing materials in these applications. None-the-less, beyond all the efforts highlighted, significant progress is still need to be made, in order to optimize the implementation of this chemistry in the electrochemical energy storage field.

In the light of these results, it has been demonstrated that transcarbamoylation reactions are susceptible to happen in the presence of catalysts, thus, this strategy can be especially relevant in industrial applications. If a more dynamic system is needed, alkoxyamine chemistry and hindered urea bond have proved to exchange faster than urethane bond. This statement is supported by the activation energies obtained by rheological characterization in each chapter. As a consequence, they can fit the specification of high added value applications. Among these two strategies, hindered urea bonds appear as the most economically and industrially scalable choice, as the synthetic pathway is much more feasible than alkoxyamine one. Nonetheless, radical chemisty offers the opportunity to reach more structural alternatives that should be researched in the future.

On the basis of these considerations, the implementation in industry of polyurethane based covalent adaptable networks is a closer reality, but a number of innovations are still required.

Methods

Fourier Transform Infrared Spectroscopy (FTIR)

FT-IR spectra were obtained by FTIR spectrophotometer (Nicolet 6700 FT-IR, Thermo Scientific Inc., USA) using attenuated total reflectance (ATR) technique (Golden Gate, spectra Tech). Spectra were recorded between 4000–525 cm^{-1} with a spectrum resolution of 4 cm^{-1}. All spectra were averaged over 10 scans.

Also, FTIR spectra were obtained using a FTIR spectrophotometer (Nicolet is20, Thermo Scientific Inc.) equipped with ATR feature with a diamond crystal. Spectra were recorded between 4000 and 600 cm^{-1} with a spectrum resolution of 4 cm^{-1}. All spectra were averaged over 16 scans.

Nuclear Magnetic Resonance (NMR) spectroscopy

^{1}H-NMR spectra were recorded with Bruker Avance DPX 300 or Bruker Avance 400 spectrometers. The NMR chemical shifts were reported as δ in parts per million (ppm) relative to the traces of non-deuterated solvent (*e.g.* δ = 2.50 ppm for DMSO-d_6 or δ = 7.26 for $CDCl_3$). COSY experiments were recorded in Bruker Avance 400 sepctrometers.

Density functional theory (DFT)

All geometry optimizations were carried out within density functional theory (DFT) using the M062X functional *(Y. Zhao and D. G. Truhlar, Theor. Chem. Acc., 2008, 120, 215–241)* combined with the 6-31+G(d,p) basis set. *(W. J. Hehre, R. Ditchfield and J. A. Pople, J. Chem. Phys., 1972, 56, 2257–2261)* To confirm that the optimized structures were minima or transition states on the potential energy surfaces, frequency calculations were carried out at the same level of theory. These frequencies were then used to evaluate the zero-point vibrational energy (ZPVE) and the thermal corrections, at T = 298.15 K, in the harmonic oscillator approximation. Single-point calculations using the 6-311++G(2df,2p) basis set *(R. Krishnan, J. S. Binkley, R. Seeger and J. A. Pople, J. Chem. Phys., 1980, 72, 650–654)* were performed on the optimized structures in order to refine the electronic energy. Solvent effects, in THF, have been estimated using the polarizable continuum model (PCM) approach *(M. Cossi, V. Barone and R. Cammi, Chem. Phys. Lett., 1996, 255, 327–335; E. Cancès, B. Mennucci and J. Tomasi, J. Chem. Phys., 1997, 107, 3032–3041; V. Barone, M. Cossi and J. Tomasi, J. Chem. Phys., 1997, 107, 3210–3221; V. Barone, M. Cossi and J. Tomasi, J. Comput. Chem., 1998, 19, 404–417)*. All the calculations were performed with the Gaussian 16 suite of programs *(M. J. Frisch, G. W. Trucks, H. B. Schlegel, G. E. Scuseria, M. A. Robb, J. R. Cheeseman, G. Scalmani, V. Barone, G. A. Petersson, H. Nakatsuji, X. Li, M. Caricato, A. V. Marenich, J. Bloino, B. G. Janesko, R. Gomperts, B. Mennucci, H. P. Hratchian, J. V. Ortiz, A. F. Izmaylov, J. L. Sonnenberg, D. Williams-Young, F. Ding, F. Lipparini, F. Egidi, J. Goings, B. Peng, A. Petrone, T. Henderson, D. Ranasinghe, V. G. Zakrzewski, J. Gao, N. Rega, G. Zheng, W. Liang, M. Hada, M. Ehara, K. Toyota, R. Fukuda, J. Hasegawa, M. Ishida, T. Nakajima, Y. Honda, O. Kitao, H. Nakai, T. Vreven, K. Throssell, J. A. Montgomery Jr., J. E. Peralta, F. Ogliaro, M. J. Bearpark, J. J. Heyd, E. N. Brothers, K. N. Kudin, V. N. Staroverov, T. A. Keith, R. Kobayashi, J. Normand, K. Raghavachari, A. P. Rendell, J. C. Burant, S. S. Iyengar, J. Tomasi, M. Cossi, J. M. Millam, M. Klene, C. Adamo, R. Cammi, J. W. Ochterski, R. L. Martin, K. Morokuma, O. Farkas, J. B. Foresman and D. J. Fox, Gaussian 16, Revision B.01, Gaussian, Inc., Wallingford CT, 2016)*

Dynamic Mechanical Thermal Analysis (DMTA)

The steady state mechanical behavior of the samples was determined by dynamic mechanical thermal analysis (DMTA) measurements, conducted in tension mode in a Dynamic Mechanical Analyzer, Triton 2000 DMA (Triton Technology). Experiments were performed in an isothermal mode and a frequency of 1Hz using rectangular shape samples. All the measurements were carried out with 5% of strain. Samples employed for these measurements (Chapter 2) had a thickness between 0.60 and 0.95 mm and a width between 5.45 and 5.95 mm in the case of aliphatic polyurethanes. In the case of aromatic polyurethanes the samples employed had around 0.75mm of thickness and between 4.75 and 4.85 mm of width. All the samples were measured with a preset length of 5.00mm.

Matrix Assisted Laser Desorption Ionization Time of Flight Mass Spectrometry (MALDI-TOF MS)

MALDI-TOF MS measurements were performed on a Bruker Autoflex Speed system (Bruker, Germany) equipped with a Smartbeam-II laser (Nd:YAG, 355nm, 2 kHz). Spectra were acquired in reflection mode; each mass spectrum was the average of 8000 shots. Samples were dissolved in THF at a concentration of 10 mg/ml. Trans-2-[3-(4-tert-Butylphenyl)-2-methyl-2-propenylidene] malononitrile (DCTB, Sigma-Aldrich) was used as a matrix. The matrix was dissolved in THF at a concentration of 20 mg/ml. Sodium trifluoroacetate (NaTFA) (Fluka) was used as cation donor (10 mg/ml dissolved in THF). The samples were mixed with the matrix and salt at a 10:2:1 (matrix/sample/salt) ratio. Approximately 1 µL of the obtained mixture was hand spotted on the ground steel target plate.

Stress relaxation measurements

Stress relaxation experiments to obtain the relaxation modulus G(t) were carried out in an ARES rheometer (Rheometrics) under the conditions indicated in the text, using a film tension fixture and 5% of strain. Employed samples in Chapter 2 and 3 had a width between 1.30 and 2.25 mm, and the thickness between 0.60 and 1.10mm. The samples employed in Chapter 4 a width between 1.30 and 1.70 mm, and a thickness between 0.15 and 0.35 mm. The temperature dependence of relaxation times is described by the Arrhenius equation:

$$\tau(T) = \tau_o exp\left(\frac{E_a}{RT}\right)$$

And activation energy was calculated from the slope of the representation of ln (τ) vs 1000/T for each sample.

Electrochemical characterization

The electrochemical testing was carried out with the aim of comparing the newly designed HUB-PU membrane with a commercial separator (Celgard® 2500) impregnated with 300 µL of the above mentioned liquid electrolyte.

The ionic conductivity was determined by electrochemical impedance spectroscopy (EIS) in the frequency range between 100 kHz and 1 Hz at open circuit potential, using a VSP-3e potentiostat (BioLogic Sciences Instruments). The activated membrane was sandwiched between two stainless steel blocking electrodes (ECC-Std test cells, EL-CELL GmbH). The assembled cells were kept in a climatic chamber (model MK53 E2.1 by BINDER GmbH) and tested between 20 and 60 °C. The resistance of the electrolyte was given by the high-frequency intercept of the Nyquist plot. The ionic conductivity was calculated at each temperature using Equation 1:

$$\sigma = \frac{l}{A} \cdot \frac{1}{R_b} \quad (1)$$

where l is the membrane thickness, A is the membrane surface area and R_b is the resistance value at the high-frequency intercept

Appendix

Chapter 2.

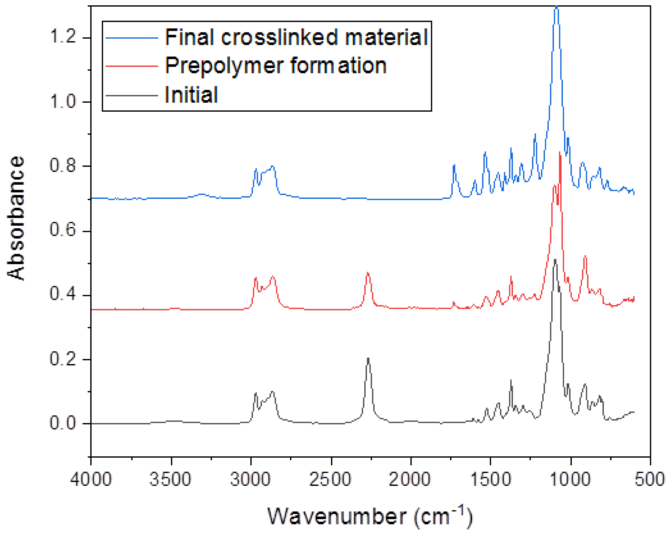

Figure S2.1. Representative FTIR spectra of the reaction of PPG triol (Mn=3740 g/mol) with MDI at t=0min (black trace) and t=300 min (pre-polymer formation, red trace). Blue trace corresponds to the final polyurethane film cross-linked for 24h at 70 °C with 1,6-Hexanediol.

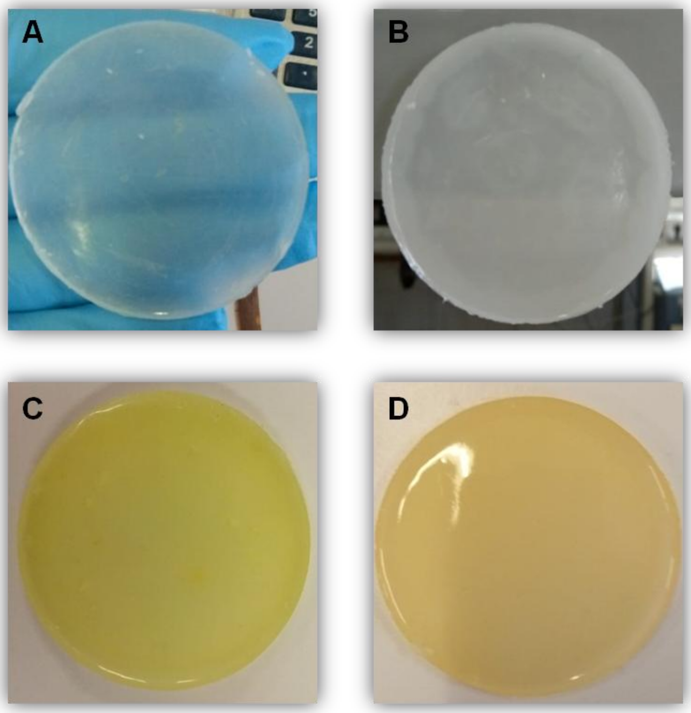

Figure S2.2. A) Aromatic polyurethane film cross-linked without catalyst. B) Aromatic polyurethane film cross-linked with DBTDL. C) Aromatic polyurethane film cross-linked with PTSA D) Aromatic polyurethane film cross-linked with TBD.

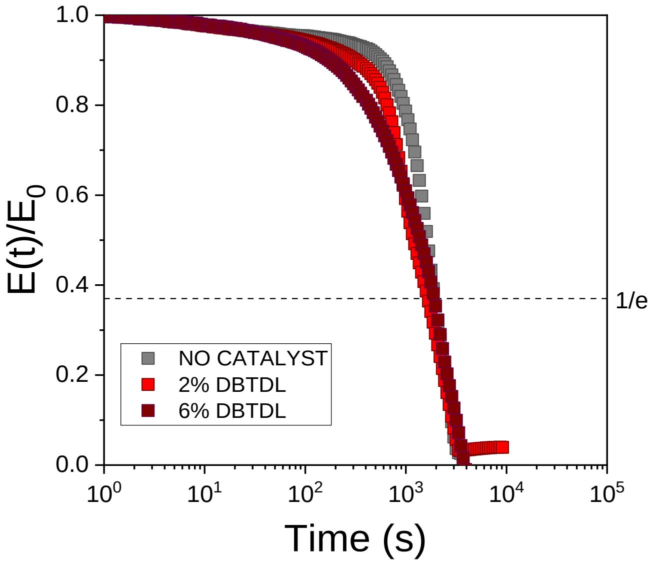

Figure S2.3. Stress-relaxation measurements for aliphatic (HDI) polyurethanes cross-linked with 2% and 6% of DBTDL performed at 120 °C.

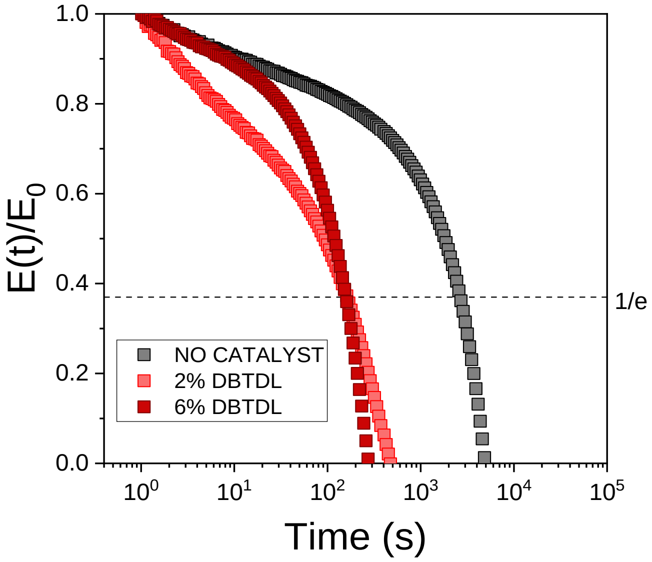

Figure S2.4. Stress-relaxation measurements for aromatic (MDI) polyurethanes cross-linked with 2% and 6% of DBTDL performed at 120 °C.

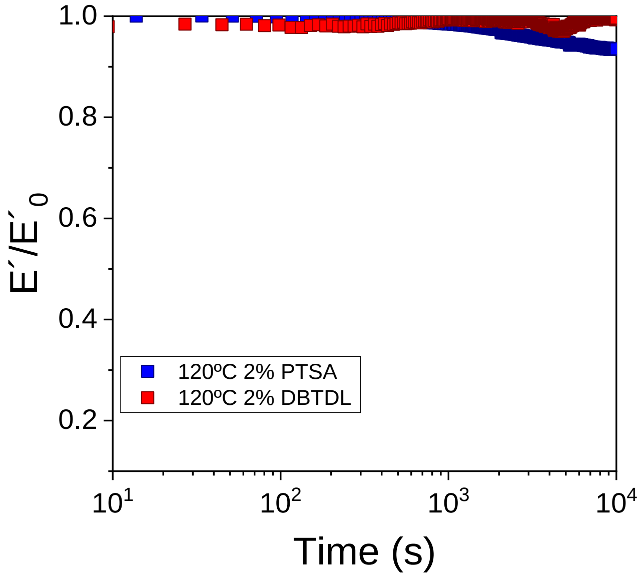

Figure S2.5. DMTA measurements for aromatic (MDI) polyurethanes cross-linked with 2% of DBTDL (red) and 2% of PTSA (blue) performed at 120 °C.

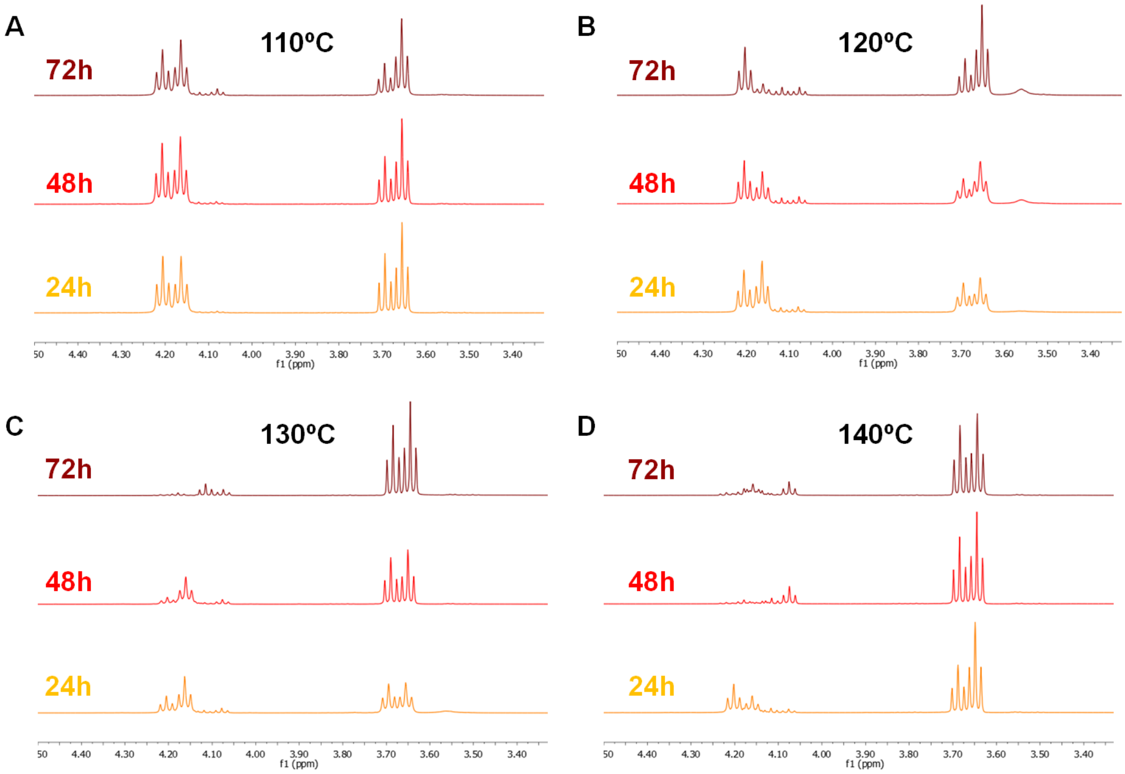

Figure S2.6. ^{1}H-NMR measurements for aromatic polyurethane model reactions catalyzed with 2% of DBTDL performed at 110 °C (A), 120 °C (B), 130 °C (C) and 140 °C (D).

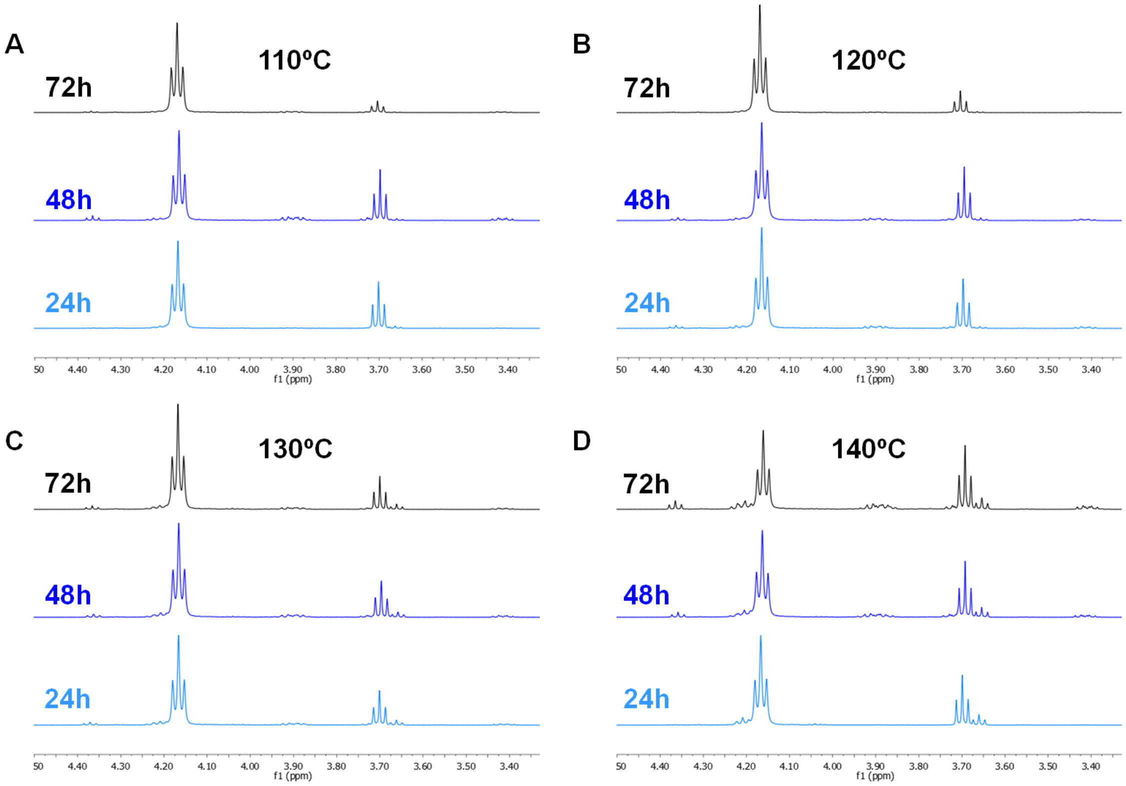

Figure S2.7. ^{1}H-NMR measurements for aromatic polyurethane model reactions catalyzed with 2% of p-TSA performed at 110 °C (A), 120 °C (B), 130 °C (C) and 140 °C (D).

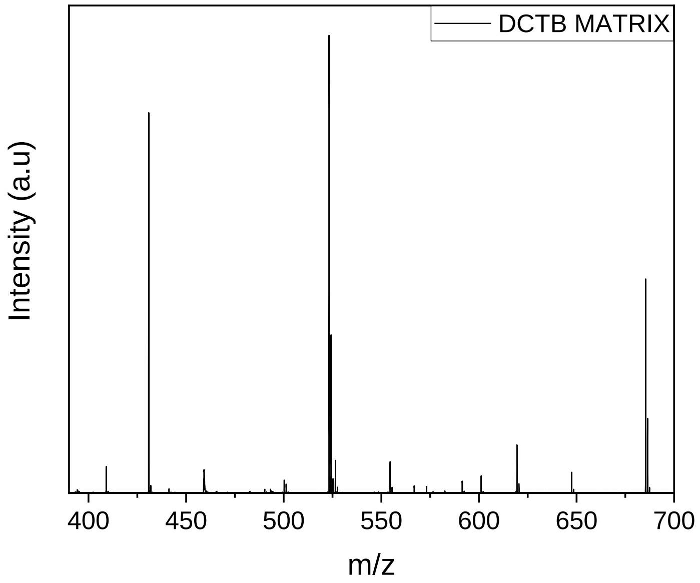

Figure S2.8. Characterization by MALDI-TOF of the employed DCTB matrix. Most relevant signals corresponding to DCTB Matrix: 409.056, 430.589, 459.233, 500.253, 523.248, 526.483, 554.514, 619.496 and 685.403.

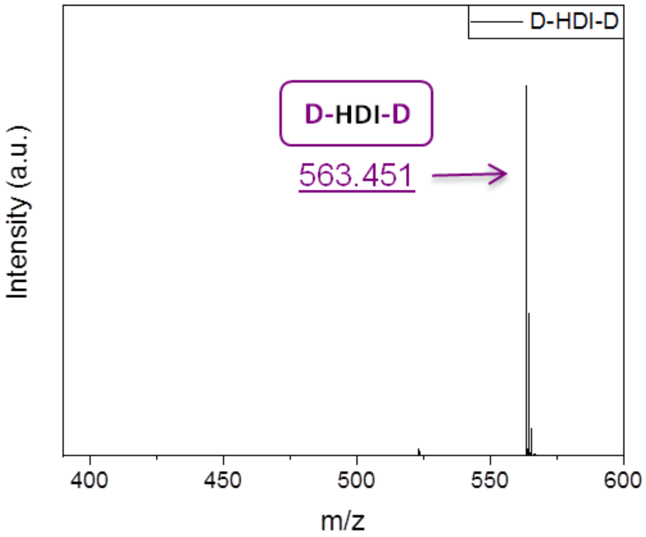

Figure S2.9. Characterization by MALDI-TOF of *Didodecyl hexane-1,6- diyldicarbamate* (D-HDI-D).

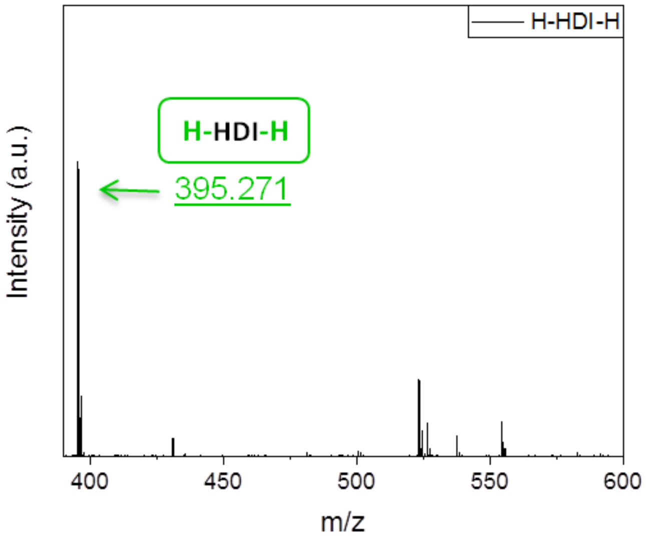

Figure S2.10. Characterization by MALDI-TOF of *Dihexyl hexane-1,6- diyldicarbamate* (H-HDI-H).

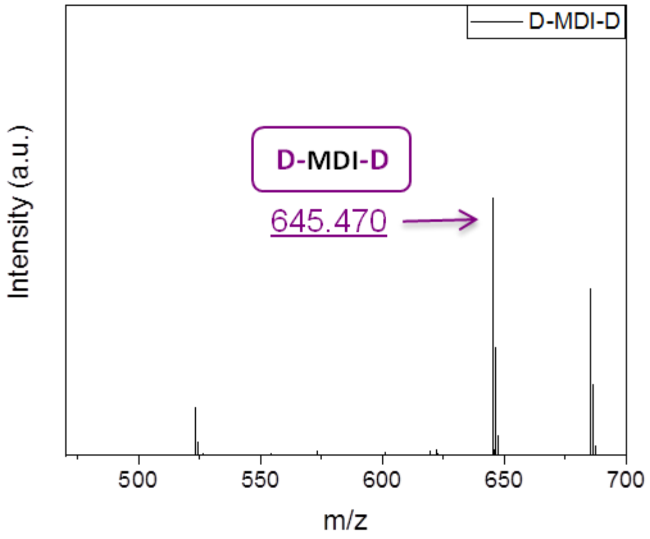

Figure S2.11. Characterization by MALDI-TOF of *Didodecyl (methylenebis(4,1-phenylene))dicarbamate* (D-MDI-D).

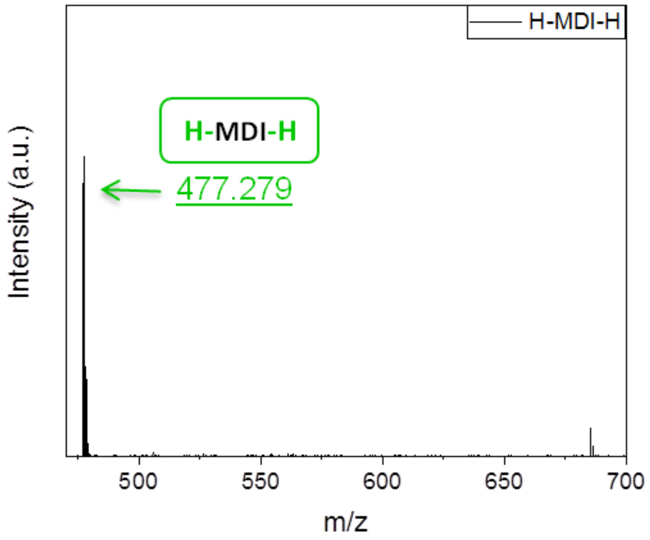

Figure S2.12. Characterization by MALDI-TOF of *Dihexyl (methylenebis(4,1-phenylene))dicarbamate* (H-MDI-H).

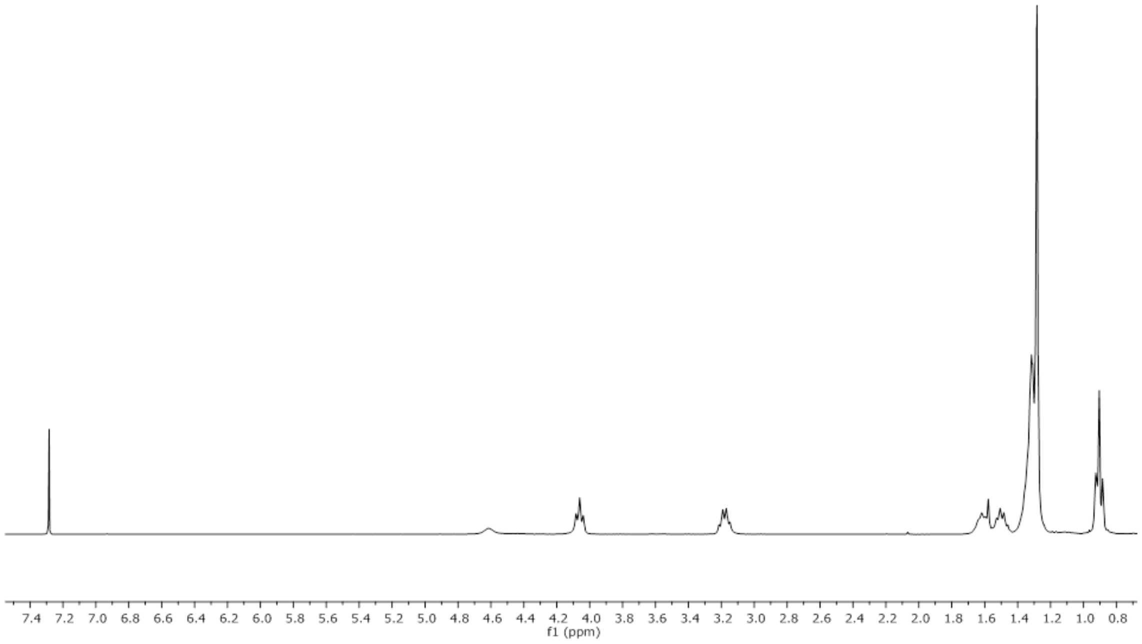

Figure S2.13. ^{1}H-NMR spectra of dodecyl hexyl carbamate.

^{1}H NMR (300 MHz, Chloroform-*d*) δ 4.61 (s, 1H), 4.06 (td, *J* = 6.7, 0.0 Hz, 2H), 3.18 (q, *J* = 6.7 Hz, 2H), 1.71 – 1.58 (m, 4H), 1.49 (q, *J* = 7.0 Hz, 2H), 1.31 (dd, *J* = 8.3, 0.0 Hz, 22H), 1.02 – 0.77 (m, 6H).

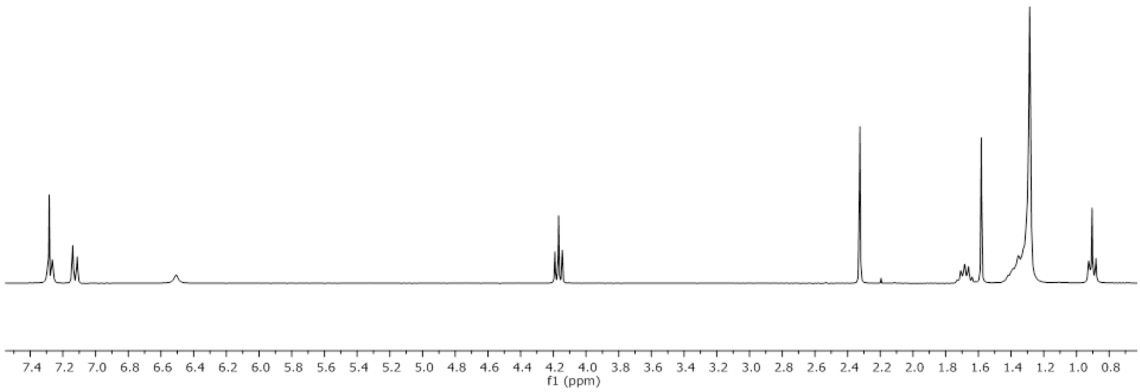

Figure S2.14. ^{1}H-NMR spectra of dodecyl p-tolyl carbamate.

^{1}H NMR (300 MHz, Chloroform-*d*) δ 7.37 – 7.19 (m, 2H), 7.13 (d, *J* = 8.3 Hz, 2H), 6.51 (s, 1H), 4.17 (t, *J* = 6.7 Hz, 2H), 2.33 (s, 3H), 1.76 – 1.62 (m, 2H), 1.29 (m, *J* = 5.2 Hz, 18H), 0.98 – 0.83 (m, 3H).

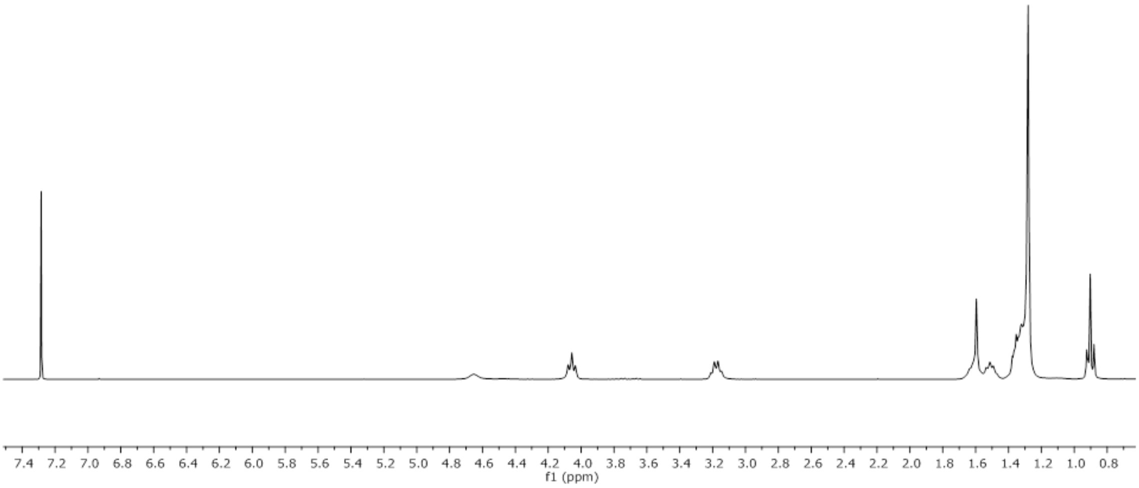

Figure S2.15. ^{1}H-NMR spectra of didodecyl hexane -1,6- diyldicarbamate.

^{1}H NMR (300 MHz, Chloroform-*d*) δ 4.65 (s, 2H), 4.06 (t, *J* = 6.7 Hz, 4H), 3.18 (q, *J* = 6.6 Hz, 4H), 1.61 (d, *J* = 6.0 Hz, 8H), 1.51 (t, *J* = 6.6 Hz, 2H), 1.42 – 1.16 (m, 38H), 0.97 – 0.81 (m, 6H).

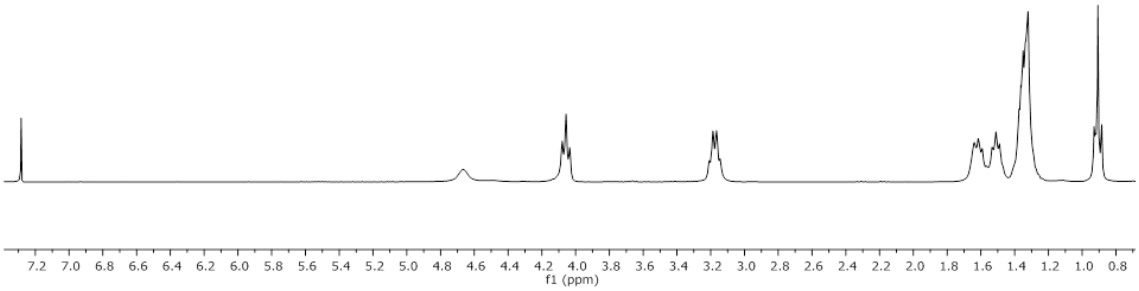

Figure S2.16. ^{1}H-NMR spectra of dihexyl hexane -1,6- diyldicarbamate.

^{1}H NMR (300 MHz, Chloroform-*d*) δ 4.67 (s, 2H), 4.06 (t, *J* = 6.7 Hz, 4H), 3.18 (q, *J* = 6.6 Hz, 4H), 1.72 – 1.55 (m, 4H), 1.51 (t, *J* = 6.6 Hz, 4H), 1.43 – 1.22 (m, 16H), 0.98 – 0.81 (m, 6H).

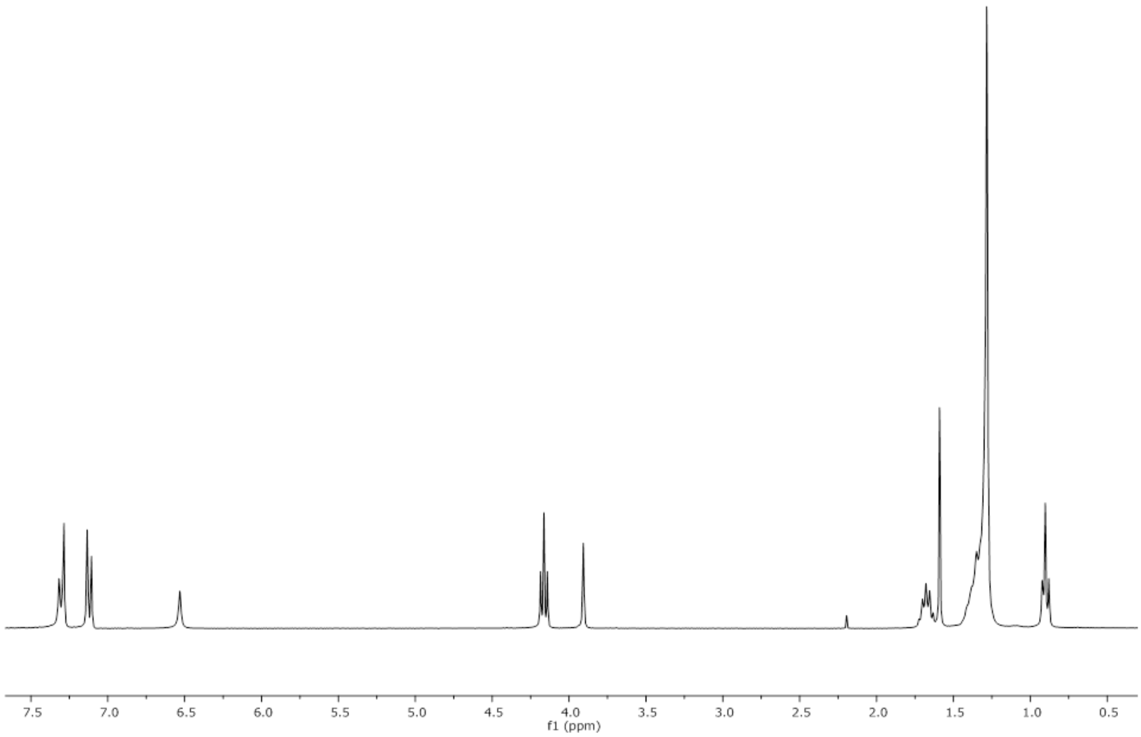

Figure S2.17. ^{1}H-NMR spectra of didodecyl (methylenebis(4,1-phenylene)) dicarbamate.

^{1}H NMR (300 MHz, Chloroform-*d*) δ 7.38 – 7.25 (m, 4H), 7.12 (d, *J* = 8.4 Hz, 4H), 6.53 (s, 2H), 4.16 (t, *J* = 6.7 Hz, 4H), 3.91 (s, 2H), 1.67 (q, *J* = 7.0 Hz, 4H), 1.29 (m, *J* = 4.6 Hz, 36H), 0.99 – 0.82 (m, 6H).

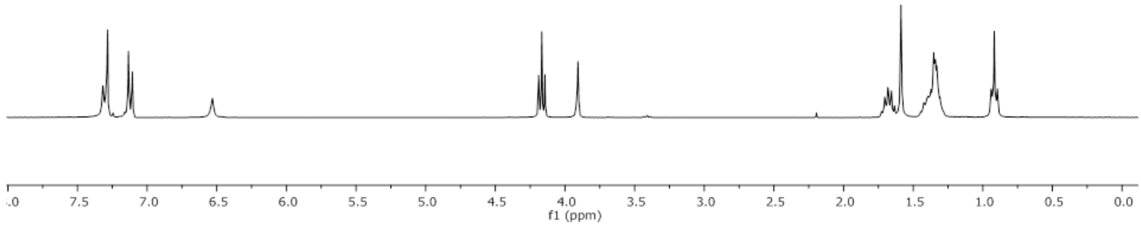

Figure S2.18. ^{1}H-NMR spectra of dihexyl (methylenebis(4,1-phenylene))dicarbamate.

^{1}H NMR (300 MHz, Chloroform-*d*) δ 7.39 – 7.27 (m, 4H), 7.20 – 7.01 (m, 4H), 6.53 (s, 2H), 4.17 (t, *J* = 6.7 Hz, 4H), 3.91 (s, 2H), 1.67 (dt, *J* = 8.0, 6.5 Hz, 4H), 1.48 – 1.18 (m, 12H), 0.92 (td, *J* = 6.9, 5.7, 2.9 Hz, 6H).

Chapter 3.

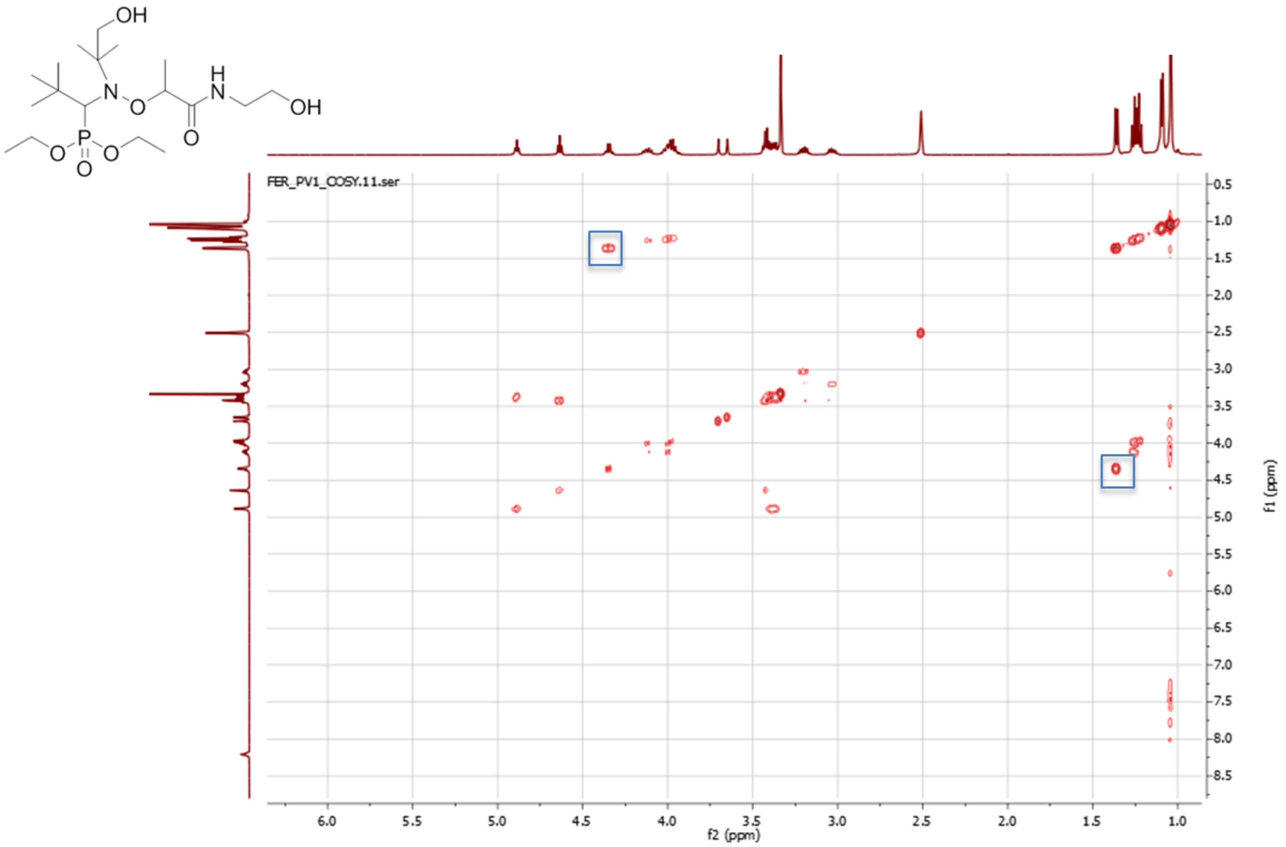

Figure S3.1. COSY characterization of PV1 alkoxyamine.

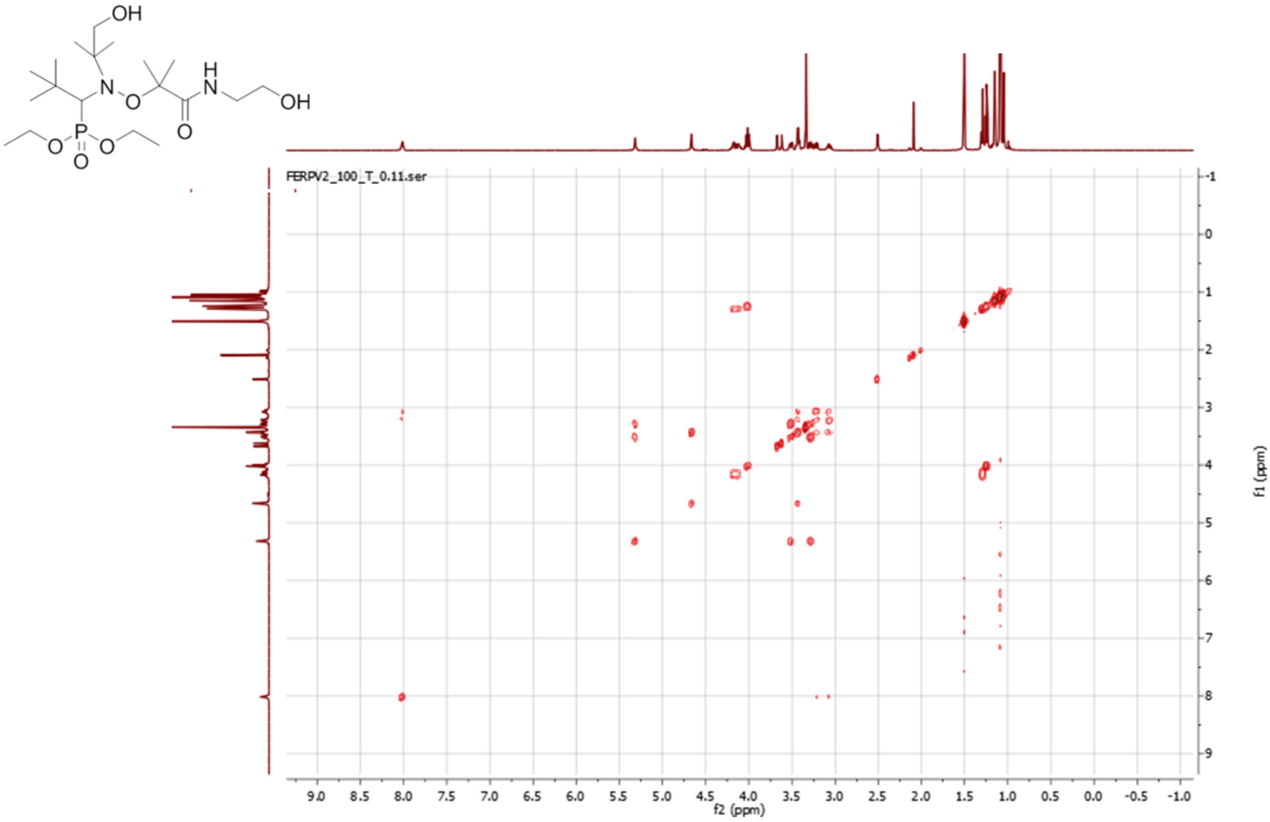

Figure S3.2. COSY characterization of PV2 alkoxyamine.

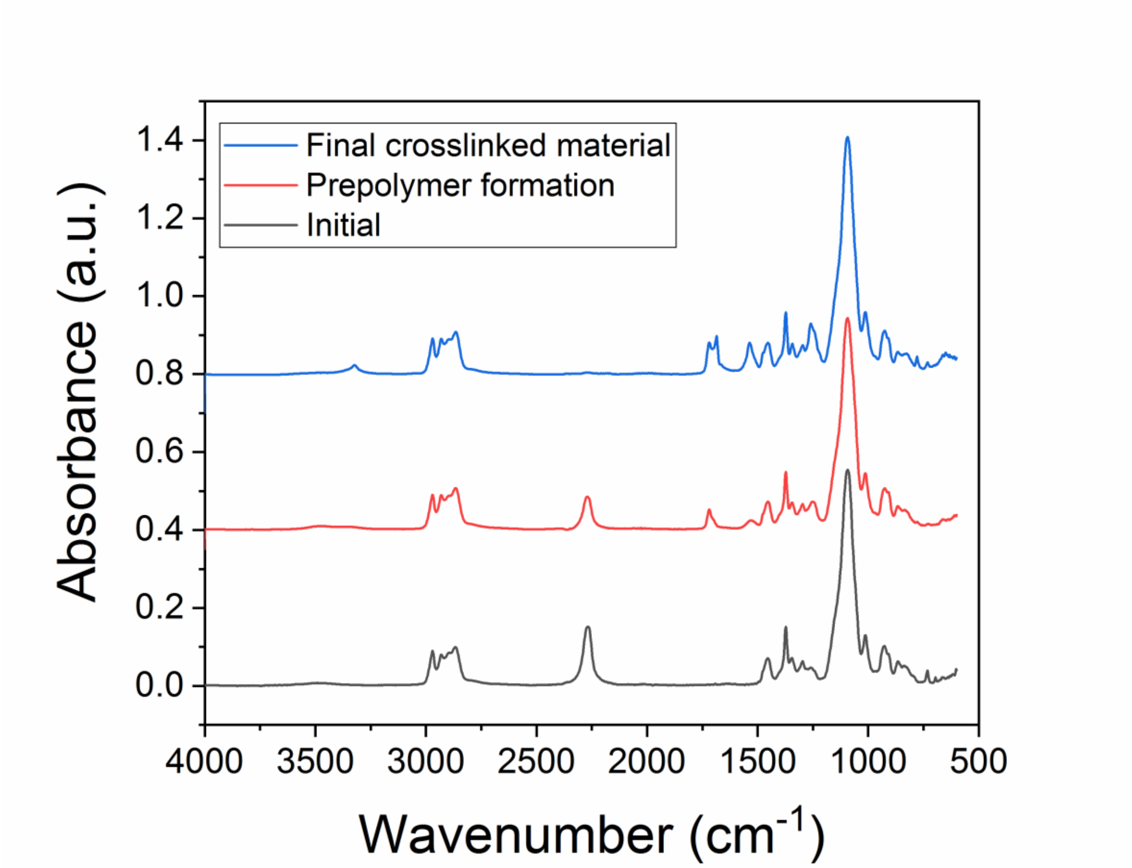

Figure S3.3. FTIR characterization of blank polyurethane thermoset (1,6 Hexanediol as chain extender). Black trace corresponds to the initial mixture of polypropylene glycol (PPG) and 1,6 Hexamethylene diisocyanate (HDI). Red trace corresponds to the tris-isocyanate terminated prepolymer and blue represents the final cured material after reacting with 1,6 Hexanediol.

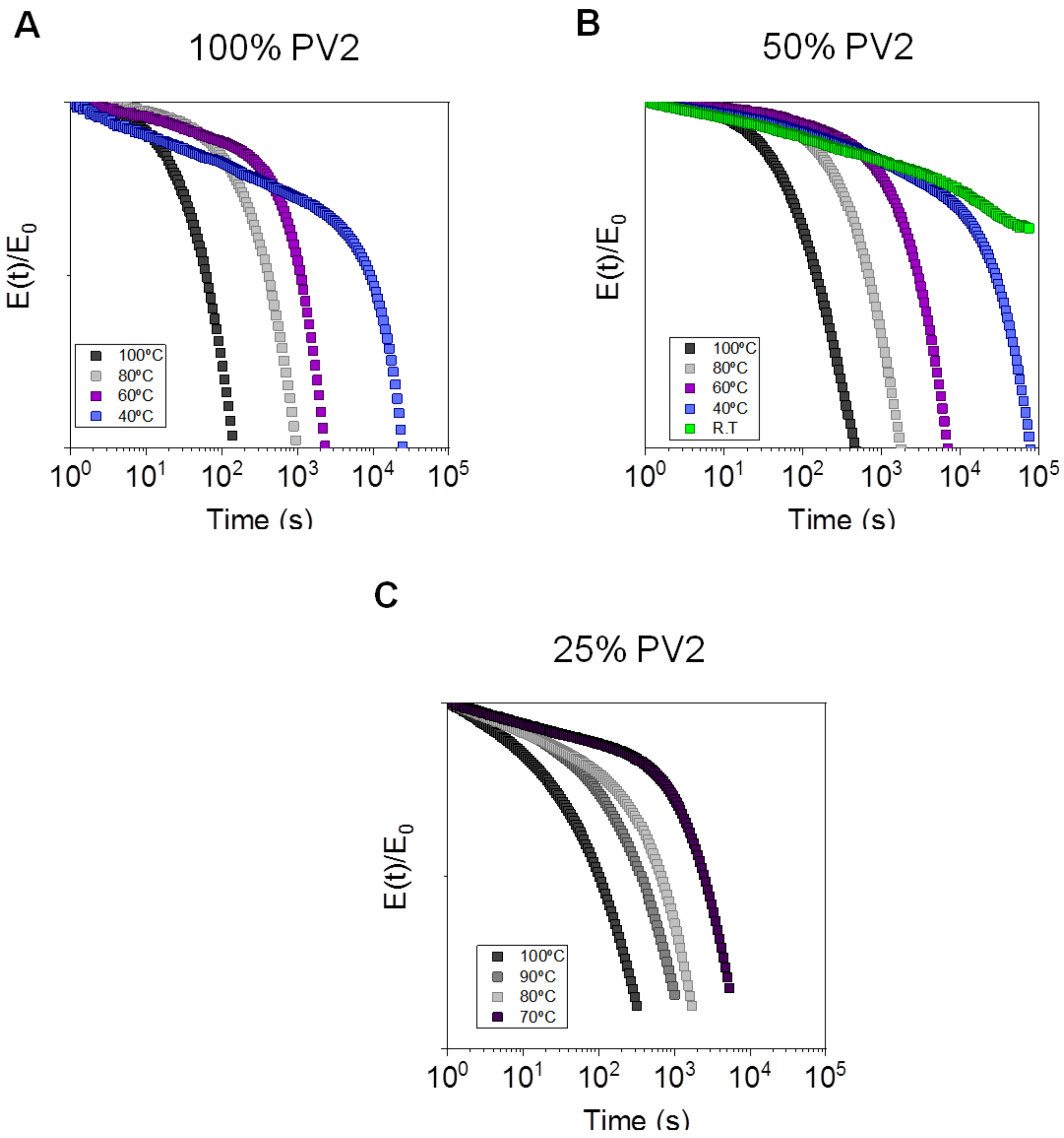

Figure S3.4. Stress-relaxation measurements of polyurethane films containing 100% of PV2 alkoxyamine (A), 50/50(%) of PV2 alkoxyamine/1,6-Hexanediol (B), and 25/75(%) of PV2 alkoxyamine/1,6-Hexanediol (C).

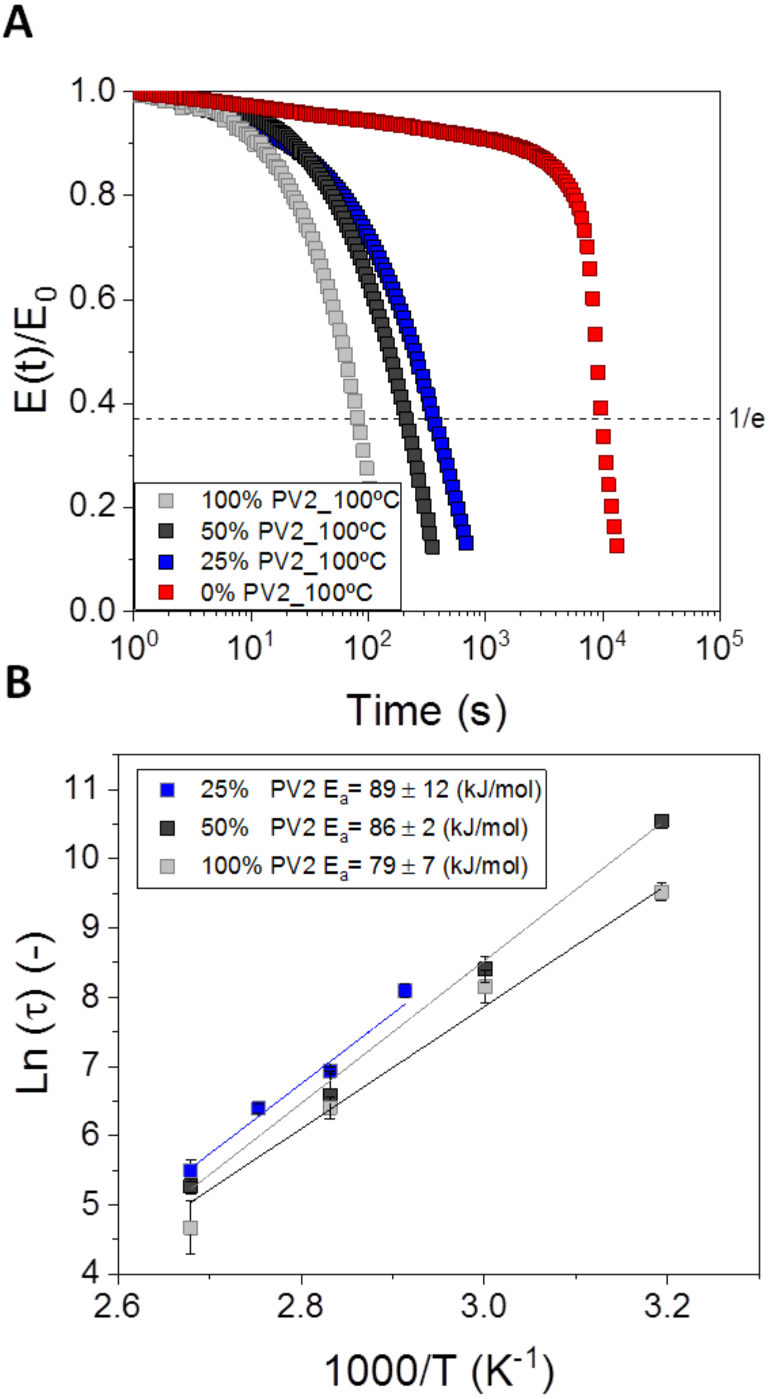

Figure S3.5. A) Influence of the alkoxyamine concentration in the relaxation time at 100ºC. B) Arrhenius plot of characteristic relaxation times of cross-linked polyurethanes with different amounts of PV2 alkoxyamine and their respective activation energies (E_a).

Chapter 4.

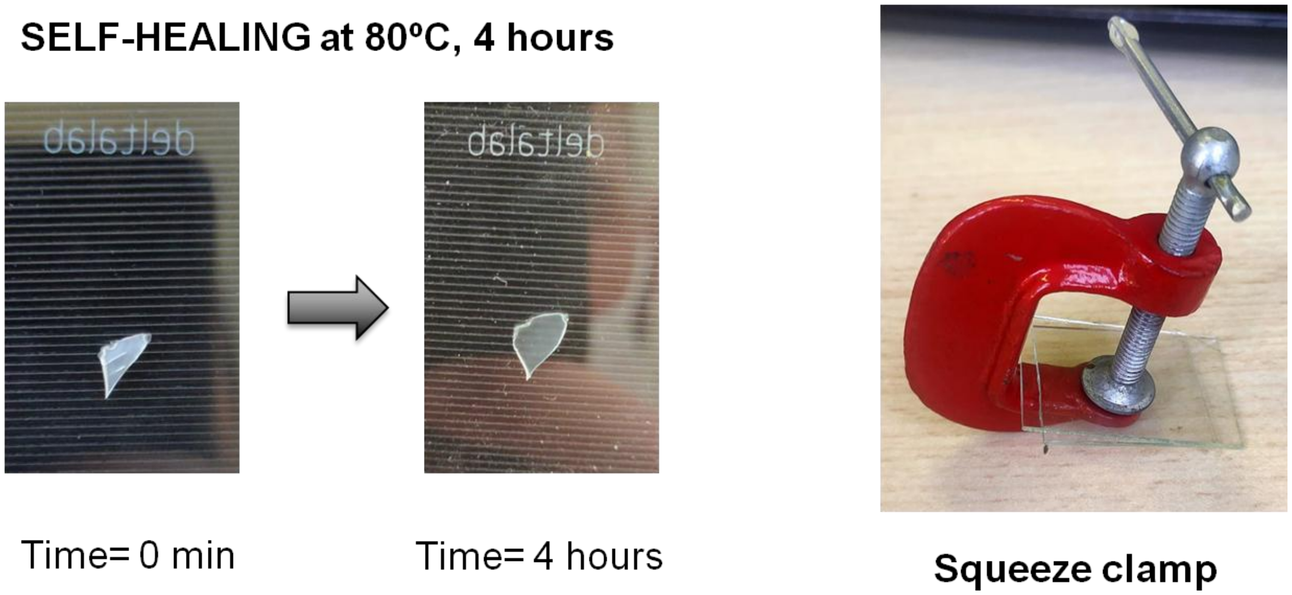
SELF-HEALING at 80ºC, 4 hours
Time= 0 min
Time= 4 hours
Squeeze clamp

Figure S4.1. Representative image of self-healing process at 80 °C applying pressure with a squeeze clamp for 4 h.

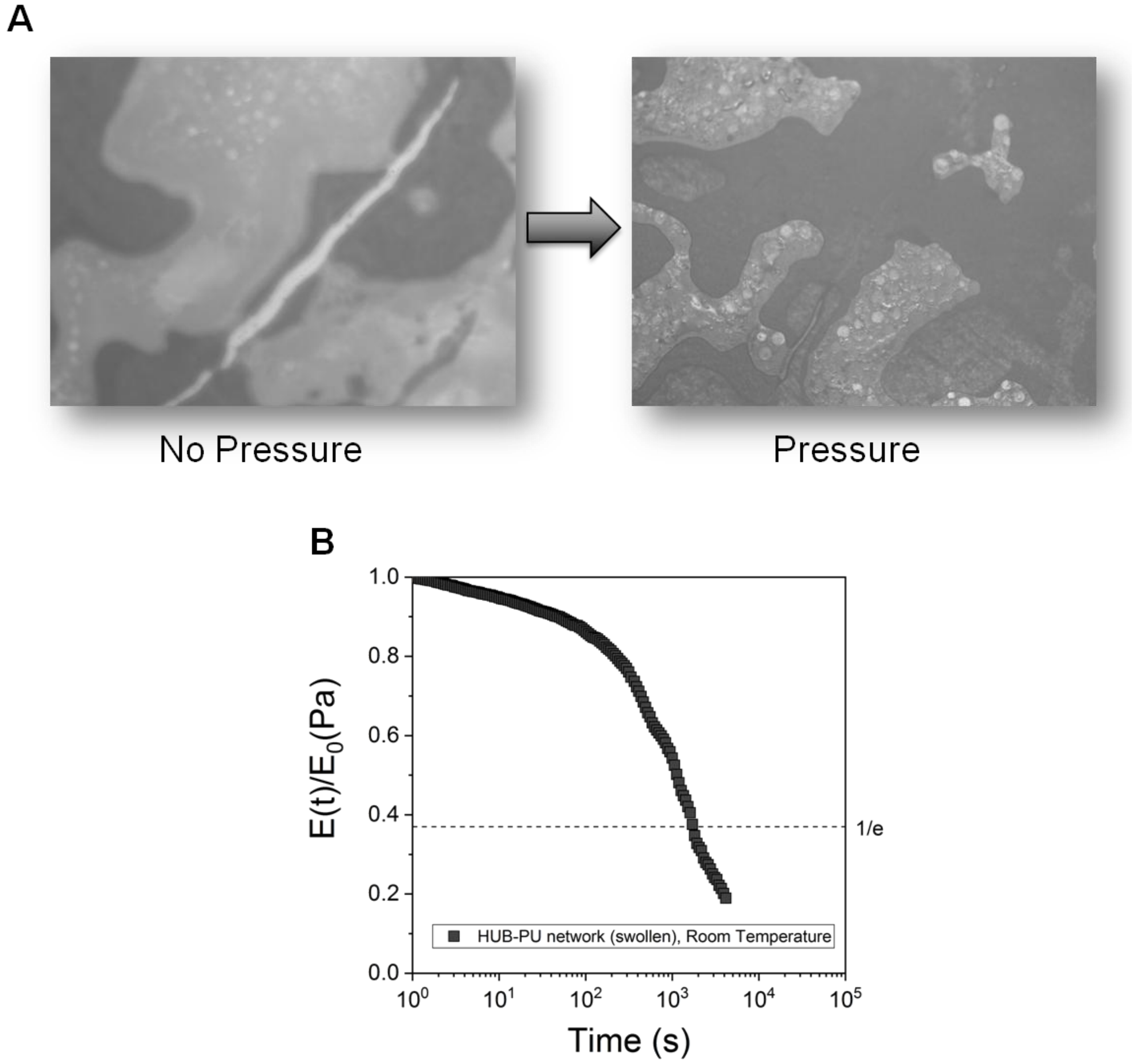

Figure S4.2. A) Microscopic image of scratch disappearance and B) Stress-relaxation measurement at room temperature of swollen HUB-PU network.

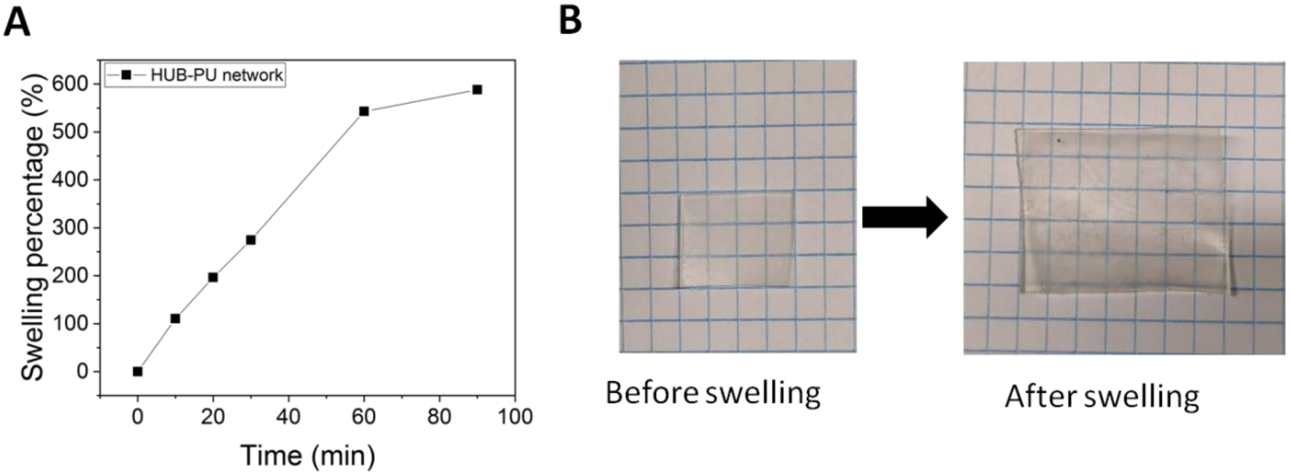

Figure S4.3. A) Swelling percentage (%) upon time (min) of HUB-PU network. B) Representative image before and after swelling of HUB-PU network in $LiPF_6$ EC:DEC (1:1 v:v).

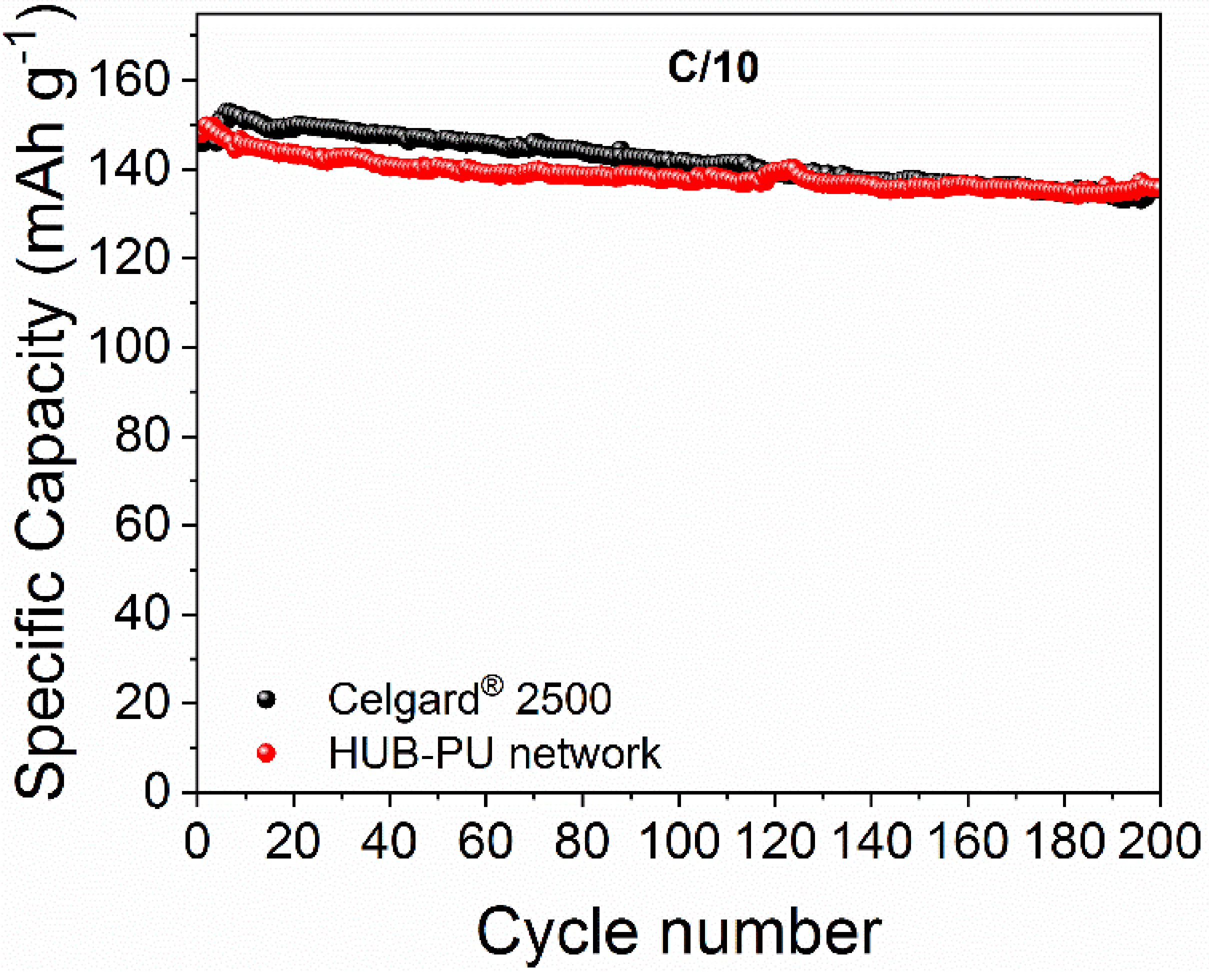

Figure S4.4. Comparison of specific capacities vs. cycle number of Celgard® 2500 and HUB-PU network at C/10 for 200 cycles.

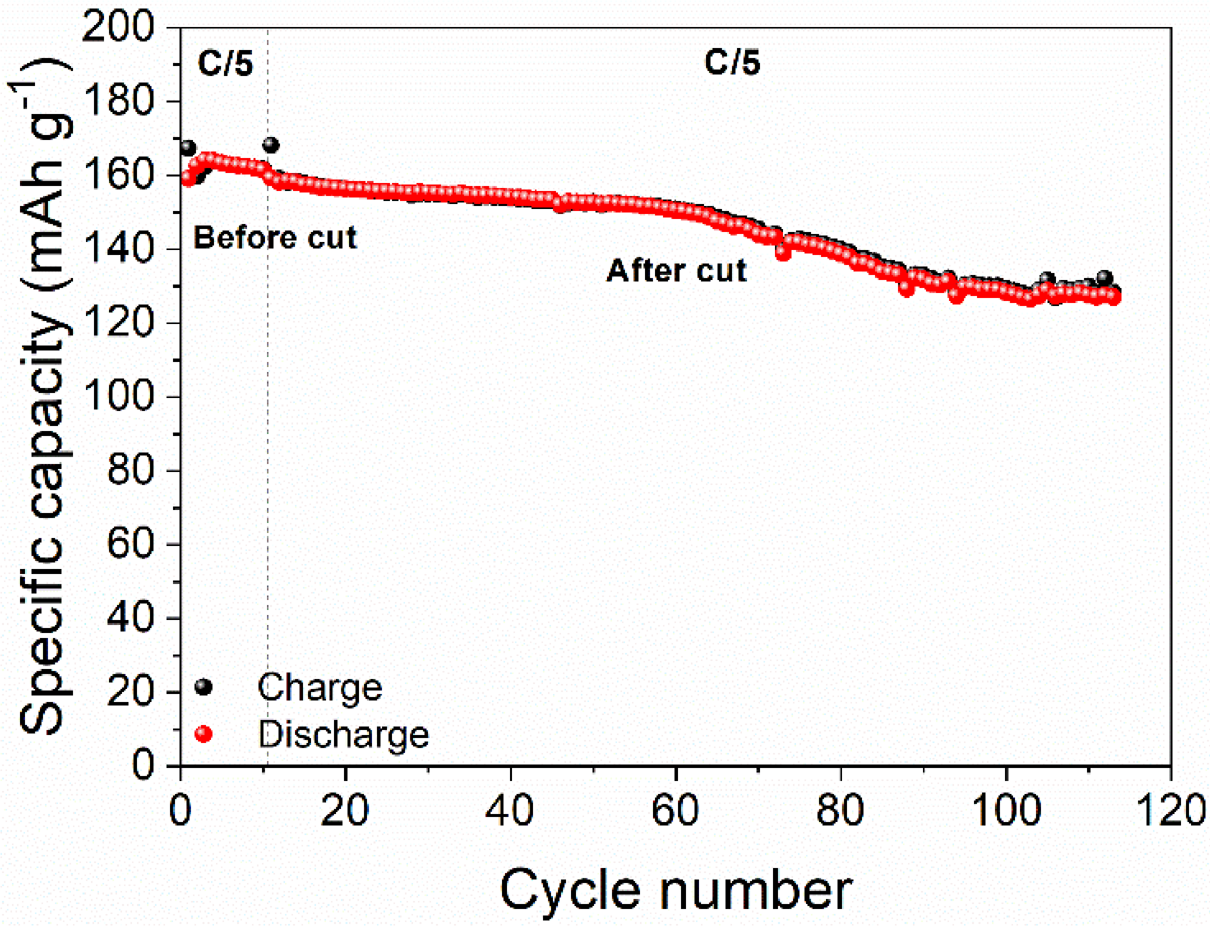

Figure S4.5. Cycling performances for 116 cycles of HUB-PU network mechanically damaged after 10 cycles.

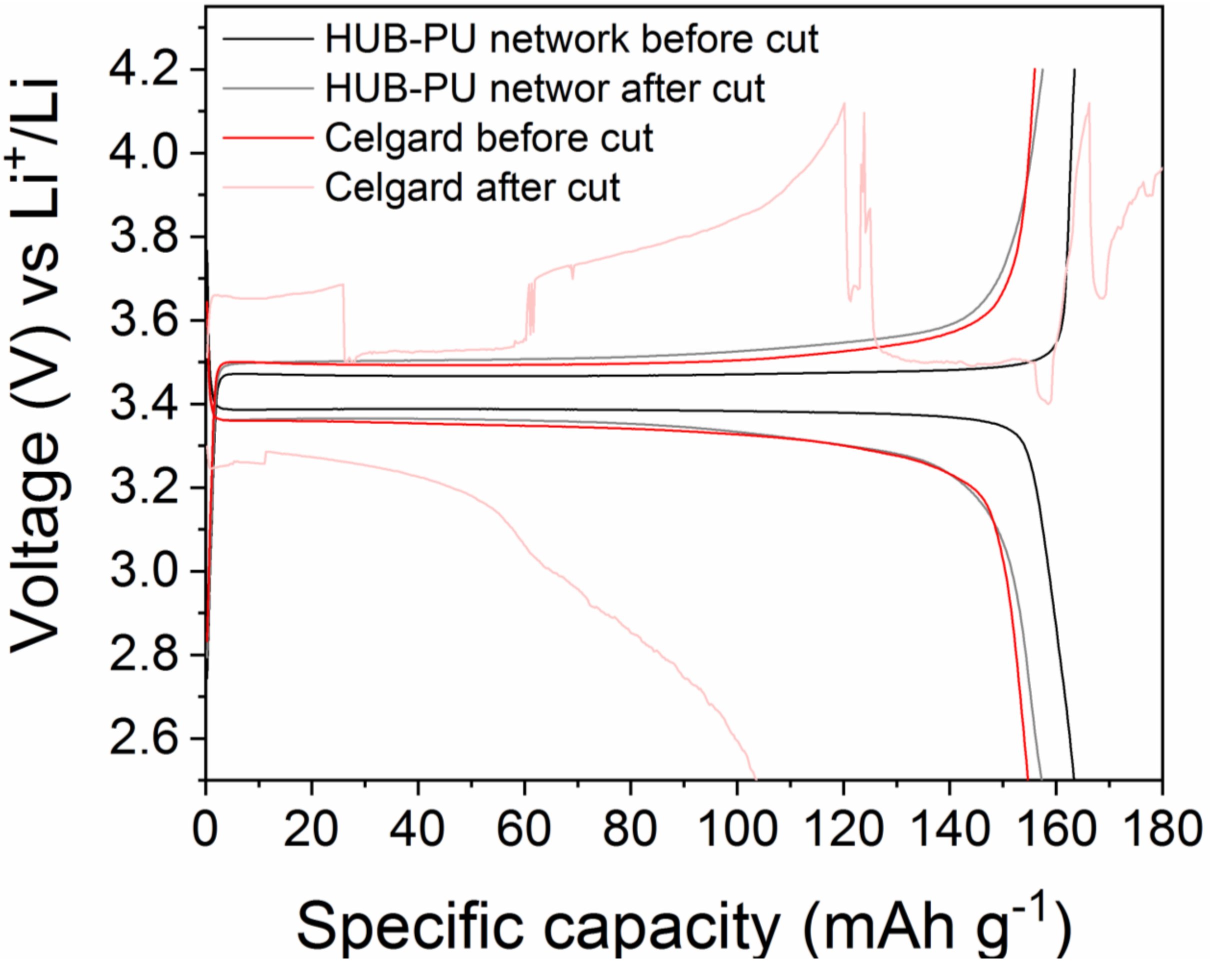

Figure S4.6. Comparison of voltage profiles before and after cut of commercial Celgard® 2500 and HUP-PU network.

Table S4.1. Comparison among the most authoritative publications in the field of self-healing polymer electrolytes for LIBs. Note: in the present work, the data relative to the last two columns are the following: 161 mAh g^{-1} (1^{st} cycle), then 159 mAh g^{-1} after the cut (11^{th} cycle) and 127 mAh g^{-1} at the 100^{th} cycle.

Ref.	Electrolyte	Self-healing mechanism	Electrode and its theoretical capacity	Cycles	Specific capacity of first and last cycles	Self-healing electrochemical test
[1]	CSE, PolyIL, 2D BN nanosheets, EMIMTFSI, LiTFSI	Electrostatic interaction between IL cations and salt anions	LFP 0.8, CB 0.1, PVDF 0.1, 170 mAh g^{-1}, *vs.* Li-metal	200	152 and 132.4 mAh g^{-1} (@ 0.1C, 55 °C)	Cut and healed outside, then used in cell, cycled @ 0.1C, 55°C
[2]	Ceramic-in-polymer, SPE, SiO_2 NPs, PEG, PEO, LiTFSI	Chemical interaction of Li dendrites with silica	LFP 0.8, CB 0.1, PVDF 0.1, 170 mAh g^{-1}, *vs.* Li-metal	55	94 and and 156 mAh g^{-1} (@ 0.05C, 70 °C)	None
[3]	SPE, dicationic quaternary ammonium 6-armed, EMIMTFSI	Electrostatic interaction between IL cations and salt anions	LFP 0.8, CB 0.1, PVDF 0.1, 170 mAh g^{-1}, *vs.* Li-metal	50	147 and 138 mAh g^{-1} (@ 0.1C, 60 °C)	None
[4]	IGPE, NH_2-PEG-NH_2, TPB, BMImTFSI	Dynamic covalent imine bonds	LFP 0.8, CB 0.1, PVDF 0.1, 170 mAh g^{-1}, *vs.* Li-metal	50	154 and 132 mAh g^{-1} (@ 0.1C, RT)	None
[5]	GPE, NH_2-PEG-NH_2, BTA, LiFSI, LiDFOB, $LiPF_6$	Dynamic covalent imine bonds	LFP 0.8, CB 0.1, PVDF 0.1, 170 mAh g^{-1}, *vs.* Li-metal	125	142 and 139 mAh g^{-1} (@ 1C, 30 °C)	Cut and healed outside, then used in cell, cycled @ 0.1C, 55 °C
[6]	GPE, NH_2-PEG-NH_2, TFB, $LiPF_6$	Dynamic covalent imine bonds	LFP 0.8, CB 0.1, PVDF 0.1, 170 mAh g^{-1}, *vs.* Li-metal	300	150 and 126 mAh g^{-1} (@ 0.1C, RT)	None

[7]	SPE, SBMA, HFBM, EMITFSI, LiTFSI	Ion-dipole interaction	LFP 0.8, CB 0.1, PVDF 0.1, 170 mAh g^{-1}, *vs.* Li-metal	100	144 and 118 mAh g^{-1} (@ 0.2C, 60 °C)	None
[8]	SIGPE, PEGMA, UPy-MA, SSPSILi	Hydrogen bonding	LFP 0.8, CB 0.1, PVDF 0.1, 170 mAh g^{-1}, *vs.* Li-metal	60	129 and 129 mAh g^{-1} (@ 0.1C, 60 °C)	None
[9]	SPE, PVT, EMIMTFSI, LiTFSI	Electrostatic interaction between IL cations and salt anions	LFP 0.8, CB 0.1, PVDF 0.1, 170 mAh g^{-1}, *vs.* Li-metal	40	145 and 144 mAh g^{-1} (@ 0.1C, RT)	None
[10]	SPE, UPy-MA, PEGMA, LiTFSI	Quadruple hydrogen bonding	LFP 0.8, CB 0.1, PVDF 0.1, 170 mAh g^{-1}, *vs.* Li-metal	100	157 and 143 mAh g^{-1} (@ 0.1C, 60 °C)	Cut and healed outside, then used in a cell, cycled @ 0.1C, 60 °C

BMIm *= bis-trifluoromethanesulphonimide;* ***BN*** *= boron nitride;* ***BTA*** *= benzene-1,3,5-tricarbaldehyde;* ***CSE*** *= composite solid electrolyte;* ***DFOB*** *= difluoro(oxalato)borate;* ***EMIMTFSI*** *= 1-ethyl-3-methylimidazoliumbis (trifluoromethylsulfonyl) imide;* ***HFBM*** *= hexafuorobutyl methacrylate;* ***IGPE*** *= ionic gel polymer electrolyte;* ***IL*** *= ionic liquid;* ***NPs*** *= nanoparticles;* ***PolyIL*** *= poly(N,N,N-trimethyl-N-(1-vinlyimidazolium-3-ethyl)-ammonium bis(trifluorome thanesulfonyl)imide);* ***PVT*** *= poly(4-vinylpyridine)(propyl-trimethylammonium);* ***SBMA*** *= sulfobetaine methacrylate;* ***SIPE*** *= single-ion conducting gel polymer electrolyte;* ***SPE*** *= solid-state polymer electrolyte;* ***TPB*** *= 1,3,5-benzenetricarboxaldehyde;* ***TFB*** *= 1,3,5-triformylbenzene.*

References

[1] J. Li, L. Yang, H. Zhang, X. Ji. Self-healing composite solid electrolytes with enhanced Li^+ transport and mechanical properties for safe lithium metal batteries. *Chem. Eng. J.* **2022**, *438*, 135418. https://doi.org/10.1016/j.cej.2022.135418

[2] L. Mezzomo, S. Bonato, S. Mostoni, B. Di Credico, R. Scotti, M. D'Arienzo, P. Mustarelli, R. Ruffo. Composite solid-state electrolyte based on hybrid poly(ethylene glycol)-silica fillers enabling long-life lithium metal batteries. *Electrochim. Acta* **2022**, *411*, 140060. https://doi.org/10.1016/j.electacta.2022.140060

[3] R. Li, Z. Fang, C. Wang, X. Zhu, X. Fu, J. Fu, W. Yan, Y. Yang. Six-armed and dicationic polymeric ionic liquid for highly stretchable, nonflammable and notch-insensitive intrinsic self-healing solid-state polymer electrolyte for flexible and safe lithium batteries. *Chem. Eng. J.* **2022**, *430*, 132706. https://doi.org/10.1016/j.cej.2021.132706

[4] L. Wan, X. Cao, X. Xue, Y. Tong, S. Ci, H. Huang, D. Zhou. Self-Healing and Flexible Ionic Gel Polymer Electrolyte Based on Reversible Bond for High-Performance Lithium Metal Batteries. *Energy Technol.* **2022**, *10*, 2100749. https://doi.org/10.1002/ente.202100749

[5] K. Deng, S. Zhou, Z. Xu, M. Xiao, Y. Meng. A high ion-conducting, self-healing and nonflammable polymer electrolyte with dynamic imine bonds for dendrite-free lithium metal batteries. *Chem. Eng. J.* **2022**, *428*, 131224. https://doi.org/10.1016/j.cej.2021.131224

[6] L. Zhang, P. Zhang, C. Chang, W. Guo, Z. H. Guo, X. Pu. Self-Healing Solid Polymer Electrolyte for Room-Temperature Solid-State Lithium Metal Batteries. *ACS Appl. Mater. Interfaces* **2021**, *13*, 46794. https://doi.org/10.1021/acsami.1c14462

[7] C. Wang, R. Li, P. Chen, Y. Fu, X. Ma, T. Shen, B. Zhou, K. Chen, J. Fu, X. Bao, W. Yan, Y. Yang. Highly stretchable, non-flammable and notch-insensitive intrinsic self-healing solid-state polymer electrolyte for stable and safe flexible lithium batteries. *J. Mater. Chem. A* 2021, *9*, 4758. https://doi.org/10.1039/D0TA10745J

[8] H. Gan, Y. Zhang, S. Li, L. Yu, J. Wang, Z. Xue. Self-Healing Single-Ion Conducting Polymer Electrolyte Formed via Supramolecular Networks for Lithium Metal Batteries. *ACS Appl. Energy Mater.* **2021**, *4*, 482. https://doi.org/10.1021/acsaem.0c02384

[9] X. Tian, P. Yang, Y. Yi, P. Liu, T. Wang, C. Shu, L. Qu, W. Tang, Y. Zhang, M. Li, B. Yang. Self-healing and high stretchable polymer electrolytes based on ionic bonds with high conductivity for lithium batteries. *J. Power Sources* **2020**, *450*, 227629. https://doi.org/10.1016/j.jpowsour.2019.227629

[10] B. Zhou, D. He, J. Hu, Y. Ye, H. Peng, X. Zhou, X. Xie, Z. Xue. A flexible, self-healing and highly stretchable polymer electrolyte *via* quadruple hydrogen bonding for lithium-ion batteries *J. Mater. Chem. A* **2018**, *6*, 11725. https://doi.org/10.1039/C8TA01907J

Experimental section

Chapter 2.

Synthesis of model urethane compounds

Hexyl isocyanate based urethane

Hexyl isocyanate (2.54 g, 20 mmol) was added to 1-dodecanol (4.1 g, 22 mmol) in a previously dried round bottom reaction flask. The mixture was stirred at 55°C overnight under dry N_2 flux. After the reaction, the mixture was allowed to cool and was subjected to column chromatography(Silica gel, [Hexane]/[[Ethyl acetate]= 9/1, v/v]) to give pure dodecyl hexyl carbamate, 3.91 g, 62% yield. The identity and purity of the product was confirmed by ^{1}H-NMR (Fig. S11).

p-Tolyl isocyanate based urethane

p-Tolyl isocyanate (1.33 g, 10 mmol) was dissolved in anhydrous THF and was added to 1-dodecanol (2.80 g, 15 mmol) in a previously dried round bottom reaction flask. The mixture was stirred at 55°C overnight under dry N_2 flux. After the reaction, the mixture was allowed to cool and was subjected to column chromatography (Silica gel, [Hexane]/[[Ethyl acetate]= 8/2, v/v]) to give pure dodecyl *p*-tolylcarbamate, 2.09 g, 65% yield. The identity and purity of the product was confirmed by ^{1}H-NMR (Fig. S12).

Synthesis of model diurethane compounds

HDI (5.04g, 0.03 mol) was added to 1-dodecanol (44.7g, 0.24 mol) or 1-hexanol (12.26 g, 0.12 mol) dissolved in 60 mL of anhydrous THF in a round bottom reaction flask.

The mixture was stirred under reflux overnight under dry N_2 flux. The white solid was filtered off and rinsed with cold anhydrous ethanol. It was recrystallized in anhydrous ethanol and dried under high vacuum overnight. White crystals formed. Yield: Didodecyl hexane-1,6-diyldicarbamate: 11.8 g, 73% . Dihexyl hexane-1,6-

diyldicarbamate: 8.4 g, 52%. The identity and purity of the product was confirmed by ^{1}H-NMR (Fig. S13 and S14).

MDI (7.50 g, 0.03 mol) was added to 1-dodecanol (27.95 g, 0.15 mol) or 1-hexanol (15.32 g, 0.15 mol) dissolved in 100 mL of anhydrous THF in a round bottom reaction flask.

The mixture was stirred under reflux overnight under dry N_2 flux. A white precipitate was formed and recrystallized in anhydrous ethanol. Hexane was added to promote the precipitation. The white solid was dried under high vacuum overnight. White crystals formed. Yield: Didodecyl (methlyenebis(4,1-phenylene))dicarbamate: 15.63 g, 84%. Dihexyl (methlyenebis(4,1-phenylene))dicarbamate: 9.00 g, 66%. The identity and purity of the product was confirmed by ^{1}H-NMR (Fig. S15 and S16).

Synthesis of reprocessable polyurethane thermosets

Synthesis of aliphatic tris-isocyanate-terminated pre-polymer

A mixture of PPG (3740g/mol) (90 g, 24.06mmol) and HDI (12.11 g, 72.18 mmol) were fed into a round bottom flask equipped with a stirrer and a N_2 inlet. The mixture was stirred for 7 hours at 90°C and the reaction was monitored by FTIR spectroscopy. The resulting tris-isocyanate-terminated pre-polymer was obtained in a form of colorless liquid, and was stored under vacuum in the freezer. Yield 92 g, 90%.

Synthesis of aromatic tris-isocyanate-terminated pre-polymer

A mixture of PPG (3740 g/mol) (90 g, 24.06 mmol) and previously dissolved MDI (18.06 g, 72.18 mmol) in anhydrous THF (36 mL) were fed into a round bottom flask equipped with a stirrer and a N_2 inlet. The mixture was stirred for 5 hours at 90°C and the reaction was monitored by FTIR spectroscopy. The resulting tris-isocyanate-terminated pre-polymer was obtained in a form of colorless liquid, and was stored under vacuum in the freezer. Yield 103 g, 95%.

Synthesis of aliphatic cross-linked polyurethane films

1,6-Hexanediol (137.9 mg, 1.16 mmol) previously dissolved in 0.2 mL of anhydrous THF were mixed with aliphatic tris-isocyanate terminated pre-polymer (3 g, 0.71mmol) and stirred vigorously. The mixture was degassed under vacuum and was place in an open mold.

For the introduction of catalysts in the polymer networks, PTSA or TBD were dissolved in anhydrous THF (12-15 g/mL) and an aliquot of the solution was added to the mixture to obtain 2 mol % of catalyst. DBTDL was directly added to the mixture.

Synthesis of aromatic cross-linked polyurethane films

1,6-Hexanediol (137.9 mg, 1.16 mmol) previously dissolved in 0.2 mL of anhydrous THF were mixed with aromatic tris-isocyanate terminated pre-polymer (3.7 g (82% solid content), 0.71 mmol) and stirred vigorously. The mixture was degassed under vacuum and was place in an open mold.

PTSA or TBD were dissolved in anhydrous THF and an aliquot of the solution was added to the mixture to obtain 2 mol % of catalyst. DBTDL was directly added to the mixture.

Chapter 3.

Synthesis of reprocessable polyurethane thermosets

Synthesis of aliphatic tris-isocyanate-terminated pre-polymer

The prepolymer was synthesized as explained in the previous Experimental Section of Chapter 2.

Synthesis of aliphatic cross-linked polyurethane films (Blank, PV1 and PV2)

1,6-Hexanediol (127 mg, 1.06 mmol) previously dissolved in 0.2 mL of anhydrous THF was mixed with aliphatic tris-isocyanate terminated pre-polymer (3 g, 0.71 mmol) and stirred vigorously. 2 mol % of NCO content of DBTDL was directly added to the mixture. The mixture was degassed under vacuum and was place in an open mold. The curing was carried out at 80 ^{o}C for 2 hours.

For the synthesis of 50% PV1 and 50% PV2 alkoxyamines in the polymer networks, PV1 (225.8 mg, 0.53 mmol) or PV2 (233.5 mg, 0.53 mmol) were dissolved in 1 mL THF and were added with 1,6-Hexanediol (63.5 mg, 0.53 mmol) to the aliphatic tris-isocyanate terminated pre-polymer (3 g, 0.71mmol) and stirred vigorously. 2 mol % of NCO content of DBTDL was directly added to the mixture.

For the materials containing 25% of PV2 alkoxyamine, 117 mg (0.265 mmol) of the alkoxyamine were added with 1,6-Hexanediol (95,3 mg, 0,8 mmol) and the films were prepared following the same procedure abovementioned.

For the materials containing 100% of PV2 alkoxyamine, 467 mg (1.06 mmol) of the alkoxyamine were dissolved in 2 mL of anhydrous THF and mixture with the prepolymer. Films were prepared following the same procedure abovementioned.

Chapter 4.

Synthesis of HUB-PU network: In order to synthesize self-healable crosslinked poly(urea-urethane) network (Figure 4.2 A), HDI (1.5 mmol, 252 mg) was dissolved, in quite diluted conditions, using anhydrous THF (13 mL) as a solvent. The solution was kept stirring vigorously at room temperature. Subsequently, tris[2-(isopropylamino)ethyl]amine (0.5 mmol, 136 mg) was added dropwise in order to form free isocyanate group end capped hindered urea trimmers. The mixture was stirred for 15 min and, successively, previously dried PEG2000 (0.75 mmol, 1.6 g) was added to the solution. Once PEG2000 was properly dissolved, DBTDL (2 mol% with respect to NCO content, 9.5 mg) was added and, after 5 min stirring, the mixture was deposited in a rectangular Teflon mold. Before the curing step, the mixture was degassed in vacuum oven and then heated up to 80 °C overnight.

Cathode preparation: To obtain the LFP electrode as a cathode for the cell testing, a slurry consisting of LFP, C65 and PVDF, at a weight ratio of 70:20:10, was mixed in NMP solvent. Then, the slurry was coated on an Al foil and dried overnight at room temperature. The as-obtained electrode was cut into 15 mm-diameter discs and dried under vacuum at 120 °C for 4 h.

Membrane activation: HUB-PU network membrane was cut into 12 mm discs, dried under vacuum at 50 °C for 12 h before being transferred in a glovebox and activated by swelling in $LiPF_6$ 1.0 M in EC:DEC (1:1, v:v) for 30 min.

Materials

Chapter 2

p-Tolyl Isocyanate (99%), Hexyl isocyanate (99%), 1-Dodecanol (98%), 3-Methyl-1-butanol (99%) were purchased from Fisher (Acros Organics) and used as received.

1-Hexanol (≥99%), Dibutyltin dilaurate (DBTDL,95%), 1,5,7-Triazabicyclo[4.4.0]dec-5-ene (TBD, 98%), p-Toluenesulfonic acid monohydrate (PTSA, ≥99%), Hexamethylene diisocyanate (HDI, ≥98.0%) and 4,4′-Methylenebis(phenyl isocyanate) (MDI, 98%) anhydrous tetrahydrofuran (THF,≥99.9%), were purchased from Aldrich and used as received.

Poly(propylene glycol) (PPG) (Mn=3,740) was purchased from Bayer Materials Science and dried in the oven overnight prior to use. 1,6-Hexanediol was purchased from Aldrich and dried prior to use.

Ethyl acetate (reagent grade) and Hexane (96%) were purchased from Scharlab.

Chapter 3

Dibutyltin dilaurate (DBTDL, 95%), Hexamethylene diisocyanate (HDI, ≥98.0%), Triethylamine (TEA), 2-amino-2-methylpropan-1-ol, 2-bromopropionyl bromide (97%) and anhydrous tetrahydrofuran (THF,≥99.9%), were purchased from Aldrich and used as received. 1,6-Hexanediol was purchased from Aldrich and dried prior to use.

Pivaldehyde was purchased from TCI and used as received.

Copper, Copper Bromide, m-CPBA, Ethanolamine, 2-Bromo-2-methylpropionyl Bromide (98%) and PMDETA were purchased from Fisher and used as received.

Poly(propylene glycol) (PPG) (M_n=3740 g/mol) was purchased from Bayer Materials Science and dried in the oven overnight prior to use.

Ethyl acetate (reagent grade), Chloroform (reagent grade) and Hexane (96%) were purchased from Scharlab.

Chapter 4

Tris[2-(isopropylamino)ethyl]amine (90%), dibutyltin dilaurate (DBTDL, 95%), hexamethylene diisocyanate (HDI, ≥98.0%) and anhydrous tetrahydrofuran (THF, ≥99.9%), were purchased from Merck and used as received. PEG (Mn=2130) was purchased from Merck and dried in the oven (70 °C) overnight prior to use.

$LiPF_6$ 1.0 M solution in EC:DEC (1:1, v:v) was purchased from Solvionic and used in the glove box. Poly(vinylidenedifluoride) (PVDF-HSV900:ADX160 90:10 wt:wt, Arkema; 10 wt.% in N-methyl-2-pyrrolidinone (NMP) solution), Li disk (Chemetall Foote Corporation, Ø 16 mm), polypropylene polymeric membrane (Celgard® 2500, 25 µm-thick, Ø 19 mm), LFP (Aleees) and carbon black powder (C65, C-NERGY Super C65, Timcal) were used as received.

List of Publications

Part of this thesis has been published or will be published in a near future. Apart from that, different collaborations have been carried out during this time that lead to publications. The list of articles that would be issued from this work is as follows (the authors list and/or article title might be changed).

(1) Verde-Sesto, E.; Goujon, N.; Sardon, H.; Ruiz, P.; Huynh, T. V.; **Elizalde, F**.; Mecerreyes, D.; Forsyth, M.; O'Dell, L. A. DNP NMR Studies of Crystalline Polymer Domains by Copolymerization with Nitroxide Radical Monomers. *Macromolecules* 2018, *51* (20), 8046–8053. https://doi.org/10.1021/acs.macromol.8b01665.

(2) **Elizalde, F**.; Aguirresarobe, R. H.; Gonzalez, A.; Sardon, H. Dynamic Polyurethane Thermosets: Tuning Associative/Dissociative Behavior by Catalyst Selection. *Polym. Chem.* 2020, *11* (33), 5386–5396. https://doi.org/10.1039/d0py00842g.

(3) Gallastegui, A.; Gabirondo, E.; **Elizalde, F**.; Aranburu, N.; Mecerreyes, D.; Sardon, H. Chemically Recyclable Glycerol-Biobased Polyether Thermosets. *Eur. Polym. J.* 2021, *143* (November 2020), 110174. https://doi.org/10.1016/j.eurpolymj.2020.110174.

(4) Gomez-Lopez, A.; **Elizalde, F**.; Calvo, I.; Sardon, H. Trends in Non-Isocyanate Polyurethane (NIPU) Development. *Chem. Commun.* 2021, *57* (92), 12254–12265. https://doi.org/10.1039/d1cc05009e.

(5) Hernández, A.; Houck, H. A.; **Elizalde, F**.; Guerre, M.; Sardon, H.; Du Prez, F. E. Internal Catalysis on the Opposite Side of the Fence in Non-Isocyanate Polyurethane Covalent Adaptable Networks. *Eur. Polym. J.* 2022, *168* (October 2021). https://doi.org/10.1016/j.eurpolymj.2022.111100.

(6) **Elizalde, F**.; Amici, J.; Trano, S.; Vozzolo, G.; Aguirresarobe, R.; Versaci, D.; Bodoardo, S.; Mecerreyes, D.; Sardon, H.; Bella, F. Self-Healable Dynamic Poly(Urea-Urethane) Gel Electrolyte for Lithium Batteries. *J. Mater. Chem. A* 2022. https://doi.org/10.1039/d2ta02239g.

(7) **Elizalde, F**.; Aguirresarobe, R.; Lezama, L.; Ruipérez, F.; Gigmes, D. Tuning Reprocessing Temperature of Aliphatic Polyurethane Networks by Alkoxyamine Selection. In preparation.

Some other collaborations have been carried out and will be published soon. Please note that the author list and/or article title might be changed.

(*) **Elizalde, F**.; Trano, S.; Vozzolo, G.; J. Ayestaran; Amici, J.; Aguirresarobe, R.; Versaci, D.; Bodoardo, S.; Mecerreyes, D.; Sardon, H.; Bella, F. 3D printable and self-healable hindered urea bond based polyurethane electrolytes for Lithium ion batteries.